d) Galvin (1969), hereafter referred to as GA69, performed laboratory experiments with regular wave on plane beach and combined his data with the data of Iversen (1952) and McCowan (1894). The breaking criterion was developed by fitting empirical relationship between h_b / H_b and m.

$$H_b = h_b \frac{1}{1.40 - 6.85m} \qquad \text{for } m \le 0.07 \tag{4.4.1}$$

$$H_b = \frac{h_b}{0.92} \qquad \text{for } m > 0.07 \tag{4.4.2}$$

e) Collins and Weir (1969), hereafter referred to as CW69, derived a breaking height formula from linear wave theory and empirically included the slope effect into the formula. The experimental data from three sources (Suquet, 1950; Iversen, 1952; and Hamada, 1963) were used to fit the formula.

$$H_b = h_b(0.72 + 5.6m) \tag{4.5}$$

f) Goda (1970), hereafter referred to as GO70, analyzed several sets of laboratory data on breaking waves on slopes obtained by several researchers (Iversen, 1952; Mitsuyasu, 1962; and Goda, 1964) and proposed a diagram presenting criterion for predicting breaking wave height. Then Goda (1974) gave an approximate expression for the diagram as

$$H_b = 0.17L_o\left\{1 - \exp\left[-1.5\frac{\pi h_b}{L_o}\left(1 + 15m^{4/3}\right)\right]\right\} \tag{4.6}$$

g) Weggel (1972), hereafter referred to as WE72, proposed an empirical formula for computing breaking wave height from five sources of laboratory data (Iversen, 1952; Galvin, 1969; Jen and Lin, 1970; Weggel and Maxwell, 1970; and Reid and Bretschneider, 1953). The experiments cover a range of 1/50 < m < 1/5.

$$H_b = \frac{h_b g T^2 1.56/[1+\exp(-19.5m)]}{gT^2 + h_b 43.75[1-\exp(-19m)]} \tag{4.7}$$

h) Komar and Gaughan (1972), hereafter referred to as KG72, used linear wave theory to derive a breaker height formula from energy flux conservation and assumed a constant H_b / h_b. After calibrating the formula to the laboratory data of Iversen (1952), Galvin (1969), and unpublished data of Komar and Simons (1968), and the field data of Munk (1949), the formula was proposed to be

$$H_b = 0.56H_o\left(\frac{H_o}{L_o}\right)^{-1/5} \tag{4.8}$$

i) Sunamura and Horikawa (1974), hereafter referred to as SH74, used the same data set as Goda (1970) to plot the relationship between H_b / H_o, H_o / L_o, and m. After fitting the curve the following formula was proposed

$$H_b = H_o m^{0.2}\left(\frac{H_o}{L_o}\right)^{-0.25} \tag{4.9}$$

j) Madsen (1976), hereafter referred to as MA76, combined the formulas of Galvin (1969) and Collins (1970) to be

$$H_b = 0.72h_b(1+6.4m) \qquad \text{for} \qquad m < 0.10 \tag{4.10}$$

Black and Rosenberg (1992) found that the formula of Madsen (1976) gives good predictions for individual breaking wave height in laboratory and field experiments.

k) Ostendorf and Madsen (1979), hereafter referred to as OM79, modified the formula of Miche (1944) by including the beach slope in to the formula. After calibrating to the laboratory data, the Miche (1944)'s formula was modified to be

$$H_b = 0.14L_b \tanh\left[(0.8+5m)\frac{2\pi h_b}{L_b}\right] \qquad \text{for} \qquad m \le 0.1 \tag{4.11.1}$$

$$H_b = 0.14L_b \tanh\left[(0.8+5(0.1))\frac{2\pi h_b}{L_b}\right] \qquad \text{for} \qquad m > 0.1 \tag{4.11.2}$$

l) Sunamura (1980), hereafter referred to as SU80, conducted an empirical formula based on an analysis of various laboratory data (Iversen, 1952; Bowen et al., 1968; Goda, 1970; and Sunamura, 1980) and obtained the following formula

$$H_b = 1.1h_b\left(\frac{m}{\sqrt{H_o/L_o}}\right)^{1/6} \tag{4.12}$$

m) Singamsetti and Wind (1980), hereafter referred to as SW80, conducted a laboratory experiment and proposed two empirical formulas based on their own data. The experiments cover a range of 1/40 < m < 1/5 and 0.02 < H_o/L_o < 0.065.

$$H_b = 0.575H_o m^{0.031}\left(\frac{H_o}{L_o}\right)^{-0.254} \tag{4.13}$$

and

$$H_b = 0.937h_b m^{0.155}\left(\frac{H_o}{L_o}\right)^{-0.13} \tag{4.14}$$

n) Ogawa and Shuto (1984), hereafter referred to as OS84, obtained the following formula from the same data sets as Goda (1970). The formula is limited to use for the range of 1/100 < m < 1/10 and 0.003 < H_o/L_o < 0.065.

$$H_b = 0.68H_c m^{0.09}\left(\frac{H_o}{L_o}\right)^{-0.25} \tag{4.15}$$

o) Larson and Kraus (1989), hereafter referred to as LK89, developed a breaking criterion based on the large wave tank data of Kajima et al. (1983). The breaking height index H_b/h_b was related to the deepwater wave steepness and the local beach slope seaward of the breaking point.

$$H_b = 1.14 h_b \left(\frac{m}{\sqrt{H_o / L_o}} \right)^{0.21} \tag{4.16}$$

p) Hansen (1990), hereafter referred to as HA90, used the laboratory data from Van Dorn (1978) and unpublished data of ISVA to plot the relationship between H_b / h_b and mL_b / h_b and proposed the following empirical formula

$$H_b = 1.05 h_b \left(m \frac{L_b}{h_b} \right)^{0.2} \tag{4.17}$$

q) Smith and Kraus (1990), hereafter referred to as SK90, proposed 2 empirical formulas based on the analysis of 11 sources of laboratory data performed on plane beach conditions. The experiments cover a range of 1/80 < m < 1/10 and 0.001 < H_o / L_o < 0.092.

$$H_b = h_b \left\{ \frac{1.12}{1 + \exp(-60m)} - 5.0[1 - \exp(-43m)] \frac{H_o}{L_o} \right\} \tag{4.18}$$

and

$$H_b = H_o (0.34 + 2.47m) \left(\frac{H_o}{L_o} \right)^{-0.30 + 0.88m} \tag{4.19}$$

r) Gourlay (1992), hereafter referred to as GL92, proposed an empirical formula based on seven sources of laboratory data (Bowen et al., 1968; Smith, 1974; Visser, 1977; Gourlay, 1978; Van Dorn, 1976; Stive, 1984; and Hansen and Svendsen, 1979). The experiments cover a range of 1/45 < m < 1/10 and 0.001 < H_o / L_o < 0.066. The data was used to plot the relationship between H_b / H_o and H_o / L_o, the curve fitting yields

$$H_b = 0.478 H_o \left(\frac{H_o}{L_o} \right)^{-0.28} \tag{4.20}$$

s) Present study: the author proposed 3 empirical formulas (PS1-PS3, see section 2.1) based on the re-analysis of existing models. The published experimental data from 24 sources were used to calibrate the formulas. The experiments cover a range of 0 < m < 0.44 and 0.001 < H_o / L_o < 0.10.

PS1: $$H_b = 0.1 L_o \tanh\left[\left(-81.07m^2 + 35.27m + 7.88\right) \frac{h_b}{L_o} \right] \tag{2.12}$$

PS2: $$H_b = \left(-2.06m^2 + 0.67m + 0.46\right) L_o \left(\frac{H_o}{L_o} \right)^{0.75} \tag{2.16}$$

PS3: $$\frac{H_b}{L_o} = 0.48 \left(\frac{H_o}{L_o} \right)^{0.75} \tag{2.18}$$

4.1.2 Comparison of the breaker height formulas

From section 4.1.1, we see that there are 23 formulas for computing H_b (i.e., Eqs. 4.1-4.20, 2.12, 2.16, and 2.18). The accuracy of the 23 formulas is examined against a wide range of measured breaking wave heights (shown in Table 4.1). The experimental data cover a wide range of wave and bottom conditions ($0.001 \le H_o / L_o \le 0.100$, and $0 \le m \le 0.44$). In order to evaluate the accuracy of the prediction, the examination results are presented in terms of root mean square relative error, ER, which is defined as Eq. (2.19).

The measured breaking wave heights are grouped into different ranges of bottom slope. According to the bottom slope conditions in Eqs. 4.4 and 4.11, the group of bottom slope may be classified to be $m \le 0.07$, $0.07 < m \le 0.10$, and $m > 0.10$. However some formulas (i.e., MK67, SH74, SU80, SW80, OS84, LK89 and HA90) are not valid for the bottom slope $m = 0$. Therefore, in this study, the bottom slope is classified into 4 groups, i.e., horizontal ($m = 0$), gentle ($0 < m \le 0.07$), intermediate ($0.07 < m \le 0.10$), and steep ($m > 0.10$).

The computations of the breaker wave height formulas are carried out with 24 sources of collected data (see Table 4.1). Table 4.2 shows the error ER of each formula for 4 groups of bottom slope. The examination results from Table 4.2 can be summarized as follows.

a) The errors ER shown in Table 4.2 vary from 9.8 to 110.3. The formula of GO70 gives the best prediction (ER = 9.8) for the breaking wave on the bottom slope of $0 < m \le 0.07$ while the formula of CW69 gives the worst prediction (ER = 110.3) for the breaking wave on the bottom slope of $m > 0.10$.

b) The formula of PS1 gives the best prediction (ER = 10.8%) over a wide range of experiments. However higher overall accuracy rating of a formula does not guarantee that the formula is superior to others under all conditions. The accuracy rating of a formula may vary depending on the bottom slope conditions. The best formulas for predicting the breaking wave heights on the bottom slopes of $m = 0$, $0 < m \le 0.07$, $0.07 < m \le 0.1$, $m > 0.10$, and all cases are the formulas of PS2, GO70, OM79, PS2, and PS1, respectively.

c) Most formulas (except MC94, GA69, CW69, MA76, and SW80b) give well predictions ($ER < 15$) for the breaking height on the gentle slope ($0 < m \le 0.07$). However, for the steep slope ($m > 0.10$), the error ER of most formulas (except GA69, WE72, KG72, OM79, SW80a, and GL92) give fair predictions ($ER > 20$).

d) The formulas of CW69, GO70, SH74, and MA76 give unrealistically very large errors ($ER > 50$) for breaking wave on the steep slope ($m > 0.10$). This may cause by an inappropriate bottom slope effect including in the formulas.

Table 4.2: The root mean square relative error (ER) of each formula for four groups of bottom slope and all cases.

Formulas	$m = 0$ (64 cases)	$0 < m \le 0.07$ (338 cases)	$0.07 < m \le 0.1$ (102 cases)	$m > 0.10$ (70 cases)	All 574 cases
MC94 (Eq. 4.1)	14.77	16.98	21.83	27.91	19.26
MI44 (Eq. 4.2)	13.94	11.13	18.04	25.37	14.93
MK67 (Eq. 4.3)	100.00	12.23	17.28	28.02	32.07
GA69 (Eq. 4.4)	15.84	21.05	25.49	17.61	20.83
CW69 (Eq. 4.5)	15.57	25.89	41.31	110.31	48.02
GO70 (Eq. 4.6)	13.86	9.82	23.04	81.57	32.21
WE72 (Eq. 4.7)	14.77	13.03	18.16	19.02	14.76
KG72 (Eq. 4.8)	10.89	10.69	12.42	12.55	11.19
SH74 (Eq. 4.9)	100.00	12.54	31.95	52.89	37.26
MA76 (Eq. 4.10)	15.57	22.55	32.01	86.97	38.70
OM79 (Eq. 4.11)	18.86	11.13	11.68	14.44	12.45
SU80 (Eq. 4.12)	100.00	14.42	14.51	20.18	31.72
SW80a (Eq. 4.13)	100.00	12.75	17.21	17.32	31.17
SW80b (Eq. 4.14)	100.00	15.73	15.53	20.66	32.23
OS84 (Eq. 4.15)	100.00	10.64	18.40	24.08	31.32
LK89 (Eq. 4.16)	100.00	13.39	14.43	23.54	31.73
HA90 (Eq. 4.17)	100.00	14.72	20.34	29.83	33.18
SK90a (Eq. 4.18)	30.01	11.03	11.83	21.09	15.12
SK90b (Eq. 4.19)	13.90	12.61	15.61	26.78	15.71
GL92 (Eq. 4.20)	21.23	14.54	16.43	13.18	15.23
PS1 (Eq. 2.12)	13.22	9.96	12.49	11.33	10.76
PS2 (Eq. 2.16)	10.04	10.67	12.69	11.31	10.96
PS3 (Eq. 2.18)	11.64	10.87	11.83	11.77	11.17

4.2 Wave Models

For computing beach transformation, the wave model should be kept as simple as possible because of the frequent updating of wave field for accounting the variability of mean water surface and the change of bottom profiles. The common equation for computing wave height transformation is the energy flux conservation expressed as Eq. (2.1).

$$\frac{\partial\left(Ec_g\cos\theta\right)}{\partial x} = -D_B \tag{2.1}$$

The wave height transformation can be computed from Eq. (2.1) by substituting the formula of energy dissipation rate, D_B, and numerical integration from offshore to shoreline.

The energy dissipation rate is the most importance parameter in the computation of wave height transformation. During the past decades, many dissipation models have been proposed. Due to the complication of the wave breaking mechanism, most of the dissipation models have to be based on an empirical or semi-empirical formula calibrated from the experimental data. In order to make the models reliable, it is necessary to calibrate or verify the models against wide range and large amount of experimental data.

Some of the existing dissipation models were developed with the limited experimental conditions. Therefore, the coefficient in those models may not be the optimal values for a wide range of experimental conditions. Therefore, the objective of this study is to re-calibrate and compare some existing models based on wide range of experimental data.

Experimental data from 19 sources, including 877 cases, have been collected for calibration and comparison of the selected models. The experiments cover wide range of wave and bottom topography conditions, including small-scale and large-scale and field experiments. The using of these independent data sources and wide range of experimental conditions are expected to clearly demonstration the applicability of the models. A summary of the collected experimental results is given in Table 4.3 (Table 4.3a is for regular waves and Table 4.3b is for irregular waves.

This section is divided into two main parts. The first part presents the dissipation models for regular wave and the second part is for irregular waves.

Table 4.3a: Summary of collected experimental data of regular waves.

Sources	No. of cases	Bed condition	Apparatus
Horikawa and Kuo (1966)	213	plane and stepped beach	small-scale
Nadaoka et al. (1982)	2	plane beach	small-scale
Kajima et al. (1983)	79	sandy beach	large-scale
Nagayama (1983)	12	plane, stepped and barred beach	small-scale
Hansen and Svendsen (1984)	1	plane beach	small-scale
Shibayama and Horikawa (1985)	10	sandy beach	small-scale
Okayasu et al.(1988)	10	plane beach	small-scale
Sato et al. (1988)	3	plane beach	small-scale
Sato et al. (1989)	2	plane beach	small-scale
Hurue (1990)	1	plane beach	small-scale
Smith and Kraus (1990)	101	plane and barred beach	small-scale
SUPERTANK project (Kraus and Smith, 1994)	57	sandy beach	large-scale
Cox and Kobayashi (1997)	1	plane beach	small-scale
Total	492		

Table 4.3b: Summary of collected experimental data of irregular waves.

Sources	No. of cases	Bed condition	Apparatus
Thornton and Guza (1986)	4	sandy beach	field
Hurue (1990)	1	plane beach	small-scale
Smith and Kraus (1990)	12	plane and barred beach	small-scale
DELILAH Project (Smith et al., 1993)	4	sandy beach	field
SUPERTANK project (Kraus and Smith, 1994)	128	sandy beach	large-scale
LIP 11D project (Roelvink and Reniers,1995)	95	sandy beach	large-scale
Sultan (1995)	1	plane beach	small-scale
MAST III - SAFE project (Dette et al.,1998)	138	sandy beach	large-scale
Grasmeijer and Rijn (1999)	2	sandy beach	small-scale
Total	385		

4.2.1 Energy dissipation for regular breaking waves

A number of works on theoretical and experimental studies have been performed to draw a clearer picture of the energy dissipation rate, D_B. During the past few decades, various models have been proposed for computing the energy dissipation rate (D_B). Widely used concepts for computing energy dissipation rate (D_B) are the bore concept and the stable energy concept. Several researchers have proposed slightly different forms of the energy dissipation rate. Some brief reviews of the models based on these two concepts are described as follows.

4.2.1.1 Bore concept

This concept was proposed by Le Mahaute (1962), based on the similarity between the breaking wave and the hydraulic jump. The average rate of energy dissipation of bore concept can be calculated as

$$D_B = \frac{1}{4}\rho g \frac{(h_2 - h_1)^3}{h_1 h_2} Q \tag{4.21}$$

where h_1 is the lower conjugate depth (see Fig. 4.1 for definition sketch), h_2 is the higher conjugate depth, Q is the volume discharge per unit area across the bore which is equal to ch/L or h/T (Hwang and Divoky, 1970), c is the phase velocity, h is the mean water depth, L is the wavelength, and T is the wave period.

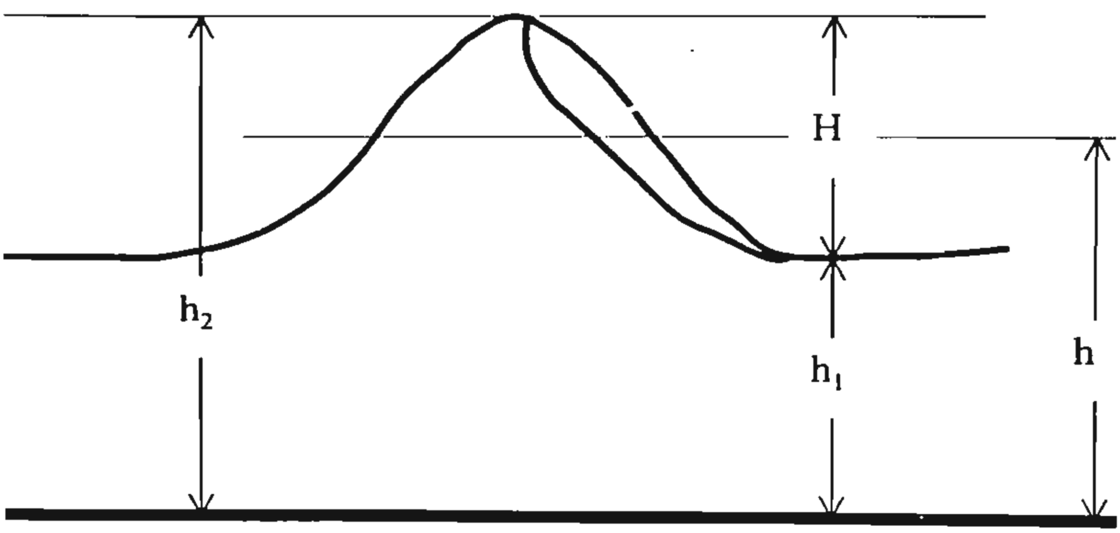

Figure 4.1: Definition sketch of the bore concept.

Substituting $Q = h/T$ and $h_2 - h_1 = H$ into Eq. (4.21), the dissipation model of bore concept can be written as

$$D_B = \frac{1}{4}\frac{\rho g h H^3}{T h_1 h_2} \tag{4.22}$$

Several researchers have proposed slightly different forms of the dissipation model based on this assumption. The following models were developed based on the bore concept.

a) Battjes and Janssen (1978) developed the dissipation model from the bore concept by assuming that $h_1 h_2 = h^2$ and $H/h = 1$. Therefore Eq. (4.22) is modified to be

$$D_B = C_1 \frac{\rho g H^2}{4T} \tag{4.23}$$

where C_1 is the empirical coefficient introduced to account for the difference between a breaking wave and hydraulic jump. The proposed value of C_1 is 1.00.

b) Thornton and Guza (1983) proposed a refinement of Battjes and Janssen's (1978) formula by assuming that $h_1 h_2 = h^2$ in Eq. (4.22). Therefore the general form of the energy dissipation rate can be expressed as

$$D_B = C_2 \frac{\rho g H^3}{4Th} \tag{4.24}$$

where C_2 is the empirical coefficient. The proposed value of C_2 is 0.51 for the laboratory.

c) Deigaard et al. (1991) developed the formula to express the rate of energy dissipation of a broken wave. The energy dissipation is expressed through the energy loss in a bore. They assumed that $h_1 = h - (H/2)$ and $h_2 = h + (H/2)$. Therefore Eq. (4.22) is modified to be

$$D_B = C_3 \frac{\rho g h H^3}{T(4h^2 - H^2)} \tag{4.25}$$

where C_3 is the empirical coefficient. The proposed value of C_3 is 1.00.

4.2.1.2 Stable energy concept

a) Dally et al. (1985) assumed that the energy dissipation rate is proportional to the difference between the local energy flux and the stable energy flux, divided by the water depth as

$$D_B = \frac{C_4}{h}\left[E c_g - E_s c_g\right] \tag{4.26}$$

where C_4 is the decay coefficient, $E_s = \rho g H_s^2/8$ is the stable wave energy, and H_s is the stable wave height. Dally et al. (1985) proposed to compute the stable wave height (H_s) as a function of water depth as

$$H_s = 0.4h \tag{4.27}$$

Substituting $E = \rho g H^2/8$, $E_s = \rho g H_s^2/8$, and $H_s = 0.4h$ into Eq. (4.26), the dissipation rate can be written as

$$D_B = C_4 \frac{c_g \rho g}{8h}\left[H^2 - (0.4h)^2\right] \tag{4.28}$$

The proposed coefficient C_4 is 0.15.

b) Rattanapitikon and Shibayama (1998) assumed that the energy dissipation rate is proportional to the difference between the energy per unit width (EL) and the stable energy per unit width ($E_s L$), divided by the local water depth and wave period as

$$D_B \propto \frac{[EL - E_s L]}{hT} \tag{4.29}$$

or $$D_B = C_5 \frac{L}{hT}[E - E_s] = C_5 \frac{c}{h}[E - E_s] \tag{4.30}$$

where C_5 is the proportional constant. Rewriting Eq. (4.30) in terms of wave height yields

$$D_B = C_5 \frac{c \rho g}{8h}\left[H^2 - H_s^2\right] \tag{4.31}$$

The stable wave height (H_s) was proposed to be

$$H_s = h \exp\left(-0.36 - 1.25 \frac{h}{\sqrt{LH}}\right) \tag{4.32}$$

Substituting Eq. (4.32) into Eq. (4.31) the dissipation rate becomes

$$D_B = C_5 \frac{c \rho g}{8h}\left[H^2 - \left(h \exp\left(-0.36 - 1.25 \frac{h}{\sqrt{LH}}\right)\right)^2\right] \tag{4.33}$$

The proposed value of C_5 is 0.15.

4.2.1.3 Model Calibrations and Comparisons

Since some dissipation models were developed with limited experimental conditions, the coefficients in those models may not be the optimal values for a wide range of experimental conditions. Therefore the re-calibrations of the coefficients in the 5 models are performed before examining the validity of the models. However, the value of dissipation rate D_B could not be measured directly from the experiment. In order to determine the proper coefficients $C_1 - C_5$, Eqs. (4.23), (4.24), (4.25), (4.28), and (4.33) are calibrated by using the measured regular wave heights inside the surf zone.

The computed wave heights can be determined from the energy flux conservation (Eq. 2.1). Substituting $E = \rho g H^2/8$ into Eq. (2.1), the energy flux conservation can be written in the term of wave height as

$$\frac{\rho g}{8}\frac{\partial(H^2 c_g \cos\theta)}{\partial x} = -D_B \tag{4.34}$$

The computed wave heights are determined from Eq. (4.34), by substituting the expression of D_B (Eqs. 4.23, 4.24, 4.25, 4.28, and 4.33) and numerical integration from breaking point to shoreline. The measured regular wave heights from 13 sources (totally 492 cases) of published experimental results have been used in this section (see Table 4.3a). The experiments are divided into 2 groups based on the experiment scale, i.e., small-scale and large-scale experiments.

In this study, the basic parameter for determination of the accuracy of a model is the root mean square (rms) relative error, which is defined as

$$ER_g = 100\sqrt{\frac{\sum_{i=1}^{ng}(H_{ci} - H_{mi})^2}{\sum_{i=1}^{ng} H_{mi}^2}} \tag{4.35}$$

where ER_g is the rms relative error of the data group, i is the wave height number, H_{ci} is the computed wave height of number i, H_{mi} is the measured wave height of number i, and ng is the total number of measured wave heights in each data group. The average error (ER_{avg}) is defined as

$$ER_{avg} = \frac{\sum_{j=1}^{tn} ER_{gj}}{tn} \tag{4.36}$$

where j is the group number, tn is the total number of groups, and ER_{gj} is the rms relative error of the group number j. The small value of average error (ER_{avg}) represents a good accuracy of the model. The average error is used to judge the applicability of the model.

The calibration of each dissipation model is conducted by varying the empirical coefficient (C) in each dissipation model until the minimum average error (ER_{avg}) between the measured and computed wave height is obtained.

The calibrated coefficients $C_1 - C_5$ are summarized in the second column of Table 4.4. Using the calibrated coefficients, the errors (ER_g and ER_{avg}) of each model have been computed and shown in Table 4.4. The results can be summarized as follows.

a) The accuracy of models for general cases in descending order are Rattanapitikon and Shibayama (1998), Dally et al. (1985), Deigaard et al. (1991), Thornton and Guza (1983), and Battjes and Janssen (1978).

b) Overall, the stable energy concept gives better prediction than that of bore concept.

c) The errors of most models (except Battjest and Janssen, 1978) for small-scale wave flume are nearly the same as that of large-scale wave flume. It means that those models may not have scale effect.

d) The model proposed by Battjes and Janssen (1978) gives quite large error ($ER > 25$) for all conditions. It may not be suitable for using. The model may be too much simplified.

e) The model of Rattanapitikon and Shibayama (1998) gives the best prediction for all conditions.

Table 4.4: The error ER_g for 2 groups of experiment scales, and ER_{avg} of each model comparing with regular wave data shown in Table 4.3a.

Models	Coeff. C	ER_g		ER_{avg}
		Small-scale (356 cases)	Large-scale (136 cases)	
Battjes and Janssen, 1978 (Eq. 4.23)	C_1 = 0.48	34.7	48.7	41.7
Thornton and Guza, 1983 (Eq. 4.24)	C_2 = 0.68	22.3	25.8	24.0
Deigaard et al., 1991 (Eq. 4.25)	C_3 = 0.49	23.3	23.0	23.1
Dally et al., 1985 (Eq. 4.28)	C_4 = 0.15	17.3	20.2	18.7
Rattanapitikon and Shibayama, 1998 (Eq. 4.33)	C_5 = 0.15	16.3	16.6	16.4

4.2.2 Energy dissipation for irregular breaking waves

Irregular wave breaking is more complex than regular wave breaking. In contrast to regular waves there is no well-defined breaking point for irregular waves. The highest waves tend to break at greatest distances from the shore. Thus, the energy dissipation of irregular waves occurs over a considerably greater area than that of regular waves. Much work has been done on the energy dissipation. Three main approaches have been proposed for describing the energy dissipation of irregular waves, i.e., probabilistic approach, spectral approach, and parametric approach (Hamm et al., 1993). The probabilistic and spectral approaches are computationally intensive and may not suitable to use in the beach deformation model. Therefore this section focuses only on the models in parametric approach because of their computation efficiency. This approach relies on the macroscopic features of breaking waves and predicts only the transformation of rms wave height.

The energy dissipation rate in the parametric approach is described by combining an energy dissipation of a single broken wave with a parametric description of the wave height distribution. Widely used concept in the parametric approach was proposed by Battjes and Janssen (1978). Several researchers have proposed slightly different forms of the energy dissipation rate. The main differences are the probability density function of breaking wave height, the dissipation formula of a broken wave and the breaking wave height formula. The brief reviews of selected 6 dissipation models are described as follows.

a) Battjes and Janssen (1978) proposed to compute D_B by multiplying the fraction of irregular breaking waves (Q_b) by the energy dissipation of a single broken wave. The energy dissipation of a broken wave is described by the bore analogy and assuming that all broken waves have a height equal to breaking wave height (H_b).

$$D_B = C_6 \frac{Q_b \rho g H_b^2}{4T_p} \tag{4.37}$$

where T_p is the peak period of the wave spectrum, C_6 is the coefficient and the published value of C_6 is 1.0.

The fraction of breaking waves, Q_b, was derived based on the assumption that the shape of probability distribution function of non-broken wave inside the surf zone is Rayleigh distribution.

$$\frac{1-Q_b}{-\ln Q_b} = \left(\frac{H_{rms}}{H_b}\right)^2 \tag{4.38}$$

The breaking wave height is determined from a Miche's (1944) criterion with an adjustable coefficient. After calibration, the breaking wave height was suggested to be

$$H_b = \frac{0.88}{k_p}\tanh(0.91k_p h) \tag{4.39}$$

where k_p is the wave number related to T_p.

Since Eq. (4.38) is an implicit equation, the iteration process is necessary to compute the fraction of breaking waves, Q_b. Quicker method is possible by using the explicit formula of Rattanapitikon and Shibayama (1998), i.e.,

$$Q_b = \begin{cases} 0 & for\ \dfrac{H_{rms}}{H_b} \le 0.43 \\ -0.738\left(\dfrac{H_{rms}}{H_b}\right) - 0.280\left(\dfrac{H_{rms}}{H_b}\right)^2 + 1.785\left(\dfrac{H_{rms}}{H_b}\right)^3 + 0.235 & for\ \dfrac{H_{rms}}{H_b} > 0.43 \end{cases} \tag{4.40}$$

Since Eqs. (4.38) and (4.40) give almost identical results (correlation coefficient R^2 = 0.999), only Eq. (4.40) is used in this study.

b) Thornton and Guza (1983) proposed to compute D_B by integrating from 0 to ∞ of the product of the dissipation for a single broken wave of height H and the probability of wave breaking at that height. The energy dissipation of a single broken wave is described by the bore analogy. The probability density function of breaking wave height is expressed as weighting of the Rayleigh distribution.

$$D_B = C_7 \frac{3\sqrt{\pi}}{4}\left(\frac{H_{rms}}{0.42h}\right)^2 \left\{1 - \frac{1}{\left[1 + (H_{rms}/0.42h)^2\right]^{2.5}}\right\} \frac{\rho g H_{rms}^3}{4T_p h} \tag{4.41}$$

where C_7 is the coefficient introduced to account for the different between breaking wave and hydraulic jump. The published value of C_7 for laboratory is 0.51.

c) Battjes and Stive (1984) used the same energy dissipation model as Battjes and Janssen (1978).

$$D_B = K_{18} \frac{Q_b \rho g H_b^2}{4T_p} \tag{4.42}$$

where C_8 is the coefficient (the published value of C_8 is 1.0), and Q_b is computed from Eq. (4.38) or Eq. (4.40). Battjes and Stive (1984) modified the breaking wave height formula to be

$$H_b = \frac{0.88}{k_p}\tanh\left\{\left[0.57 + 0.45\tanh\left(33\frac{H_{rmso}}{L_{op}}\right)\right]k_p h\right\} \tag{4.43}$$

where H_{rmso} is the deepwater rms wave height and L_{op} is the deepwater wavelength related to T_p.

Hence the model of Battjes and Stive (1984) is similar to that of Battjes and Janssen (1978), except the formula of H_b.

d) Southgate and Nairn (1993) modified the model of Battjes and Janssen (1978) by changing the expression of energy dissipation of a broken wave.

$$D_B = C_9 \frac{Q_b \rho g H_b^3}{4T_p h} \tag{4.44}$$

where C_9 is the coefficient (the published value of C_9 is 1.0), and Q_b is computed from Eq. (4.38) or Eq. (4.40). The breaking wave height is determined from the formula of Nairn (1990).

$$H_b = h\left[0.39 + 0.56\tanh\left(33\frac{H_{rmso}}{L_{op}}\right)\right] \tag{4.45}$$

e) Baldock et al. (1998) proposed to compute D_B by integrating from H_b to ∞ of the product of the dissipation for a single broken wave of height H and the probability of that wave height occurring. The energy dissipation of a single broken wave is described by the bore analogy. The probability density function of wave height was assumed to be the Rayleigh distribution.

$$D_B = C_{10}\exp\left[-\left(\frac{H_b}{H_{rms}}\right)^2\right]\frac{\rho g\left(H_b^2 + H_{rms}^2\right)}{4T_p} \qquad \text{for } H_{rms} < H_b \tag{4.46}$$

In the saturated surf zone $(H_{rms} \geq H_b)$, H_{rms} is set to be equal to H_b. The published coefficient C_{10} is 1.0. The breaking wave height (H_b) is determined from the formula of Nairn (1990) as shown in Eq. (4.45).

f) Rattanapitikon and Shibayama (1998) modified the model of Battjes and Janssen (1978) by changing the expression of energy dissipation of a broken wave from the bore concept to be the stable energy concept.

$$D_B = C_{11}\frac{Q_b c_p \rho g}{8h}\left[H_{rms}^2 - \left(h\exp(-0.58 - 2.00\frac{h}{\sqrt{L_p H_{rms}}})\right)^2\right] \tag{4.47}$$

where C_{11} is the coefficient (the published value of C_{11} is 0.1), L_p is the wavelength related to T_p, and Q_b is the computed from Eq. (4.38) or Eq. (4.40). The breaking wave height (H_b) is computed by using breaking criterion of Goda (1970).

$$H_b = 0.1L_{op}\left\{1 - \exp\left[-1.5\frac{\pi h}{L_{op}}\left(1 + 15m_a^{4/3}\right)\right]\right\} \tag{4.48}$$

where m_a is the average bottom slope.

4.2.2.1 Model calibrations and comparisons

The value of dissipation rate D_B could not be measured directly from the experiment. In order to determine the proper coefficients $C_6 - C_{11}$, Eqs. (4.37), (4.41), (4.42), (4.44), (4.46) and (4.47) are calibrated by using the measured irregular wave heights. Only the measured wave heights inside the surf zone should be used in the calibration. However the surf zone of irregular waves could not be clearly defined. Therefore all measured wave heights (from offshore to shoreline) are used in this section. The computed wave heights are determined from the energy flux conservation (Eq. 2.1). From linear wave theory, the wave energy density (E) is equal to $\rho g H_{rms}^2/8$. Therefore, Eq. (2.1) can be written in the term of wave height as

$$\frac{\rho g}{8}\frac{\partial(H_{rms}^2 c_{gp}\cos\theta)}{\partial x} = -D_B \tag{4.49}$$

where c_{gp} is the group velocity related to T_p.

Snell's law is applied to describe wave refraction as

$$\frac{\sin\theta}{c_p} = \text{constant} \tag{4.50}$$

where c_p is the phase velocity related to T_p.

The computed wave heights are determined from Eq. (4.49), by substituting the expression of D_B (Eqs. 4.37, 4.41, 4.42, 4.44, 4.46 and 4.47) and numerical integration from offshore to shoreline.

The measured irregular wave heights from 9 sources of published experimental results (totally of 385 cases) have been used in this section. A summary of the collected experimental data is shown in Table 4.3b. The experiments are grouped into 3 groups based on the experiment scale, i.e., small-scale, large-scale, and field experiments.

Because some dissipation models were developed with limited experimental conditions, the coefficients in each model may not be the optimal values for a wide range of experimental conditions. Therefore the re-calibrations of the coefficients in the 6 models are performed before examining the validity of the models.

The calibration of each dissipation model is conducted by varying the empirical coefficient C in each dissipation model until the minimum average error (ER_{avg}) between the measured and computed wave height is obtained.

The calibrated coefficients $C_6 - C_{11}$ are summarized in the second column of Table 4.5. Using the calibrated coefficients, the errors (ER_g and ER_{avg}) of each model have been computed and shown in Table 4.5. The results can be summarized as follows.

a) The models developed by Battjes and Janssen (1978), Thornton and Guza (1983), Battjes and Stive (1984), Southgate and Nairn (1993), Baldock et al. (1998) give quite large error (ER_g > 15%) for field application.

b) The model of Rattanapitikon and Shibayama (1998) gives very good prediction for general cases.

Table 4.5: The error ER_g for 3 groups of experiment scales, and ER_{avg} of each model comparing with irregular wave data shown in Table 4.3b.

Models	Coeff. C	ER_g			ER_{avg}
		Small-scale (16 cases)	Large-scale (361 cases)	Field (8 cases)	
Battjes and Janssen, 1978 (Eq. 4.37)	C_6 = 1.2	11.0	10.0	17.6	12.9
Thornton and Guza, 1983 (Eq. 4.41)	C_7 = 0.22	12.9	12.1	18.6	14.5
Battjes and Stive, 1984 (Eq. 4.42)	C_8 = 1.0	8.7	7.1	18.8	11.6
Southgate and Nairn, 1993 (Eq. 4.44)	C_9 = 1.4	9.8	8.0	19.8	12.5
Baldock et al., 1998 (Eq. 4.46)	C_{10} = 0.9	12.0	7.3	21.1	13.5
Rattanapitikon and Shibayama, 1998 (Eq. 4.47)	C_{11} = 0.1	10.1	7.4	14.5	10.7

4.3 Undertow Models

From laboratory and field observations, it is well known that, water waves induce a steady drift of fluid particles (mass transport velocity) in additional to an oscillatory motion both for non-breaking and breaking waves. The pioneering experiment in this phenomenon was carried out in by Bagnold (1940).

Because of the additional mass flux caused by surface roller, the mass transport velocity induced by breaking waves, commonly referred to as <u>undertow</u>, is larger than that induced by non-breaking waves (Hansen and Svendsen, 1984).

The undertow velocity is important in the prediction of cross-shore suspended sediment transport rate. Dyhr-Nielsen and Sorensen (1970) were the first to give a qualitative analysis on the undertow. The undertow velocity can be computed by using momentum equation or eddy viscosity concept. In order to compute the undertow velocity accurately, the mean undertow velocity (vertically averaged from the bed to wave trough) should be known as the boundary condition. This section concentrates only on the comparison of the existing models for computing the mean undertow velocity induced by regular and irregular waves.

For computing the undertow velocity, the mean undertow velocity (depth average velocity) is an essential requirement. Widely used concept for computing mean undertow velocity (U_m) is the concept of Svendsen (1984b). Svendsen (1984b) proposed to separate the mean velocity (U_m) to be two components, one is due to the wave motion (U_w) and the other one due to the surface roller (U_r).

$$U_m = U_w + U_r \tag{3.15}$$

Various formulas for computing U_m have been suggested by the previous researchers. However, no direct literature has been published to describe clearly the applicability and accuracy of each formula. Therefore, the objective of this section is to investigate the performance of each formula based on wide range of the experimental data.

Published experimental data of undertow profiles from 9 sources, including 751 undertow profiles, have been collected for calibration of the present formulas. These include small-scale, large-scale and field experimental data obtained from a variety of wave and bottom conditions. A summary of the collected experimental data is given in Table 4.6 (Table 4.6a is for regular waves, and Table 4.6b is for irregular waves)

Table 4.6a: Summary of collected experimental data for regular breaking waves.

Sources	Apparatus	Bed condition	Wave condition	Total No. of cases	Total No. of profiles
Nadaoka et al. (1982)	small-scale	plane beach	regular	2	11
Hansen and Svendsen (1984)	small-scale	plane beach	regular	1	4
Okayasu et al. (1988)	small-scale	plane beach	regular	9	56
Cox et al. (1994)	small-scale	rough beach	regular	1	5
Total				13	76

Table 4.6b: Summary of collected experimental data for irregular breaking waves.

Sources	Apparatus	Bed condition	Wave condition	Total No. of cases	Total No. of profiles
Dette and Uliczka (1986)	large-scale	sandy beach	irregular	1	4
Okayasu and Katayama (1992)	small-scale	plane beach	irregular	1	6
SUPERTANK (1994)	large-scale	sandy beach	irregular	111	643
Shimisu and Ikeno (1996)	large-scale	sandy beach	irregular	4	14
Rodriguez et al. (1994)	field	sandy beach	irregular	2	8
Total				119	675

4.3.1 Mean undertow velocity induced by regular waves

4.3.1.1 Description of the models

From the previous studies, the following explicit formulas have been suggested to compute the mean undertow velocity induced by regular wave actions:

a) Svendsen (1984) proposed to separate the mean undertow velocity into two parts, one is due to wave motion and the other one due to surface roller. The following formula was suggested to compute U_m throughout the surf zone:

$$U_m = -k_{S1} B_o c \left(\frac{H}{h} \right)^2 - k_{S2} \frac{H^2}{Th} \tag{4.51}$$

where k_{S1} and k_{S2} are the coefficients. The published value of k_{S1} is 1.0, and k_{S2} is 0.9.

b) Stive and Wind (1986) proposed an empirical formula for computing the mean undertow velocity for entire surf zone as

$$U_m = -k_{W1} H \sqrt{\frac{g}{h}} - k_{W2} H \sqrt{\frac{g}{h}} \tag{4.52}$$

where k_{W1} and k_{W2} are the coefficients. The published value of $k_{W1} + k_{W2}$ is 0.1.

c) De Vriend and Stive (1987) used the same concept as Svendsen (1984) but different formula:

$$U_m = -k_{V1} \frac{gH^2}{8cd_t} - k_{V2} \frac{h}{L} \frac{gH^2}{8cd_t} \tag{4.53}$$

where k_{V1} and k_{V2} are the coefficients. The published value of k_{V1} is 1.0, and k_{V2} is 7.0.

d) Hansen and Svendsen (1987) modified Eq. (4.51) by introducing the new formula of U_r, i.e.,

$$U_m = -k_{H1} B_o c \left(\frac{H}{h} \right)^2 - k_{H2} \frac{cH}{h} \tag{4.54}$$

where k_{H1} and k_{H2} are the coefficients. The published value of k_{H1} is 0.7, and k_{H2} is 0.07

e) Rattanapitikon and Shibayama (2000a) re-analysis of the existing formulas and proposed to compute U_m from

$$U_m = -k_{RS1} \frac{B_o g H^2}{ch} - k_{RS2} b \frac{B_o c H}{h} \tag{4.55}$$

where k_{RS1} and k_{RS2} are the coefficients and b is the coefficient which expressed as

$$b = \begin{cases} 0 & \textit{offshore zone} \\ \dfrac{1/\sqrt{H} - 1/\sqrt{H_b}}{1/\sqrt{H_t} - 1/\sqrt{H_b}} & \textit{transition zone} \\ 1 & \textit{inner surf zone} \end{cases}$$

where subscript b indicates the value at the breaking point, and subscript t indicates the value at the transition point.

4.3.1.2 Comparison of the models

It should be noted that the models of Svendsen (1984), Stive and Wind (1986), De Vriend and Stive (1987), and Hansen and Svendsen (1987) do not account the effect of transition zone. Trial simulations of the above 4 models (Eqs. 4.51-4.54) indicate that the models give poor estimations for the undertow in the transition zone. Therefore, the above 4 models (Eqs. 4.51-4.54) have been modified to include the influence of the transition zone by multiplying the formula of U_r by the coefficient b as in Eq. (4.55). Using the collected experimental data at the breaking point and inner surf zone, the existing 5 models (Eqs. 4.51-4.55) are re-calibrated to determine the best-fit coefficients in the models. The verification results are presented in term of rms relative error (ER) and summarized in Table 4.7. From Table 4.7, it is found that the coefficients in all models (Eqs. 4.51-4.55) are slightly differed from the published values and Eq. (4.55) shows the best prediction.

Table 4.7: Verification results of Eqs. (4.51)-(4.55) (measured data at the breaking point and inner surf zone from Nadaoka et al., 1982; Hansen and Svendsen, 1984; Okayasu et al., 1988; and Cox et al., 1994).

Formulas	Best-fit coefficients		ER
	k_{n1}	k_{n2}	
Svendsen (Eq. 4.51): $U_m = -k_{S1} B_o c \left(\frac{H}{h}\right)^2 - k_{S2} b \frac{H^2}{Th}$	$k_{S1} = 1.00$	$k_{S2} = 1.79$	30.8
Stive and Wind (Eq. 4.52): $U_m = -k_{W1} H \sqrt{\frac{g}{h}} - k_{W2} bH \sqrt{\frac{g}{h}}$	$k_{W1} = 0.05$	$k_{W2} = 0.10$	21.3
DeVriend and Stive (Eq. 4.53): $U_m = -k_{V1} \frac{gH^2}{8cd_t} - k_{V2} b \frac{h}{L} \frac{gH^2}{8cd_t}$	$k_{V1} = 0.42$	$k_{V2} = 10.81$	36.9
Hansen and Svendsen (Eq. 4.54): $U_m = -k_{H1} B_o c \left(\frac{H}{h}\right)^2 - k_{H2} b \frac{cH}{h}$	$k_{H1} = 0.83$	$k_{H2} = 0.10$	20.7
Rattanapitikon and Shibayama (Eq. 4.55): $U_m = -k_{RS1} \frac{B_o g H^2}{ch} - k_{RS2} b \frac{B_o c H}{h}$	$k_{RS1} = 0.76$	$k_{RS2} = 1.12$	20.1

4.3.2 Mean undertow velocity induced by irregular waves

Irregular wave breaking is more complex than regular wave breaking. The highest wave tends to break at greatest distance from the shore. Since the width of surf zone and the transition zone varies with each individual wave, the influence of the transition zone is not significantly observed in the irregular wave surf zone (Nairn et al., 1990). To make the formula simple, most of the models exclude the influence of the transition zone.

4.3.2.1 Description of the models

From the previous studies, the following explicit formulas have been suggested to compute the mean undertow velocity induced by irregular wave actions:

a) Rodriguez et al. (1994) modified the formula of De Vriend and Stive (1987) to predict the mean undertow velocity induced by irregular wave actions:

$$U_m = -k_{R1}\frac{gH_{rms}^2}{8cd_t} - k_{R2}Q_b\frac{h}{L}\frac{gH_{rms}^2}{8cd_t} \qquad (4.56)$$

where Q_b is the fraction of breaking wave which is computed from Eqs. (2.55) and (2.56), k_{R1} and k_{R2} are the coefficients. The published value of k_{R1} is 1.0, and k_{R2} is 7.0.

b) Grasmeijer and Van Rijn (1997) proposed:

$$U_m = -k_{G1}\sqrt{\frac{g}{h}}\frac{H_{rms}^2}{d_t} \qquad (4.57)$$

where k_{G1} is the coefficient. The published value of k_{G1} is 0.125.

c) Kennedy et al. (1998) proposed:

$$U_m = -k_{K1}\frac{\sqrt{gh}}{8}\left(\frac{H_{rms}}{h}\right)^2 \qquad (4.58)$$

where k_{K1} is the coefficient.

d) Present study (see section 3.2.2) modified our undertow model for regular wave for computing the undertow for irregular wave as

$$U_m = -k_{P1}\frac{gH_{rms}^2}{ch} - k_{P2}\frac{Q_b cH_{rms}}{h} \qquad (3.59)$$

where Q_b is the fraction of breaking wave which is computed from Eqs. (2.55) and (2.56), k_{P1} and k_{P2} are the coefficients. The published value of k_{P1} is 0.57, and k_{P2} is 0.5.

4.3.2.2 Re-calibration and comparison of the formulas

Using the collected experimental data at the breaking point and inner surf zone, the above 4 models (Eqs. 4.56-4.59) are re-calibrated to determine the best-fit coefficients in the models. The verification results are presented in term of *rms* relative error (ER) and summarized in Table 4.8. From Table 4.8, it is found that the coefficients in Eqs. (4.56) – (4.58) need to be slightly changed and Eq. (4.59) shows the best prediction.

Table 4.8: Verification results of Eqs. (4.56) – (4.59) (measured data from Dette and Uliczka, 1986; Okayasu and Katayama, 1992; SUPERTANK, 1994; Shimisu and Ikeno, 1996; and Rodriguez et al., 1994).

Formulas	Best-fit coefficients		ER
	k_{n1}	k_{n2}	
Rodriguez et al. (Eq. 4.56): $U_m = -k_{R1}\dfrac{gH_{rms}^2}{8cd_t} - k_{R2}Q_b\dfrac{h}{L}\dfrac{gH_{rms}^2}{8cd_t}$	$k_{R1} = 0.47$	$k_{R2} = 4.92$	56.1
Grasmeijer and Van Rijn (Eq. 4.57): $U_m = -k_{G1}\sqrt{\dfrac{g}{h}}\dfrac{H_{rms}^2}{d_t}$	$k_{G1} = 0.09$	-	58.0
Kennedy et al. (Eq. 4.58): $U_m = -k_{K1}\dfrac{\sqrt{gh}}{8}\left(\dfrac{H_{rms}}{h}\right)^2$	$k_{K1} = 1.20$	-	47.0
Rattanapitikon and Shibayama (Eq. 4.59): $U_m = -k_{P1}\dfrac{gH_{rms}^2}{ch} - k_{P2}\dfrac{Q_bcH_{rms}}{h}$	$k_{P1} = 0.57$	$k_{P2} = 0.50$	42.6

Chapter 5: CONCLUSIONS

Based on a large amount of published experimental results covering a wide range of test conditions under regular irregular wave actions, simple models are developed for computing the breaker wave height, wave height transformation, and undertow profile. The following is the summary of the conclusions of the present study.

1. Data from small scale, large scale, and field experiments in a total of 41 sources were collected and utilized in development of the present models (see Table 5.1).

2. A total of 574 cases from 24 sources of published experimental results were used to develop the new breaker height formulas. The experimental data cover wide range of wave and bottom conditions ($0.001 \leq H_o / L_o \leq 0.100$, and $0 \leq m \leq 0.44$). The development of the present formulas was separated into two stages. Firstly, the measured data of breaking waves on the horizontal slope were analyzed to identify the basic forms of breaker indices. After that, based on the measured data of the breaking waves on various bottom slopes, the equations of bottom slope effect were derived and explicitly included into the basic formulas. The present formulas were examined against the measured data. The examination results were presented in terms of root mean square relative error (ER). It was found that the present formulas predict well for wide range of wave and bottom slope conditions. The error ER of the present formula is 10.8%. As mention before that the validity of empirical formulas may be limited according to the range of experimental conditions that used in the calibrations or verifications. The use of the present formula become questionable for the beaches having slope greater than 0.44 and for the deepwater wave steepness greater than 0.1.

3. For the wave model: the wave height transformation from offshore to shoreline is computed from the energy flux conservation. To solve the energy flux conservation, the energy dissipation model should be known. The energy dissipation model for regular breaking waves was developed based on the analysis of energy dissipation models of previous researchers. The energy dissipation model for irregular breaking waves was developed based on the parametric approach and the present regular breaking wave model. The models were examined using published experimental data from 13 sources (638 wave profiles in total). For regular wave conditions, the model was verified by using small and large scale laboratory data. The average rms relative error by the present regular wave model is 15.8 %. For irregular wave conditions, the model was capable in simulating the increase in rms wave height due to shoaling and subsequent decrease due to wave breaking over wide range of

wave conditions and various shapes of beach profiles. The validity of model was confirmed by small and large scale laboratory and field data. The average rms relative error of the present irregular wave model is 10.1 %.

4. A simple explicit model was developed to compute undertow profile induced by regular breaking waves and then applied to the irregular breaking waves. The main formula of undertow profile was derived from the eddy viscosity model. In solving the eddy viscosity model, the expression of τ / ν_t should be known. The ratio of shear stress and eddy viscosity coefficient (τ / ν_t) was proposed as a function of energy dissipation rate of a broken wave. The validity of proposed formulas (for determining the shape of undertow) were calibrated using the published experimental data from 9 sources (751 undertow profiles in total). The present model gives reasonably well estimations of the undertow profiles above the bottom boundary layers. The rms relative error, ER, of the proposed formulas for regular and irregular are 15% and 21%, respectively.

5. A total of 574 breaker heights from 24 sources of published experimental results were used to examine and compare the accuracy of the 24 existing breaker height formulas. Comparisons were made of overall accuracy as well as the accuracy within different ranges of bottom slope. It was found that the present formula gives the best overall predictions.

6. A total of 877 wave profiles from 19 sources of published experimental results were used to calibrate and compare the accuracy of 11 existing dissipation models (5 for regular waves and 6 for irregular waves). The experimental data cover a wide range of wave and beach conditions. The calibration of each model was conducted by varying the empirical coefficients in each model until the minimum error ER, between the measured and computed wave heights, is obtained. Using the calibrated coefficients, the errors ER of each model for various conditions were computed and compared. The comparisons show that the present models give the minimum error for all conditions.

7. A total of 751 undertow profiles from 9 sources of published experimental results were used to calibrate and compare the accuracy of 9 models of mean undertow velocity (5 for regular waves and 4 for irregular waves). The calibration of each model was conducted by varying the empirical coefficients in each model until the minimum error ER, between the measured and computed mean velocity, is obtained. It was found that the present model gives the best predictions.

Table 5.1: Sources and number of collected data for present study.

No	Sources	H_b	H_{reg}	H_{irr}	u_{reg}	u_{irr}
1	Cox et al. (1994)				5	
2	Cox and Kobayashi (1997)		1			
3	Dette et al. (1998); MAST III - SAFE			138		
4	Dette and Uliczka (1986)					4
5	Galvin (1969)	19				
6	Grasmeijer and Rijn (1999)			2		
7	Hansen and Svendsen (1979)	17				
8	Hansen and Svendsen (1984)		1		4	
9	Hattori and Aono (1985)	3				
10	Horikawa and Kuo (1966)	158	213			
11	Hurue (1990)		1	1		
12	Hwung et al. (1992)	2				
13	Iversen (1952)	63				
14	Iwagaki et al. (1974)	39				
15	Kajima et al. (1983)		79			
16	Kraus and Smith (1994); SUPERTANK		57	128		643
17	Maruyama et al. (1983)	1				
18	Mizuguchi (1980)	1				
19	Nadaoka et al. (1982)	12	2		11	
20	Nagayama (1983)	12	12			
21	Okayasu et al. (1986)	2				
22	Okayasu et al. (1988)	10	10		56	
23	Okayasu and Katayama (1992)					6
24	Ozaki et al. (1977)	20				
25	Rodriguez et al. (1994)					8
26	Roelvink and Reniers (1995); LIP 11D			95		
27	Saeki and Sasaki (1973)	2				
28	Sato et al. (1988)	3	3			
29	Sato et al. (1989)	2	2			
30	Sato et al. (1990)	7				
31	Shibayama and Horikawa (1985)		10			
32	Shimisu and Ikeno (1996)					14
33	Singamsetti and Wind (1980)	95				
34	Smith and Kraus (1990)	80	101	12		
35	Smith et al. (1993); DELILAH			4		
36	Stive (1984)	2				
37	Sultan (1995)			1		
38	Thornton and Guza (1986)			4		
39	Ting and Kirby (1994)	2				
40	Visser (1982)	7				
41	Walker (1974)	15				
	Total	574	492	385	76	675

REFERENCES

[1] Bagnold, R.A. (1940). Beach formation by waves: some model experiments in wave tank, J. Ins. Civil Eng., Vol. 15, pp. 27-52.

[2] Baldock, T.E., Holmes, P., Bunker, S. and Van Weert, P. (1998). Cross-shore hydrodynamics within an unsaturated surf zone, Coastal Engineering, Vol. 34, pp. 173-196.

[3] Basco, D.R. and Yamashita, T. (1986). Toward a simple model of wave breaking transition region in surf zones, Proc. 20th Coastal Engineering Conf., ASCE, pp. 955-970.

[4] Battjes, J.A. and Janssen, J.P.F.M. (1978). Energy loss and set-up due to breaking of random waves, Proc. 16th Coastal Engineering Conf., ASCE, pp. 569-589.

[5] Battjes, J.A. and Stive M. J. F. (1984). Calibration and verification of a dissipation model for random breaking waves, Proc. 19th Coastal Engineering Conf., ASCE, pp. 649-660.

[6] Battjes, J.A. and Stive, M.J.F. (1985). Calibration and verification of a dissipation model for random breaking waves, J. Geophysical Research, Vol. 90, C5, pp. 9159-9167.

[7] Black, K.P. and Rosenberg, M.A. (1992). Semi-empirical treatment of wave transformation outside and inside the breaker line, Coastal Engineering, Vol. 16, pp. 313-345.

[8] Bowen, A.J., Inman, D.L. and Simmons, V.P. (1968). Wave set-down and set-up, J. Geophysical Research, Vol. 73, No. 8, pp. 2569-2577.

[9] Collins, J.I. and Weir, W. (1969). Probabilities of wave characteristics in the surf zone, Tetra Tech. Report, TC-149, Pasadena, California, USA.

[10] Collins, J.I. (1970). Probabilities of breaking wave characteristics, Proc. 12nd Coastal Engineering Conf., ASCE, pp. 399-414.

[11] Cox, D.T., Kobayashi, N., and Okayasu, A. (1994). Vertical variations of fluid velocities and shear stress in surf zones, Proc. 24th Coastal Engineering Conf., ASCE, pp. 98-112.

[12] Cox, D.T. and Kobayashi, N. (1997). Kinematic undertow model with logarithmic boundary layer, J. Waterways, Port, Coastal, and Ocean Eng., Vol. 123, No. 6, pp. 354-360.

[13] Dally, W.R., Dean, R.G., and Dalrymple, R.A. (1985). Wave height variation across beach of arbitrary profile, J. Geophysical Research, Vol. 90, No. C6, pp. 11917-11927.

[14] Dally, W.R. (1992). Random breaking waves: Field verification of a wave-by-wave algorithm for engineering application, Coastal Engineering, Vol. 16, pp. 369-397.

[15] Danel, P. (1952). On the limiting clapotis, Gravity Waves, U.S. Dept. of Commerce, National Bureau of Standards, Circular 521, pp. 35-45.

[16] Dean, R. and Dalrymple, R.A. (1984). Water Wave Mechanics for Engineers and Scientists, Prentice-Hall, Inc., New Jersey.

[17] Deigaard, R., and Fredsoe, J. (1991). Modelling of undertow by a one-equation turbulence model, Coastal Engineering, No. 15, pp. 431-458.

[18] Dette, H.H. and Uliczka, K. (1986). Velocity and sediment concentration field. Proc. 20th Coastal Engineering Conf., ASCE, pp. 1062-1076.

[19] Dette, H.H, Peters, K. and Newe, J. (1998). MAST III – SAFE Project: Data documentation, Large wave flume experiments '96/97, Report No. 825 and 830, Leichtweiss-Institute, Technical University Braunschweig.

[20] De Vriend, H.J. and Stive, M.J.F. (1987). Quasi-3D modelling of nearshore currents. Coastal Engineering, Vol. 11, pp. 565-601.

[21] Duncan J.H. (1981). An experimental investigation of breaking waves produced by a towed hydrofoil, Proc. Royal Soc. London, Ser. A 377, pp. 331-348.

[22] Dyhr-Nielsen, M. and Sorensen, T. (1970). Sand transport phenomena on coasts with bars, Proc. 12th Coastal Engineering Conf., ASCE, pp. 855-866.

[23] Ebersole, B. A. (1987). Measurement and prediction of wave height decay in the surf zone, Proc. Coastal Hydrodynamics '87, ASCE, pp. 1-16.

[24] Fredsoe, J., and Deigaard, R. (1992). Mechanics of Coastal Sediment Transport, Adv. Series on Ocean Eng. Vol. 3, World Scientific, USA.

[25] Galvin, C.J. (1969). Breaker travel and choice of design wave height, J. Waterways and Harbors Division, ASCE, Vol. 95, No. WW2, pp.175-200.

[26] Goda, Y. (1964). Rept. Port and Harbor Res. Inst., No. 8.

[27] Goda, Y. (1970). A synthesis of breaker indices, Trans. JSCE, Vol. 2, pp. 227-230.

[28] Goda, Y. (1974). New wave pressure formula for composite breakwater, Proc. 14th Coastal Engineering Conf., ASCE, pp. 1702-1720.

[29] Gourlay, M.R. (1978). Wave Generated Currents, Ph.D. Thesis, Dept. of Civil Eng., University of Queensland.

[30] Gourlay, M.R. (1992). Wave set-up, wave run-up and beach water table: Interaction between surf zone hydraulics and groundwater hydraulics, Coastal Engineering, Vol. 17, pp. 93-144.

[31] Grasmeijer, B.T. and Van Rijn, L.C. (1999). Transport of fine sands by currents and waves. III: breaking waves over barred profile with ripples, J. Waterways, Port, Coastal, and Ocean Eng., Vol. 125, No. 2, pp. 71-79.

[32] Hamm, L., Madsen, P.A. and Peregrine, D.H. (1993). Wave transformation in the nearshore zone: a review, Coastal Engineering, Vol. 21, pp. 5-39.

[33] Hamada, T. (1963). Breakers and beach erosion, Port and Harbor Research Institute, Ministry of Transportation, Japan.

[34] Hansen, J.B. and Svendsen, I.A. (1979). Regular waves in shoaling water experimental data, Series paper No. 21, Institute of Hydrodynamics and Hydraulic Eng., Technical University of Denmark, Denmark.

[35] Hansen, J.B., and Svendsen, I.A. (1984). A theoretical and experiment study of undertow, Proc. 19th Coastal Engineering Conf., ASCE, pp. 2246-2262.

[36] Hansen, J.B. and Svendsen, I.A. (1987). Surf zone breakers with current, Nonlinear Water Waves, IUTAM Symposium, Tokyo/Japan, pp. 169-177.

[37] Hansen, J.B. (1990). Periodic waves in the surf zone: Analysis of experimental data, Coastal Engineering, Vol. 14, No. 1, pp. 19-41.

[38] Hattori, M. and Aono, T. (1985). Experimental study on turbulence structures under breaking waves, Coastal Engineering in Japan, Vol. 28, pp. 97-116.

[39] Horikawa, K. and Kuo, C.T. (1966). A study of wave transformation inside the surf zone, Proc. 10th Coastal Engineering Conf., ASCE, pp. 217-233.

[40] Hwang, L.S. and Divoky, D. (1970). Breaking wave setup and decay on gentle slopes, Proc. 12th Coastal Engineering Conf., ASCE, pp. 377-389.

[41] Hwung, H.H., Chyan, J.M. and Chung, Y.C. (1992). Energy dissipation and air bubbles mixing inside surf zone, Proc. 23rd Coastal Engineering Conf., ASCE, pp. 308-321.

[42] Hurue, M. (1990). Two-Dimensional Distribution of Undertow due to Irregular Waves, Bach. Thesis, Dept. of Civil Eng., Yokohama National University, Japan.

[43] Iversen, H.W. (1952). Laboratory study of breakers, Gravity Waves, Circular 52, US Bureau of Standards, pp. 9-32.

[44] Iwagaki, Y., Sakai, T., Tsukioka, K. and Sawai, N. (1974). Relationship between vertical distribution of water particle velocity and type of breakers on beaches, Coastal Engineering in Japan, JSCE, Vol. 17, pp. 51-58.

[45] Jen, Y. and Lin, P.M. (1970). Plunging wave pressures on a semi-cylindrical tube, Proc. 12nd Coastal Engineering Conf., ASCE, pp. 1469-1490.

[46] Kajima, R., Shimizu, T., Maruyama, K. and Saito, S. (1983). On-offshore sediment transport experiment by using large scale wave flume. Collected data No. 1-8, Central Research Institute of Electric Power Industry, Japan (in Japanese).

[47] Kamphuis, J.W. (1991). Incipient wave breaking, Coastal Engineering, Vol. 15, pp. 185-203.

[48] Kamphuis, J.W. (1994). Wave height from deep water through breaking zone, J. of Waterway, Port, Coastal, and Ocean Eng., Vol. 120, No. 4, pp. 347-367.

[49] Karambas, Th. V. and Koutitas, C. 1992. A breaking wave propagation model based on the Boussinesq equations, Coastal Engineering, Vol. 18, pp. 1-19.

[50] Kennedy, D.L., Cox, D.T. and Kobayashi, N. (1998). Application of an undertow model to irregular waves on barred beaches and reflective coastal structures, Proc. 26th Coastal Engineering Conf., ASCE, pp. 311-324.

[51] Komar, P.D. and Gaughan, M.K. (1972). Airy wave theory and breaker height prediction, Proc. 13rd Coastal Engineering Conf., ASCE, pp. 405-418.

[52] Kraus, N.C., and Smith, J.M. (1994). SUPERTANK Laboratory Data Collection Project, Technical Report CERC-94-3, U.S. Army Corps of Engineers, Waterways Experiment Station, Vol. 1-2.

[53] Larson, M. and Kraus, N.C. (1989). SBEACH: Numerical model for simulating storm-induced beach change, Report 1, Tech. Report CERC-89-9, Waterways Experiment Station, US Army Crops of Engineers.

[54] Le Mehaute (1962). On non-saturated breakers and the wave run-up, Proc. 8th Coastal Engineering Conf., ASCE, pp. 77-92.

[55] Le Mehaute, B. and Koh, R.C.Y. (1967). On the breaking of waves arriving at an angle to the shore, J. Hydraulic Research, Vol. 5, No. 1, pp. 67-88.

[56] Madsen, O.S. (1976). Wave climate of the continental margin: Elements of its mathematical description, D.J. Stanley and D.J.P. Swift (Editors), Marine Sediment Transport in Environmental Management. Wiley, New York, pp. 65-87.

[57] Maruyama, K., Sakakiyama, T., Kajima, R., Saito, S. and Shimizu, T. (1983). Experimental study on wave height and water particle velocity near the surf zone using a large wave flume, Civil Eng. Lab. Report No. 382034, The Central Research Institute of Electric Power Industry, Chiba, Japan (in Japanese).

[58] Massel, S.R. (1996). On the largest wave height in water of constant depth, Ocean Engineering, Vol. 23, pp. 553-573.

[59] McCowan, J. (1894). On the highest waves of a permanent type, Philosophical Magazine, Edinburgh, Ser. 5, Vol. 38, pp. 351-358.

[60] Miche, R. (1944). Mouvements ondulatoires des mers en profondeur constante on decroissante, Ann. des Ponts et Chaussees, Ch.114, pp.131-164, 270-292, and 369-406.

[61] Mitsuyasu, H. (1962). Rept. Transportation Techical Res. Inst., No. 47.

[62] Mizuguchi, M. (1980). An heuristic model of wave height distribution in surf zone, Proc. 17th Coastal Engineering Conf., ASCE, pp. 278-289.

[63] Munk, W.H. (1949). The solitary wave theory and its applications to surf problems, Annals of the New York Academy of Sciences, Vol. 51.

[64] Nadaoka, K., Kondoh, T. and Tanaka. N. (1982). The structure of velocity field within the surf zone revealed by means of laser-doppler anemometry, Port and Harbor Research Institute, Vol. 21, No. 2, pp. 50-102 (in Japanese).

[65] Nagayama, S. (1983). Study on the change of wave height and energy in the surf zone, Bach. Thesis, Civil Eng., Yokohama National University, Japan.

[66] Nairn, R.B. (1990). Prediction of cross-shore sediment transport and beach profile evolution, Ph.D. thesis, Dept. of Civil Eng., Imperial College, London.

[67] Nairn, R.B., Roelvink, J.A., and Southgate, H.N. (1990). Transition zone width and implications for modelling surfzone hydrodynamics, Proc. 22nd Coastal Engineering Conf., ASCE, pp. 68-81.

[68] Okawa, Y. and Shuto, N. (1984). Run-up of periodic waves on beaches of non-uniform slope, Proc. 19th Coastal Engineering Conf., ASCE, pp. 328-344.

[69] Okayasu, A., Shibayama, T. and Mimura, N., (1986). Velocity field under plunging waves, Proc. 20th Coastal Engineering Conf., ASCE, pp. 660-674.

[70] Okayasu, A., Shibayama, T. and Horikawa, K. (1988). Verification of undertow in the surf zone, Proc. 21st Coastal Engineering Conf., ASCE, pp. 478-491.

[71] Okayasu, A. (1989). Characteristics of Turbulence Structure and Undertow in Surf Zone, D. Eng. Dissertation, Civil Eng., Univ. of Tokyo, Japan.

[72] Okayasu, A. and Katayama, H. (1992). Distribution of undertow and long-wave component velocity due to random waves, Proc. 23rd Coastal Engineering Conf., ASCE, pp. 883-893.

[73] Ostendorf, D.W. and Madsen, O.S. (1979). An analysis of longshore current and associated sediment transport in the surf zone, Report No. 241, Dept. of Civil Eng., M.

[74] Ozaki, A., Sasaki, M. and Usui, Y. (1977). Study on rip currents: experimental observation of nearshore circulation on a sloping bottom, Coastal Engineering in Japan, JSCE, Vol. 20, pp. 147-158.

[75] Rakha, K.A. and Kamphuis, J.W. (1995). Numerical and hydraulic model study of wave decay on a shelf beach, Coastal Engineering, Vol. 24, pp. 275-296.

[76] Rattanapitikon, W. and Shibayama, T. (1993). Vertical distribution of suspended sediment concentration in and outside surf zone, Coastal Engineering in Japan, Vol. 36, No. 1, pp. 49-65.

[77] Rattanapitikon, W. and Shibayama T. (1998). Energy dissipation model for regular and irregular breaking waves, Coastal Eng. Journal, JSCE, Vol. 40, No.4, pp. 327-346.

[78] Rattanapitikon, W. and Shibayama, T. (2000a). Simple model for undertow profile, Coastal Engineering Journal (JSCE), Vol. 42, No. 1, pp.1-30

[79] Rattanapitikon, W. and Shibayama T. (2000b). Verification and modification of breaker height formulas, Coastal Eng. Journal, JSCE, Vol. 2, No. 4, pp. 389-406.

[80] Reid, R.O. and Bretschneider, C.L. (1953). Surface waves and offshore structures, Technical Report No. 53-10, Taxas A&M University.

[81] Rodriguez, A., Arcilla, S.A., Collado, F.R., Gracia, V., Coussirat, M.G. and Prieto, J. (1994). Wave and currents at the ebro delta surf zone: measurement and modelling, Proc. 24th Coastal Engineering Conf., ASCE, pp. 2542-2556.

[82] Roelvink, J.A. and Reniers A.J.H.M. (1995). LIP 11D Delta Flume Experiments: A data set for profile model validation, Report No. H 2130, Delft Hydraulics.

[83] Saeki, H. and Sasaki, M. (1973). A study of the deformation of waves after breaking, Proc. 20th Japanese Conf. on Coastal Engineering, JSCE, pp. 559-564 (in Japanese).

[84] Sato, S., Fukuhama, M. and Horikawa, K. (1988). Measurements of near-bottom velocities in random waves on a constant slope, Coastal Engineering in Japan, JSCE, Vol. 31, No. 2, pp. 219-229.

[85] Sato, S., Isayama, T. and Shibayama, T. (1989). Long-wave component in near bottom velocity under random waves on a gentle slope, Coastal Engineering in Japan, JSCE, Vol. 32, No. 2, pp. 149-159.

[86] Sato, S., Homma, K. and Shibayama, T. (1990). Laboratory study on sand suspension due to breaking waves, Coastal Engineering in Japan, JSCE, Vol. 33, No. 2, pp. 219-231.

[87] Seyama, A. and Kimura, A. (1988). The measured properties of irregular wave breaking and wave height change after breaking on slope, Proc. 21st Coastal Engineering Conf., ASCE, pp. 419-432.

[88] Shibayama, T. and Horikawa, K. (1986). Sediment transport due to breaking waves, Proc. of JSCE, No. 357/II-3(Hydraulic and Sanitary), pp. 1509-1522.

[89] Shimizu, T. and Ikeno, M. (1996). Experimental study on sediment transport in surf and swash zones using large wave flume, Proc. 25th Coastal Engineering Conf., ASCE, pp. 3076-3089.

[90] Singamsetti, S.R. and Wind, H.G. (1980). Characteristics of breaking and shoaling periodic waves normally incident on to plane beaches of constant slope, Report M1371, Delft Hydraulic Lab., Delft, The Netherlands.

[91] Smith, D.A. (1974). Radiation stress effects on wave set-up in the surf zone, M.Sc. Thesis, Dept. of Civil Eng., University of London, Imperial College.

[92] Smith, J.M. and Kraus, N.C. (1990). Laboratory study on macro-features of wave breaking over bars and artificial reefs, Technical Report CERC-90-12, WES, U.S. Army Corps of Engineers.

[93] Smith, J.M., Larson, M. and Kraus, N.C. (1993). Longshore current on a barred beach: field measurements and calculations, J. Geophysical Research, Vol. 98, pp. 22727-22731.

[94] Southgate, H.N. and Nairn, R.B. (1993). Deterministic profile modelling of nearshore processes. Part 1. Waves and currents, Coastal Engineering, Vol. 19, pp. 27-56.

[95] Stive, M.J.F. (1984). Energy dissipation in wave breaking on gentle slopes, Coastal Engineering, Vol. 8, pp. 99-127.

[96] Stive, M.J.F., and Wind, H.G. (1986). Cross-shore mean flow in the surf zone, Coastal Engineering, No. 10, pp. 325-340.

[97] Sultan, N. (1995). Irregular wave kinematics in the surf zone, Ph.D. Dissertation, Texas A&M University, College Station, Texas, USA.

[98] Sunamura, T. and Horikawa, K. (1974). Two-dimensional beach transformation due to waves, Proc. 14th Coastal Engineering Conf., ASCE, pp. 920-938.

[99] Sunamura, T. (1980). A laboratory study of offshore transport of sediment and a model for eroding beaches, Proc. 17th Coastal Engineering Conf., ASCE, pp. 1051-1070.

[100] Suquet, F. (1950). Experimental study on the breaking of waves, La Houille Blanche, No. 3, May to June.

[101] Svendsen, I.A., Madsen, P.A., and Hansen, J.B. (1978). Wave characteristics in the surf zone, Proc. 16th Coastal Engineering Conf., ASCE, pp. 520-539.

[102] Svendsen I.A. (1984a). Wave heights and set-up in a surf zone, Coastal Engineering, No. 8, pp. 303-329.

[103] Svendsen I.A. (1984b). Mass flux and undertow in a surf zone, Coastal Engineering, No. 8, pp. 347-365.

[104] Thornton, E.B. and Guza, R.T. (1983). Transformation of wave height distribution, J. Geophysical Research, Vol. 88, pp. 5925-5983.

[105] Thornton, E.B. and Guza, R.T. (1986). Surf zone longshore currents and random waves: field data and model, J. Physical Oceanography, Vol. 16, pp. 1165-1178.

[106] Ting, C.K. and Kirby, J.T. (1994). Observation of undertow and turbulence in a laboratory surf zone, Coastal Engineering, Vol. 24, pp. 51-80.

[107] Van Dorn, W.G. (1978). Breaking invariance in shoaling waves, J. Geophysical Research, Vol. 83, C6, pp. 2981-2988.

[108] Visser, P.J. (1977). Wave set-up: experimental investigation on normally incident waves, Report No. 77-1, Laboratory of Fluid Mech., Dept. of Civil Eng., Delft University of Tech., Delft, The Netherlands.

[109] Visser, P.J. (1982). The proper longshore current in a wave basin, Report No. 82-1, Laboratory of Fluid Mech., Dept. of Civil Eng., Delft University of Tech., Delft, The Netherlands.

[110] Walker, J.R. (1974). Wave transformations over a sloping bottom and over a three-dimensional shoal, Miscellaneous Report No. 11, University of Hawaii, Look Lab-75-11, Honlulu, Hawaii, USA.

[111] Weggel, J.R. and Maxwell, W.H.C. (1970). Experimental study of breaking wave pressures, Second Annual Offshore Technology Conference, Texas, OTC-1244.

[112] Weggel J.R. (1972). Maximum breaker height, J. Waterways, Harbors and Coastal Eng. Div., Vol. 98, No. WW4, pp. 529-548.

OUTPUT

International Journals:

1) Rattanapitikon, W. and Shibayama, T. (1998). Energy dissipation model for regular and irregular breaking waves, Coastal Engineering Journal (JSCE), Vol. 40, No. 4, pp. 327-346.
2) Rattanapitikon, W. and Shibayama, T. (2000). Simple model for undertow profile, Coastal Engineering Journal (JSCE), Vol. 42, No. 1, pp.1-30.
3) Rattanapitikon, W. and Shibayama, T. (2000). Verification and modification of breaker height formulas, Coastal Engineering Journal (JSCE), Vol. 42, No. 4, pp. 389-406.
4) Rattanapitikon, W. and Shibayama, T. (2001). Comparisons of energy dissipation models for regular and irregular breaking waves, (**in preparing**).

APPENDIX: PAPER REPRINTS

A.1 Energy Dissipation Model for Regular and Irregular Breaking Waves

Reprinted from:

Rattanapitikon, W. and Shibayama, T. (1998). Energy dissipation model for regular and irregular breaking waves. Coastal Engineering Journal (JSCE), Vol. 40, No. 4, pp. 327-346.

Coastal Engineering Journal, Vol. 40, No. 4 (1998) 327–346

ENERGY DISSIPATION MODEL FOR REGULAR AND IRREGULAR BREAKING WAVES

WINYU RATTANAPITIKON
Department of Civil Engineering, Sirindhorn International Institute of Technology, Thammasat University, Klong Luang, Phatum Thani 12121, Thailand
E-mail: winyu@siit.tu.ac.th

TOMOYA SHIBAYAMA
Department of Civil Engineering, Yokohama National University, 79-5 Tokiwadai, Hodogaya-ku, Yokohama 240-8501, Japan
E-mail: tomo@coast.cvg.ynu.ac.jp

Received 25 May 1998
Revised 9 October 1998

Based on a large amount of published laboratory results, reliable models are developed for computing the average rate of energy dissipation in regular and irregular breaking waves. The average energy dissipation rate is assumed to be proportional to the difference between the local mean energy density and stable energy density. Wave height transformation is computed from the energy flux conservation law based on the linear wave theory. The models are examined and verified extensively for a variety of wave and bottom conditions, including small and large scale laboratory and field experiments. Reasonable good agreements are obtained between the measured and computed wave heights and root mean square wave heights.

Keywords: Energy dissipation, wave breaking, wave model.

1. Introduction

In studying many coastal engineering problems, it is essential to have accurate information on wave conditions in the surf zone. When waves propagate to the nearshore zone, wave profiles are steepen and eventually waves break. Once the waves start to break, a part of wave energy is transformed to turbulence and heat, and wave height decreases towards the shore. The rate of energy dissipation of breaking waves is an essential requirement for predicting wave height, sediment transport rate and beach profile change in the surf zone.

During the last few decades, a number of studies and experiments have been carried out to develop the energy dissipation models. Owing to the complexity of wave breaking mechanism, any type of model for computing the rate of energy dissipation has to be based on empirical or semi-empirical formula calibrated with the experimental results. To make the empirical formula reliable, it is necessary to

Table 1. Summary of collected experimental data used to validate the present models.

Sources	Total No. of cases	Total No. of data points	Wave condition	Bed condition	Apparatus
Hansen and Svendsen (1984)	1	5	regular	plane beach	small-scale
Horikawa and Kuo (1966)	213	2127	regular	plane and stepped beach	small-scale
Kajima *et al.* (1983)	79	1379	regular	sandy beach	large-scale
Kraus and Smith (1994)	57	429	regular	sandy beach	large-scale
	128	2223	irregular		
Nadaoka *et al.* (1982)	2	11	regular	plane beach	small-scale
Nagayama (1983)	12	171	regular	plane, stepped and barred beach	small-scale
Okayasu *et al.* (1988)	10	62	regular	plane beach	small-scale
Sato *et al.* (1988)	3	25	regular	plane beach	small-scale
Sato *et al.* (1989)	2	11	regular	plane beach	small-scale
Shibayama and Horikawa (1985)	10	85	regular	sandy beach	small-scale
Smith *et al.* (1993)	4	32	irregular	sandy beach	field
Smith and Kraus (1990)	101	506	regular	plane and barred beach	small-scale
	12	96	irregular		
Thornton and Guza (1986)	4	60	irregular	sandy beach	field
Total	638	7240			

calibrate or verify the formula with a large amount and wide range of experimental results. Since many energy dissipation models were developed based on data with the limited experimental conditions, there is still a need for more data to confirm the underlying assumptions and to make the model more reliable. At this moment, the experimental results obtained by many researchers have been accumulated and a large number of experimental results have become available. It is a good time to develop a model based on the large amount and wide range of experimental results. It is the purpose of this study to develop the energy dissipation model based on wide range of experimental conditions. Experimental data from 13 sources, including 638 cases, have been collected for calibration and verification of the present models. A summary of the collected experimental results is given in Table 1. The experiments cover wide range of wave and bottom topography conditions, including both small and large scale laboratory and field experiments. Most of the experiments were performed under fixed bed conditions, except data of Kajima *et al.* (1983), Smith *et al.* (1993), Kraus and Smith (1994), Shibayama and Horikawa (1985), Thornton and Guza (1986) which were performed under movable bed conditions.

2. Governing Equation

If we apply wave model for computing beach transformation, the wave model should be kept as simple as possible because of the frequent updating of wave field for accounting the variability of mean water surface and the change of bottom profiles. In the present study, wave height transformation will be computed from the energy flux conservation law. It is

$$\frac{\partial(Ec_g \cos\theta)}{\partial x} = -D_B \tag{1}$$

where E is the wave energy density, c_g is the group velocity, θ is the mean wave angle, x is the distance in cross shore direction, x-axis points onshore, and D_B is the energy dissipation rate which is zero outside the surf zone. The energy dissipation due to the bottom friction is neglected. Snell's law is employed to describe wave refraction.

The wave height transformation can be computed from the energy flux balance equation [Eq. (1)] by substituting the formula of the energy dissipation rate, D_B, and numerical integrating from offshore to shoreline. The main difficulty of energy flux conservation approach is how to formulate the energy dissipation rate, D_B, inside the surf zone. The phenomenon of wave breaking is very complicated. At present stage of knowledge, it is clear that any type of formula for computing the energy dissipation rate, D_B, has to be based on empirical or semi-empirical formula. The main target of the next sections is to develop an empirical formula for computing the energy dissipation rate for regular wave breaking and then for irregular wave breaking.

3. Energy Dissipation Due to Breaking of Regular Waves

3.1. *Model development*

A major problem of wave field calculation inside the surf zone is how to evaluate the rate of energy dissipation. A number of works on theoretical and experimental studies have been performed to draw a clearer picture of the energy dissipation rate, D_B. Various models have been proposed, by previous researchers, for computing the energy dissipation rate, D_B. Widely used formulas for computing energy dissipation rate are the Bore model and the model of Dally *et al.* (1985). A briefly reviews of these two models are described as follows.

(a) Bore model, originally introduced by Le Mehaute (1962), is developed based on an assumption that the energy dissipation rate of a broken wave is similar to the dissipation rate of a hydraulic jump. Several researchers have proposed slightly different forms of the energy dissipation rate, e.g.

$$\text{Battjes and Janssen (1978)}: \quad D_B = \frac{\rho g H^2}{4T} = \frac{2}{T}E \tag{2}$$

$$\text{Thornton and Guza (1983)}: \quad D_B = \frac{\rho g H^3}{4Th} = \frac{2H}{Th}E \tag{3}$$

where ρ is the density of water, g is the acceleration due to gravity, H is the wave height, T is the wave period, and h is the water depth.

(b) The model of Dally *et al.* (1985) is based on the observation of stable wave height on the horizontal bed. They assumed that the energy dissipation rate is proportional to the difference between the local energy flux and the stable energy flux, divided by the local water depth as

$$D_B \propto \frac{[Ec_g - E_s c_g]}{h} \tag{4}$$

or

$$D_B = \frac{K_d c_g}{h}[E - E_s] = \frac{K_d cn}{h}[E - E_s] \tag{5}$$

where

$$E_s = \frac{1}{8}\rho g H_s^2 = \frac{1}{8}\rho g(\Gamma h)^2 \tag{6}$$

$$n = \frac{[1 + 2kh/\sinh(2kh)]}{2} \tag{7}$$

in which K_d is a constant (decay coefficient), c is the phase velocity, E_s is the stable energy density, H_s is the stable wave height and Γ is the stable wave factor.

From the model calibration with the laboratory data of Horikawa and Kuo (1966), Dally *et al.* (1985) found that $K_d = 0.15$ and Γ is varied case by case between 0.35–0.48. However, finally, they suggested to use $\Gamma = 0.4$ for general cases. The Dally *et al.*'s model has been verified extensively for a variety of wave conditions (e.g. Ebersole, 1987; Larson and Kraus, 1989). The advantage of Dally *et al.*'s model is that it is able to reproduce the pause (or stop breaking) in the wave breaking process at a finite wave height on a horizontal bed or in the recovery zone while the bore model gives a continuous dissipation due to wave breaking.

From the above empirical formulas Eqs. (2)–(5), we see that the energy dissipation rate, D_B, may be a function of the energy density, E. Moreover, the energy dissipation rate should be equal to zero for recovered wave. Therefore, in the present study, the energy dissipation rate is assumed to be proportional to the difference between the local energy density and stable energy density:

$$D_B \propto [E - E_s] \tag{8}$$

or

$$D_B = \beta[E - E_s] \tag{9}$$

where β is the proportionality constant.

Table 2. Root mean square relative error (ER) of the four possible forms of D_B.

No	Sources	Total No of cases	D_B from Eq. (11) $K_1 = 0.90$	D_B from Eq. (12) $K_2 = 0.98$	D_B from Eq. (13) $K_3 = 0.15$	D_B from Eq. (14) $K_4 = 0.15$
1	Hansen and Svendsen (1984)	1	5.14	4.82	13.83	16.15
2	Horikawa and Kuo (1966), slope=0	101	11.98	14.21	13.87	13.30
	Horikawa and Kuo (1966), slope=1/80–1/20	112	29.44	22.99	17.86	20.64
3	Kajima *et al.* (1983)	79	26.03	19.29	20.06	18.36
4	Kraus and Smith (1994)	57	21.58	26.25	21.87	20.86
5	Nadaoka *et al.* (1982)	2	21.70	15.44	8.38	11.97
6	Nagayama (1983)	12	10.00	9.69	9.55	9.19
7	Okayasu *et al.* (1988)	10	17.39	16.06	13.57	14.18
8	Sato *et al.* (1988)	3	15.20	12.43	8.11	11.35
9	Sato *et al.* (1989)	2	25.39	17.75	24.76	31.83
10	Shibayama and Horikawa (1986)	10	19.25	17.68	17.15	16.23
11	Smith and Kraus (1990)	101	24.73	25.11	21.98	19.44
	Total	490	20.23	18.66	17.84	17.55

Rewriting Eq. (9) in terms of wave height leads to

$$D_B = \beta\frac{\rho g}{8}[H^2 - (\Gamma h)^2] \tag{10}$$

The energy dissipation rate of Eq. (10) contains two parameters β and Γ which can be determined empirically from the measured wave heights. The published experimental data from small-scale and large-scale experiments performed under regular wave actions are used to determine the parameters β and Γ. Total 11 sources of published experimental results, including 490 cases, are used in this section (see the first column of Table 2).

3.1.1. *Determination of parameter* β

By comparison of Eq. (9) to Eqs. (2), (3) and (5), respectively, we see that there may be four possible forms of β. Therefore, there are four possible models of the energy dissipation rate, D_B:

$$\text{model (1)}: \quad D_B = K_1\frac{2}{T}(E - E_s) = K_1\frac{\rho g}{4T}[H^2 - (\Gamma h)^2] \tag{11}$$

where $\beta = K_1 \frac{2}{T}$

$$\text{model (2)}: \quad D_B = K_2 \frac{2H}{Th}(E - E_s) = K_2 \frac{\rho g H}{4Th}[H^2 - (\Gamma h)^2] \tag{12}$$

where $\beta = K_2 \frac{2H}{Th}$.

$$\text{model (3)}: \quad D_B = K_3 \frac{cn}{h}(E - E_s) = K_3 \frac{\rho g c n}{8h}[H^2 - (\Gamma h)^2] \tag{13}$$

where $\beta = K_3 \frac{cn}{h}$.

$$\text{model (4)}: \quad D_B = K_4 \frac{c}{h}(E - E_s) = K_4 \frac{\rho g c}{8h}[H^2 - (\Gamma h)^2] \tag{14}$$

where $\beta = K_4 \frac{c}{h}$; in which $K_1 - K_4$ are constants, which can be found from model calibrations. Model 3 of Eq. (13) is the same model with Dally *et al.* (1985).

In order to select the proper form of β or D_B, the above four models Eqs. (11)-(14) will be examined by using measured wave heights inside the surf zone.

By rewriting Eq. (1) in term of wave height, it becomes

$$\frac{\rho g}{8} \frac{\partial (H^2 c_g \cos\theta)}{\partial x} = -D_B \tag{15}$$

The wave height transformation is computed from the energy flux balance equation [Eq. (15)] by substituting the above possible expressions of D_B and numerical integrating from breaking point to shoreline. In this subsection, $\Gamma = 0.4$ is used as suggested by Dally *et al.* (1985) and it will be modified later in Subsec. 3.1.2.

In order to evaluate the accuracy of the prediction, the verification results are presented in term of root mean square (rms) relative error, ER, as used by Dally *et al.* (1985), which is defined as

$$ER = 100\sqrt{\sum_{i=1}^{tn}(H_{ci} - H_{mi})^2 \Big/ \sum_{i=1}^{tn} H_{mi}^2} \tag{16}$$

where i is the wave height number, H_{ci} is the computed wave height of number i, H_{mi} is the measured wave height of number i, and tn is the total number of measured wave height. Smaller values of ER means better predictions.

A calibration for models 1–4 was conducted by varying the values of $K_1 - K_4$ until the minimum error (ER) between measured and computed wave heights is obtained. The optimum values of $K_1 - K_4$ are 0.90, 0.98, 0.15 and 0.15, respectively, which give the average rms relative error of each model equal to 20.23, 18.66, 17.84 and 17.55, respectively.

The rms relative errors (ER) of each model for all cases of collected experiments are shown in Table 2. From Table 2, among the four possible models, the model 4 of Eq. (14) appeared to be the best. Therefore, the proper form of the parameter β is recommended to be

$$\beta = 0.15\frac{c}{h} \tag{17}$$

Therefore, the energy dissipation rate can be written as

$$D_B = K_a \frac{c}{h}[E - E_s] = K_a \frac{c\rho g}{8h}[H^2 - (\Gamma h)^2] \tag{18}$$

where $K_a = 0.15$ is the constant.

Comparing Eq. (18) with Dally *et al.*'s model Eq. (5), we see that Eq. (18) is similar to the Dally *et al.*'s model Eq. (5) except the factor n.

It should be noted that we could get the same form as Eq. (18), if we assume that the energy dissipation rate is proportional to the difference between the energy per unit width (EL) and the stable energy per unit width (E_sL), divided by the local water depth and wave period as

$$D_B \propto \frac{[EL - E_sL]}{hT} \tag{19}$$

or

$$D_B = K_a \frac{L}{hT}[E - E_s] = K_a \frac{c}{h}[E - E_s] \tag{20}$$

where K_a is the proportional constant. Rewriting Eq. (20) in terms of wave height yields

$$D_B = K_a \frac{c\rho g}{8h}[H^2 - (\Gamma h)^2] \tag{21}$$

which is the same as Eq. (18).

3.1.2. *Determination of the parameter* Γ

Since the parameter Γ changes between 0.35–0.48 (Dally *et al.*, 1985), the objective of this subsection is to determine the empirical formula of the parameter Γ.

After substituting Eq. (18) into Eq. (1), the equation of energy flux balance can be written as

$$\frac{\partial(Ec_g \cos\theta)}{\partial x} = K_a \frac{c\rho g}{8h}[H^2 - (\Gamma h)^2] \tag{22}$$

Considering Eq. (22), the measured Γ can be determined from the measured wave height, period and water depth by using the following formula [rewriting Eq. (22)].

$$\Gamma = \frac{1}{h}\sqrt{H^2 - \frac{\partial(Ec_g \cos\theta)}{\partial x}\frac{8h}{0.15c\rho g}} \tag{23}$$

Using the measured wave heights, periods, and water depths from the experimental data of Kajima *et al.* (1983), the measured Γ can be determined from Eq. (23). An attempt is made to correlate the parameter Γ with the wave parameters. Among the various possibilities, the correlation between Γ and $h/\sqrt{LH}$ appeared to be

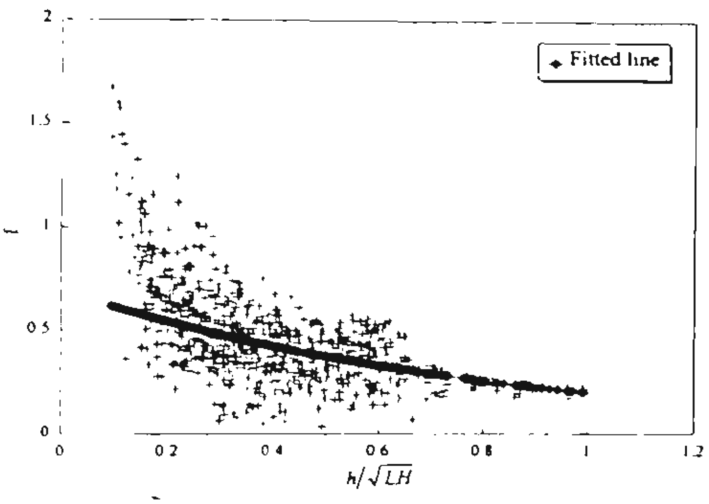

Fig. 1. Relationship between Γ and $h/\sqrt{LH}$ (laboratory data from Kajima *et al.*, 1983).

the best (see Fig. 1). A formula for the stable wave factor Γ, from Fig. 1, can be expressed as

$$\Gamma = \exp\left[-0.36 - 1.25\frac{h}{\sqrt{LH}}\right] \tag{24}$$

Substituting Γ from Eq. (24) into Eq. (18), finally, the energy dissipation rate D_B of the present study can be expressed as

$$D_B = \frac{0.15c\rho g}{8h}\left[H^2 - \left(h\exp\left(-0.36 - 1.25\frac{h}{\sqrt{LH}}\right)\right)^2\right] \tag{25}$$

3.2. *Model verification*

Comparisons between measured and computed wave heights inside the surf zone are used to verify the model. The verification is performed for 490 cases of 11 sources of collected laboratory data. The verification by using these independent data sources and wide range of experiment conditions are expected to clearly demonstrate the accuracy of the present model.

The wave height transformation is computed from the energy flux balance equation [Eq. (1)] by substituting D_B from Eq. (25) and numerical integration, using backward finite difference scheme, from breaking point to shoreline. All coefficients in the model are kept to be constant for all cases in the verification. Comparison between measured and computed wave heights for all 490 cases are shown in Fig. 2. Columns 4 and 5 of Table 3 shows the *rms* relative error, ER, of the Dally *et al.*'s model Eq. (5) and the present model Eq. (25), respectively. From Table 3, we see that the results of computed wave height of present model are better than those

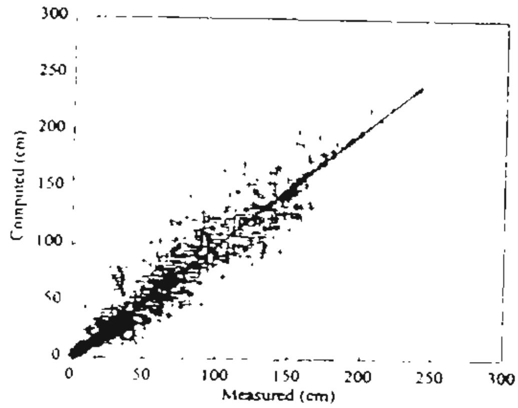

Fig. 2. Comparison between computed and measured wave height for all 490 cases (measured data from 11 sources as shown in Table 2)

Table 3. Root mean square relative error (ER) of Dally's model and present model.

No	Sources	Total No. of cases	Dally model, Eq. (5)	Present study, Eq. (25)
1	Hansen and Svendsen (1984)	1	13.83	7.00
2	Horikawa and Kuo (1966), slope = 0	101	13.87	11.66
	Horikawa and Kuo (1966), slope = 1/80-1/20	112	17.86	17.68
3	Kajima *et al.* (1983)	79	20.06	16.37
4	Kraus and Smith (1994)	57	21.87	19.16
5	Nadaoka *et al.* (1982)	2	8.38	10.81
6	Nagayama (1983)	12	9.55	8.61
7	Okayasu *et al.* (1988)	10	13.57	11.30
8	Sato *et al.* (1988)	3	8.11	7.74
9	Sato *et al.* (1989)	2	24.76	19.78
10	Shibayama and Horikawa (1986)	10	17.15	17.69
11	Smith and Kraus (1990)	101	21.98	20.44
	Total	490	17.84	15.75

of Dally *et al.*'s model. for most cases. The average *rms* relative error, for all 490 cases, by the present model is 15.8% while that by Dally *et al.*'s model is 17.8%.

4. Energy Dissipation Due to Breaking of Irregular Waves

Irregular wave breaking is more complex than regular wave breaking. In contrast to regular waves there is no well-defined breaking point for irregular waves. The highest waves tend to break at greatest distances from the shore. Thus, the energy dissipation of irregular waves occurs over a considerably greater area than that of regular waves.

4.1. *Model development*

Dally (1992) used regular wave model of Dally *et al.* (1985) to simulate transformation of irregular wave by using wave-by-wave approach. This means that Dally assumed that D_B is proportional to the difference between *local energy flux of a breaking wave* and stable energy flux. Also wave-by-wave approach requires much computation time. Therefore it may not suitable to use in a beach deformation model.

However, the model becomes simple if we set an assumption, similar to that of present regular wave model, that the average rate of energy dissipation in breaking waves is proportional to the difference between *local mean energy density* and stable energy density. After incorporating the fraction of breaking, the average rate of energy dissipation in irregular wave breaking, $\bar{D}_B$, can be expressed as

$$\bar{D}_B = \frac{K_5 Q_b c_p}{h}[E_m - E_s] \tag{26}$$

where

$$E_m = \frac{1}{8}\rho g H_{rms}^2 \tag{27}$$

$$E_s = \frac{1}{8}\rho g H_s^2 = \frac{1}{8}\rho g(\Gamma_i h)^2 \tag{28}$$

in which all variables are computed based on the linear wave theory. K_5 is the proportional constant, Q_b is the fraction of breaking waves, c_p is the phase velocity related to the peak spectral wave period T_p, h is the water depth, E_m is the local mean energy density, E_s is the stable energy density, H_{rms} is the root mean square wave height, H_s is the stable wave height and Γ_i is the stable wave factor of irregular wave.

Rewriting Eq. (26) in term of wave height yields

$$\bar{D}_B \frac{K_5 Q_b c_p \rho g}{8h}[H_{rms}^2 - (\Gamma_i h)^2] \tag{29}$$

The stable wave factor, Γ_i, is determined by applying Eq. (24) as

$$\Gamma_i = \exp\left[K_6\left(-0.36 - 1.25\frac{h}{\sqrt{L_p H_{rms}}}\right)\right] \tag{30}$$

where K_6 is the coefficient, L_p is the wavelength related to the peak spectral wave period.

$$\bar{D}_B = \frac{K_5 Q_b c_p \rho g}{8h}\left[H_{rms}^2 - \left(h\exp\left(-0.36K_6 - 1.25K_6\frac{h}{\sqrt{L_p H_{rms}}}\right)\right)^2\right] \tag{31}$$

The local fraction of breaking waves, Q_b, is determined from the derivation of Battjes and Janssen (1978) based on the assumption of truncated Rayleigh distribution at the maximum wave height:

$$\frac{1-Q_b}{-\ln Q_b} = \left(\frac{H_{rms}}{H_b}\right)^2 \tag{32}$$

where H_b is the breaking wave height that can be computed by using breaking criteria of Goda (1970):

$$H_b = K_7 L_0 \left\{1 - \exp\left[-1.5\frac{\pi h}{L_0}(1 + 15m^{4/3})\right]\right\} \tag{33}$$

where K_7 is the coefficient, L_0 is the deep-water wavelength related to the peak spectral wave period, and m is the bottom slope.

Since Eq. (32) is an implicit equation, the iteration process is necessary to compute the fraction of breaking waves, Q_b. It will be more convenient if we can compute Q_b from the explicit form of Eq. (32). From the multi-regression analysis, the explicit form of Q_b can be expressed as the following (with $R^2 = 0.999$):

$$Q_b \begin{cases} 0 & \text{for } \dfrac{H_{rms}}{H_b} \le 0.43 \\ -0.738\left(\dfrac{H_{rms}}{H_b}\right) - 0.280\left(\dfrac{H_{rms}}{H_b}\right)^2 + 1.785\left(\dfrac{H_{rms}}{H_b}\right)^3 + 0.235 & \text{for } \dfrac{H_{rms}}{H_b} > 0.43 \end{cases} \tag{34}$$

The energy dissipation model Eqs. (31), (33) and (34) contains 3 coefficients, $K_5 - K_7$, that can be found from model calibration.

4.2. *Model calibration*

The model is calibrated for determining the optimal values of the coefficients $K_5 - K_7$ in Eqs. (31) and (33). The calibration is carried out with the large-scale experimental data from the SUPERTANK Laboratory Data Collection Project (Kraus and Smith, 1994). The SUPERTANK project was conducted to investigate cross-shore hydrodynamic and sediment transport processes, during the period August 5 to September 13, 1992, at Oregon State University, Corvallis, Oregon, USA. A 76-m-long sandy beach was constructed in a large wave tank of 104 m long, 3.7 m wide, and 4.6 m deep. Wave conditions involved regular and irregular waves. The 20 major tests were performed and each major test consisted of several cases (see Table 4). Most of the major tests were performed under the irregular wave actions, except the test No. STBO, STEO, STFO, STGO, STHO, and STIO. The collected experiments for irregular waves include 128 cases of *rms* wave height profiles, covering incident wave heights from 13.9 cm to 60.1 cm, peak wave periods from 2.8 sec to 9.8 sec.

Table 4. Root mean square relative error (ER) of the present model comparing with irregular wave data of Kraus and Smith (1994).

Test No.	Description	Total No. of cases	ER. of Present study
ST10	Erosion toward equilibrium, irregular waves	26	5.77
ST20	Acoustic profiler tests, regular and irregular waves	8	6.86
ST30	Accretion toward equilibrium, irregular waves	19	10.01
ST40	Dedicated hydrodynamics, irregular waves	12	10.37
ST50	Dune erosion, Test 1 of 2, irregular waves	8	12.11
ST60	Dune erosion, Test 2 of 2, irregular waves	9	9.72
ST70	Seawall, Test 1 of 3, irregular waves	9	7.87
ST80	Seawall, Test 2 of 3, irregular waves	3	10.98
ST90	Berm flooding, Test 1 of 2, irregular waves	3	4.32
STAO	Foredune erosion, irregular waves	1	4.94
STBO	Dedicated suspended sediment, regular waves	0	-
STCO	Seawall, Test 3 of 3, irregular waves	8	10.88
STDO	Berm flooding, Test 2 of 2, irregular waves	3	12.39
STEO	Laser Doppler velocimeter, Test 1 of 2, regular waves	0	-
STFO	Laser Doppler velocimeter, Test 2 of 2, regular waves	0	-
STGO	Erosion toward equilibrium, regular waves	0	-
STHO	Erosion, transition toward accretion, regular waves	0	-
STIO	Accretion toward equilibrium, regular waves	0	-
STJO	Narrow-crested offshore mound, reg. and irreg. waves	10	10.12
STKO	Broad-crested offshore mound, reg. and irreg. waves	9	22.18

The rms wave height transformation is computed by the numerical integration of energy flux balance equation [Eq. (1)] with the energy dissipation rate $\bar{D}_B$ of Eq. (31):

$$\frac{\partial(H_{rms}^2 c_{gp}\cos\theta)}{\partial x} = \frac{K_5 Q_b c_p}{h}\left[H_{rms}^2 - \left(h\exp\left(-0.36K_6 - 1.25K_6\frac{h}{\sqrt{L_p H_{rms}}}\right)\right)^2\right] \quad (35)$$

where Q_b is computed from Eq. (34), and H_b is computed from Eq. (33).

Equation (35) is solved by backward finite difference scheme. Trial simulations indicated that $K_5 = 0.10$, $K_6 = 1.60$, and $K_7 = 0.10$ give good agreement between measured and computed rms wave heights. Finally, the energy dissipation rate of irregular wave breaking can be written as

$$\bar{D}_B = \frac{0.1 Q_b c_p \rho g}{8h}\left[H_{rms}^2 - \left(h\exp\left(-0.58 - 2.00\frac{h}{\sqrt{L_p H_{rms}}}\right)\right)^2\right] \quad (36)$$

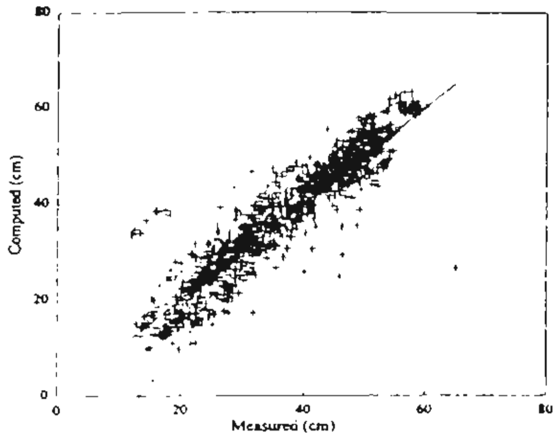

Fig. 3. Comparison between computed and measured *rms* wave height for 128 cases of large-scale experiments (measured data from Kraus and Smith, 1994).

Table 5 Root mean square relative error (ER) of the present model.

No.	Sources	No. of data set	Present study
1	Kraus and Smith (1994)	128	9.75
2	Smith and Kraus (1990)	12	11.90
3	Smith *et al.* (1993)	4	14.54
4	Thornton and Guza (1986)	4	14.41
	Total	148	10.08

Comparison between measured and computed *rms* wave heights for all 128 cases are shown in Fig. 3. Table 4 shows the *rms* relative error, ER, of the present model for each major tests. The average *rms* relative error, ER, for all 128 cases is 9.8% which indicates good prediction. Typical examples of computed *rms* wave height transformation for each major test are shown in Figs. 4 and 5. From Table 4 and Figs. 4 and 5, it can be seen that the model results generally show good prediction, except the test no. STKO (broad-crested offshore mound). Furthermore, for some cases, the model tends to under-predict the wave heights very close to the shore.

4.3. *Model verification*

Since the present model is calibrated with only the data from the large-scale experiments, there is still a need of data from small-scale and field experiments for confirming ability of the present model. Three sources of experimental results are collected to verify the model, i.e. small-scale experimental data of Smith and Kraus

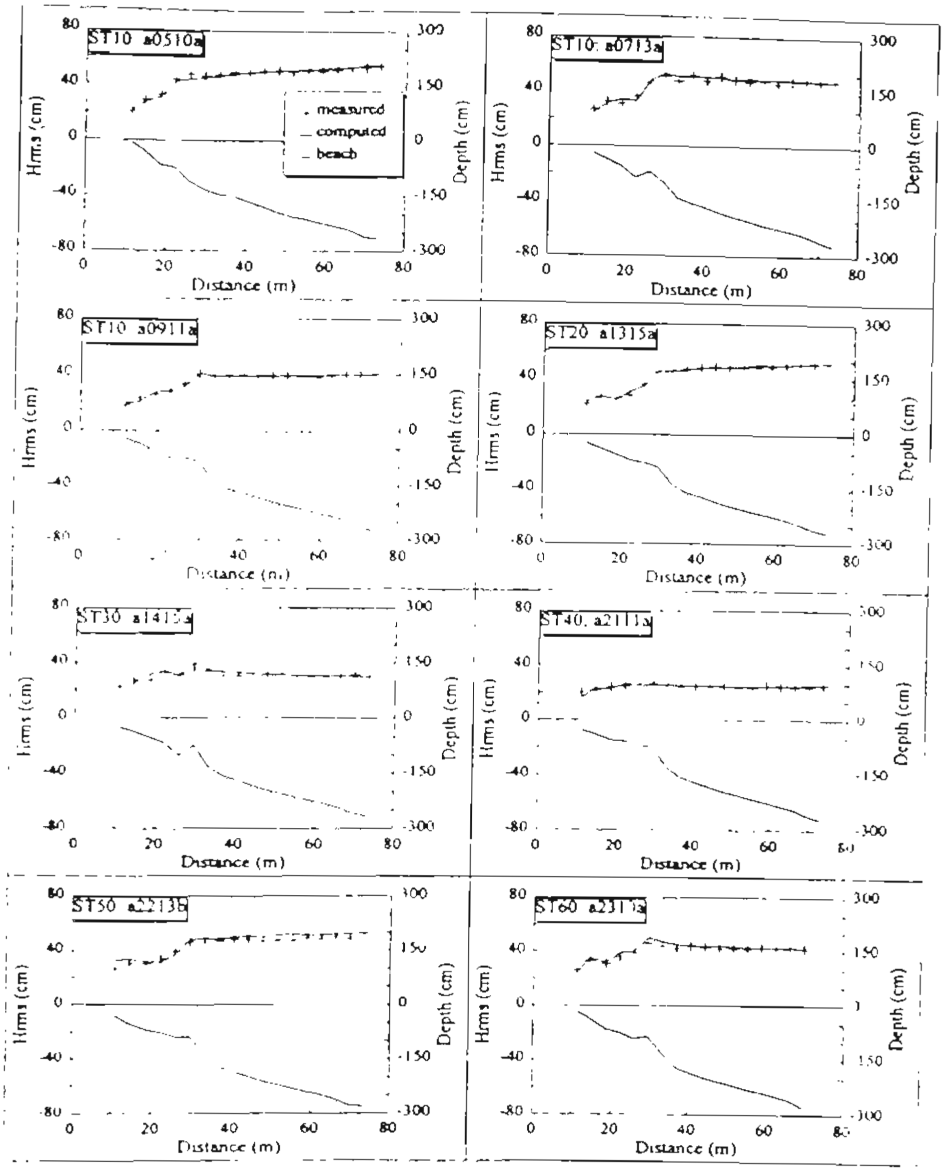

Fig. 4 Examples of computed and measured *rms* wave height transformation for Test No. ST10-ST60 (measured data from Kraus and Smith, 1994)

(1990), field data from the DELILAH project (Smith *et al.*, 1993) and field data of Thornton and Guza (1986).

The wave height transformation is computed from the energy flux balance equation [Eq. (35)] by using backward finite difference scheme, from offshore boundary to shoreline. All coefficients in the model are kept to be constant for all cases in the verification.

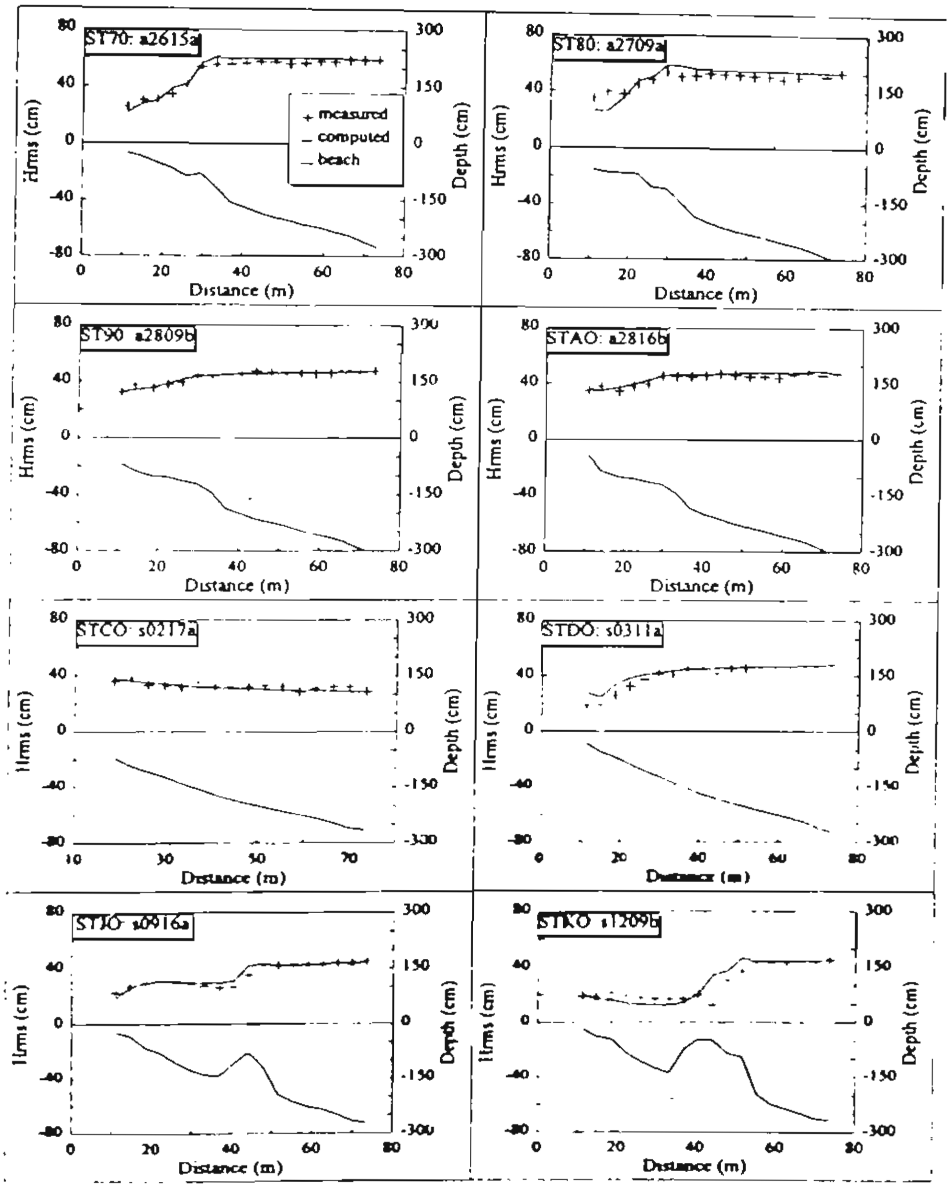

Fig. 5. Examples of computed and measured *rms* wave height transformation for Test No. ST70-STKO (measured data from Kraus and Smith, 1994).

4.3.1. *Comparison with small-scale laboratory data*

The small-scale laboratory data of Smith and Kraus's (1990) is used in this subsection. The experiment was conducted to investigate the macro-features of wave breaking over bars and artificial reefs using small wave tank of 45.70-m-long, 0.46-m-wide, and 0.91-m-deep. Both regular and irregular waves were employed in this experiment. Total 12 cases were performed for irregular wave tests. Three irregular wave conditions were generated for three bar configurations as well as for a plane beach.

Comparison between measured and computed *rms* wave heights for all cases are shown in Fig. 6. The average *rms* relative error, *ER*, for all cases is 11.9% which indicates a good prediction of the model. Figure 7 shows the typical examples of

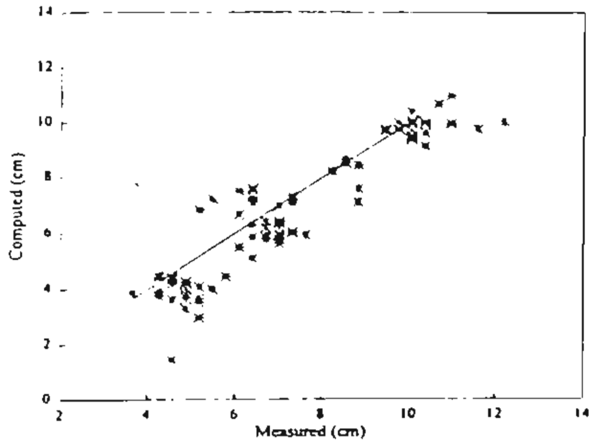

Fig. 6. Comparison between computed and measured *rms* wave height for 12 cases of small-scale experiments (measured data from Smith and Kraus, 1990)

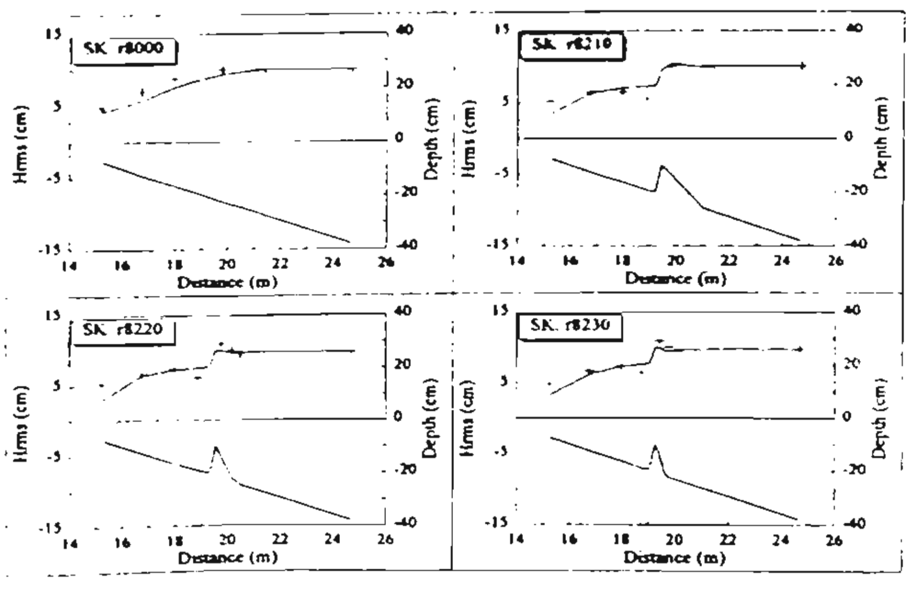

Fig. 7. Examples of computed and measured *rms* wave height transformation for incident *rms* wave height of 10 cm, peak period of 1.75 s, and four bottom conditions (measured data from Smith and Kraus, 1990).

computed *rms* wave height transformation for incident *rms* wave height of 10 cm, peak period of 1.75 s and four bottom conditions. The model results generally show good agreement with the measured data. However, the model could not predict the rapid increase and decrease in wave heights near the narrow-crested bar. Also, the model gives under prediction for the wave heights close to the shore.

4.3.2. *Comparison with field data*

Two field data from the DELILAH project (Smith *et al.*, 1993) and Thornton and Guza (1986) are used in this subsection. DELILAH (Duck Experiment on Low-frequency and Incident-band Longshore and Across-shore Hydrodynamics) project was conducted on the barred beach in Duck, North Carolina, USA, to measure currents waves, wind, tide, and beach profiles, during the period October 1–19, 1990.

Thornton and Guza's (1986) experiment was conducted on a beach with nearly straight and parallel depth contours at Leadbetter Beach, Santa Barbara, California, USA, to measure longshore currents, waves, and beach profiles, during the period January 30 to February 23, 1980.

Comparison between computed and measured wave heights for all cases are shown in Fig. 8. The average *rms* relative error, ER, comparing with the data from DELILAH project and Thornton and Guza (1986) are 14.5%, and 14.4%, respectively.

Figure 9 shows the typical examples of computed and measured *rms* wave height transformation for the cases of DELILAH project. The model results generally show good agreement with the measured data. However, the predicted wave heights are consistently smaller than the measured wave heights shoreward the bar

Figure 10 shows the typical examples of computed and measured *rms* wave height transformation for the cases of Thornton and Guza (1986). The model results also

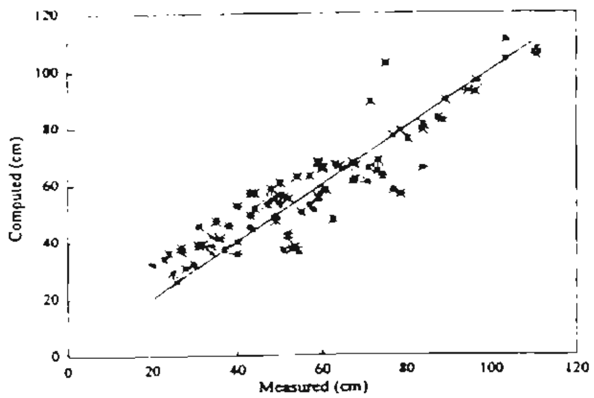

Fig. 8. Comparison between computed and measured *rms* wave height for 8 cases of field experiments (measured data from Smith *et al.*, 1993, and Thornton and Guza, 1986).

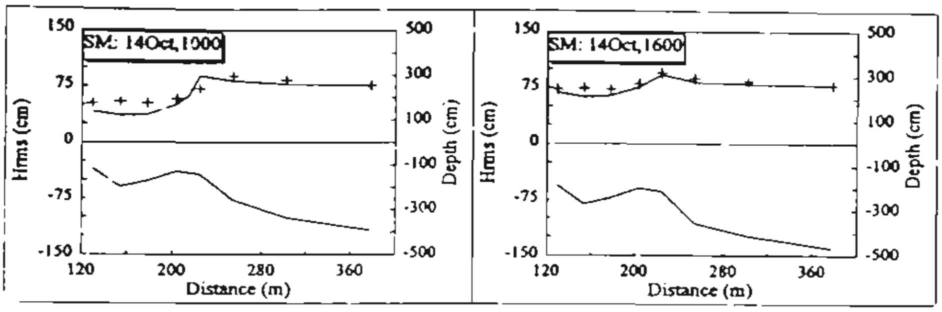

Fig. 9. Examples of computed and measured *rms* wave height transformation for cases 1000 and 1600 (measured data from Smith *et al.*, 1993).

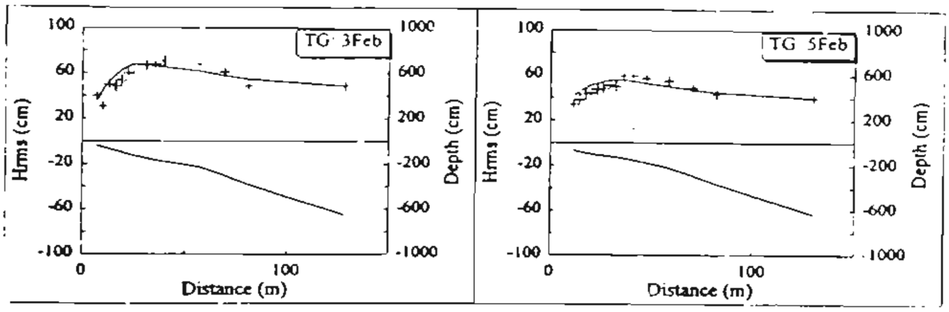

Fig. 10. Examples of computed and measured *rms* wave height transformation for cases 3 Feb and 5 Feb (measured data from Thornton and Guza, 1986).

generally show good agreement with the measured data. However, the model gives slightly over estimation in the offshore region.

5. Conclusions

The energy dissipation models for regular and irregular breaking waves were developed and applied to compute wave heights by using energy flux conservation law. The energy dissipation model for regular breaking waves was developed based on the analysis of energy dissipation models of previous researchers. The energy dissipation model for irregular breaking waves was developed based on the present regular breaking wave model and on the local fraction of breaking waves. The models were examined using published experimental data from 13 sources (638 wave profiles in total). The results of verification can be summarized as follows:

(1) For regular wave conditions, the model was verified by using small and large scale laboratory data. The results of computed wave height of present model are better than those of Dally *et al.* (1985)'s model. The average *rms* relative error by the present model is 15.8% while that by Dally *et al.*'s model is 17.8%.

(2) For irregular wave conditions, the model was capable of simulating the increase in *rms* wave height due to shoaling and subsequent decrease due to wave breaking over wide range of wave conditions and various shapes of beach profiles. The validity of model was confirmed by small and large scale laboratory and field data. The average *rms* relative error, ER, of the model is 10.0%.

Acknowledgments

The authors wish to express their gratitude to Prof. Yoshimi Goda of the Yokohama National University for his comments and fruitful discussions. This research was sponsored by the Thailand Research Fund.

References

Battjes, J. A. and Janssen, J.P.E.M. (1978). Energy loss and set-up due to breaking of random waves, *Proc. 16th Coastal Engineering Conf.*, ASCE, pp. 569–587.

Dally, W. R., Dean, R. G. and Dalrymple, R. A. (1985). Wave height variation across beach of arbitrary profile, *J. Geo. Res.* 90, C6, pp. 11917–11927.

Dally, W. R. (1992). Random breaking waves: Field verification of a wave-by-wave algorithm for engineering application, *Coastal Engineering* 16: 369–397.

Ebersole, B. A. (1987). Measurement and prediction of wave height decay in the surf zone, *Proc. Coastal Hydrodynamics '87*, ASCE, pp. 1–16.

Goda, Y. (1970). A synthesis of breaking indices, *Trans. Japan Soc. Civil Eng.* 2, Part 2, pp. 227–230.

Hansen, J. B. and Svendsen, I. A. (1984). A theoretical and experiment study of undertow, *Proc. 19th Coastal Engineering Conf.*, ASCE, pp. 2246–2262.

Horikawa, K. and Kuo, C. T. (1966). A study of wave transformation inside surf zone, *Proc. 10th Coastal Engineering Conf.*, ASCE, pp. 217–233.

Kajima, R., Shimizu, T., Maruyama, K. and Saito, S. (1983). On-offshore sediment transport experiment by using large scale wave flume, collected data No. 1–8, Central Research Institute of Electric Power Industry, Japan (in Japanese).

Kraus, N. C. and Smith, J. M. (1994). SUPERTANK Laboratory Data Collection Project, Technical Report CERC-94-3, U.S. Army Corps of Engineers, Waterways Experiment Station, Vol. 1–2.

Larson, M. and Kraus, N.C. (1989). SBEACH: Numerical model for simulating storm-induced beach change, Technical Report CERC-89-9, U.S. Army Corps of Engineers, Waterways Experiment Station.

Le Mehaute (1962). On non-saturated breakers and the wave run-up, *Proc. 8th Coastal Engineering Conf.*, ASCE, pp. 77–92.

Nadaoka, K., Kondoh, T. and Tanaka, N. (1982). The structure of velocity field within the surf zone revealed by means of laser-doppler anemometry, Report of The Port and Harbor Research Institute **21**, 2, pp. 50–102 (in Japanese).

Nagayama, S. (1983). Study on the change of wave height and energy in the surf zone, Bach. Thesis, Civil Eng., Yokohama National University, Japan.

Okayasu, A., Shibayama, T. and Horikawa, K. (1988). Vertical variation of undertow in the surf zone, *Proc. 21st Coastal Eng. Conf.*, ASCE, pp. 478–491.

Sato, S., Fukuhama, M., and Horikawa, K. (1988). Measurement of near-bottom velocities in random waves on a constant slope, *Coastal Engineering in Japan*, JSCE **31**, 2, pp. 219–229.

Sato, S., Isayama, T. and Shibayama, T. (1989). Long-wave component in near-bottom velocity under random waves on a gentle slope, *Coastal Engineering in Japan*, JSCE **32**, 2, pp. 149–159.

Shibayama, T. and Horikawa, K. (1986). Sediment transport due to breaking waves, *Proc. JSCE*, No. 357/II-3(Hydraulic and Sanitary), pp. 1509–1522.

Smith, J. M. and Kraus, N. C. (1990). Laboratory study on macro-features of wave breaking over bars and artificial reefs, Technical Report CERC-90-12, U.S. Army Corps of Engineers, Waterways Experiment Station.

Smith, J. M., Larson, M. and Kraus, N. C. (1993). Longshore current on a barred beach: Field measurements and calculations, *J. Geophys. Res.* **98**, pp. 22727–22731.

Thornton, E. B. and Guza, R. T. (1983). Transformation of wave height distribution, *J. Geophys. Res.* **88**, pp 5925–5983.

Thornton, E. B. and Guza, R. T. (1986). Surf zone longshore currents and random waves: Field data and model, *J. Physical Oceanography* **16**, pp. 1165–1178.

A.2 Simple Model for Undertow Profile

Reprinted from:

Rattanapitikon, W. and Shibayama, T. (2000). Simple model for undertow profile, Coastal Engineering Journal (JSCE), Vol. 42, No. 1, pp.1-30.

Coastal Engineering Journal, Vol. 42, No. 1 (2000) 1–30

SIMPLE MODEL FOR UNDERTOW PROFILE

WINYU RATTANAPITIKON
Department of Civil Engineering, Sirindhorn International Institute of Technology, Thammasat University, Klong Luang, Pathum Thani 12121, Thailand
E-mail: winyu@siit.tu.ac.th

TOMOYA SHIBAYAMA
Department of Civil Engineering, Yokohama National University, 79-5 Tokiwadai, Hodogaya-ku, Yokohama 240-8501, Japan
E-mail: tomo@coast.cvg.ynu.ac.jp

Received 27 May 1999
Revised 30 September 1999

Based on a re-analysis of the existing undertow models and the experimental results, a proper explicit model is proposed for computing undertow profile inside the surf zone. The model has been derived by using the eddy viscosity approach. The model is examined using published laboratory data from six sources covering small-scale and large-scale experiments, i.e. the experiments of Nadaoka *et al.* (1982), Hansen and Svendsen (1984), Okayasu *et al.* (1988), Cox *et al.* (1994), CRIEPI (Kajima *et al.*, 1983) and SUPERTANK (Kraus and Smith, 1994). The present undertow model is considerably simpler than most of existing models. Although the model is simple, it shows good agreement with the experimental results above the bottom boundary layer. The calculation is so simple that the undertow profile can be calculated by using a pocket calculator.

Keywords: Undertow, velocity profile, surf zone.

1. Introduction

Cross-shore time-averaged velocity below wave trough, or undertow, is important in the prediction of cross-shore suspended sediment transport rate. This paper concentrates on the derivation of a model for predicting the undertow profile induced by regular breaking waves.

From the previous research works, a number of models have been established for computing undertow profiles. Since the formulas or assumptions in each model are different, the computed results from various models must differ from each other and (may be) from the measured data. We cannot see clearly which model is better than the others, because every model usually shows that it gives a good prediction being compared with a limited range of the experimental conditions. At the present state of knowledge, clearly all the existing undertow models were developed based on certain assumptions. In order to confirm the underlying assumptions in the model, wide range of experimental conditions should be used in the calibration or verification

Table 1. Summary of collected laboratory data used to validate the present model.

Sources	Case No.	Total No. of profiles	Total No. of data points	Bed conditions	Apparatus
Nadaoka *et al.* (1982)	1	7	76	plane, smooth	small-scale
	5	7	73		
Hansen and Svendsen (1984)	1	4	22	plane, smooth	small-scale
Okayasu *et al.* (1988)	1	6	62	plane, smooth	small-scale
	2	6	53		
	3	6	62		
	4	6	54		
	6	7	51		
	7	6	40		
	8	7	54		
	9	6	46		
	10	6	43		
Cox *et al.* (1994)	1	6	53	plane, rough	small-scale
CRIEPI (1983)	2.1	13	36	sandy beach	large-scale
	2.3	10	20		
	3.3	16	40		
	3.4	13	37		
	4.1	10	18		
	4.2	22	58		
	4.3	48	194		
	5.2	57	142		
	6.1	21	63		
	6.2	19	59		
SUPERTANK (1994)	STEO	8	11	sandy beach	large-scale
	STFO	4	9		
	STGO	10	16		
	STHO	10	16		
	STIO	38	67		
Total		379	1475		

of the model. Therefore, there is only one way to make the model reliable, that is, to compare the computed results with the wide range of experimental conditions. Unlike many other existing models, wide range of experimental conditions is used to develop and verify the present model.

Laboratory data of undertow profiles from six sources, including 379 undertow profiles, have been collected for calibration and verification of the present model.

These include small-scale and large-scale laboratory data obtained from a variety of wave and bottom conditions. A summary of the collected laboratory data is given in Table 1. Case number in Table 1 is kept to be the same as the originals. The experiments of Nadaoka *et al.* (1982), Hansen and Svendsen (1984) and Okayasu *et al.* (1988) were performed over the smooth bed conditions, while the experiments of CRIEPI (Kajima *et al.*, 1983), SUPERTANK (Kraus and Smith, 1994) and Cox *et al.* (1994) were performed over the rough bed conditions. The experiments of CRIEPI (Kajima *et al.*, 1983) and SUPERTANK (Kraus and Smith, 1994) were performed in large-scale wave flume and other experiments were performed in small-scale wave flume.

Due limited measuring points in the large-scale experiments of CRIEPI (Kajima *et al.*, 1983) and SUPERTANK (Kraus and Smith, 1994), the measured data may be difficult to use in the model calibration. Only the measured undertow inside the surf zone of Nadaoka *et al.* (1982), Hansen and Svendsen (1984), Okayasu *et al.* (1988) and Cox *et al.* (1994) are used to calibrate the present model. However, all of the collected data are used to verify the present model.

The present paper has two main parts. The first part is model development (described in Secs. 2–5). The other is model verification (described in Sec. 6).

2. Governing Equation

For computing the beach deformation, the undertow model should be kept as simple as possible because of the frequent changing of wave and bottom profiles. Therefore the present undertow profile is calculated based on the assumption of eddy viscosity model. By considering time-averaged values, the eddy viscosity model can be expressed as

$$\tau = \rho \nu_t \frac{\partial U}{\partial z} \tag{1}$$

where τ is the time-averaged shear stress, ρ is fluid density, ν_t is the time-averaged eddy viscosity coefficient, U is the time-averaged velocity or undertow, and z is the upward vertical coordinate from the bed.

To solve the eddy viscosity model [Eq. (1)], the expression of τ/ν_t should be known and one boundary condition of velocity should be also given. The mean velocity (vertically averaged from bed to wave trough), U_m, is used as the boundary condition of Eq. (1). The following section deals with the expression of τ/ν_t. The mean velocity, U_m, is described in Sec. 4.

3. Vertical Distribution of Shear Stress and Eddy Viscosity Coefficient

In the eddy viscosity model, vertical distribution of shear stress, τ, and eddy viscosity coefficient, ν_t, are important for the analysis of vertical distribution of the undertow.

Okayasu *et al.* (1988) showed through experiments that the vertical distribution of the shear stress and eddy viscosity coefficient, from bed to wave trough, are linear functions of the vertical elevation. Since the turbulence in the surf zone is mainly caused by broken waves, the shear stress and eddy viscosity coefficient may depend on the rate of energy dissipation due to wave breaking. Thus the formula of shear stress, τ, is assumed to be

$$\tau = \rho^{1/3} D_B^{2/3} \left[k_1 \frac{z}{d} + k_2 \right] \tag{2}$$

where D_B is the energy dissipation rate of a broken wave, d is the water depth at wave trough, k_1 and k_2 are the coefficients.

The eddy viscosity coefficient, ν_t, is calculated by

$$\nu_t = k_3 \left(\frac{D_B}{\rho} \right)^{1/3} z \tag{3}$$

where k_3 is also a coefficient.

So, τ/ν_t can be expressed as

$$\frac{\tau}{\nu_t} = \rho^{2/3} D_B^{1/3} \left[\frac{k_4}{d} + \frac{k_5}{z} \right] \tag{4}$$

where $k_4 = k_1/k_3$, and $k_5 = k_2/k_3$.

The main attention in this section is to find out the appropriate values of the coefficients k_4 and k_5 in Eq. (4). It should be noted that, the ratio of turbulent shear stress and eddy viscosity coefficient in Eq. (4) depends only on energy dissipation of the breaking waves. The turbulence caused by bed roughness is not included in this equation. This means that Eq. (4) may be invalid at the region closed to the bed (inside the bottom boundary layer). For the rough bed experiments, only the laboratory data outside the boundary layer is used in the model calibration.

The experiments of Nadaoka *et al.* (1982), Hansen and Svendsen (1984), Okayasu *et al.* (1988) and Cox *et al.* (1994) are used to examine the ability of Eq. (4). Since the measured values of τ and ν_t are not available, we have to examine Eq. (4) in terms of velocity. Substituting Eq. (4) into Eq. (1), then take an integration, the time-averaged velocity or undertow profile can be expressed as

$$U = \int \left(\frac{D_B}{\rho} \right)^{1/3} \left[\frac{k_4}{d} + \frac{k_5}{z} \right] dz \tag{5}$$

Then

$$U = \left(\frac{D_B}{\rho} \right)^{1/3} \left[\frac{k_4 z}{d} + k_5 \ln z \right] + U_a \tag{6}$$

where U_a is an integral constant.

The mean velocity, U_m, is defined as

$$U_m = \frac{1}{d}\int_{z_0}^{d} U dz \tag{7}$$

where z_0 is the height of bottom roughness.

Substituting Eq. (6) into Eq. (7) then taking an integration and assuming z_0 is very small comparing with the water depth of wave trough (d), the integral constant U_a is expressed as

$$U_a = U_m - \left(\frac{D_B}{\rho}\right)^{1/3}\left[\frac{k_4}{2} + k_5(\ln d - 1)\right] \tag{8}$$

Substitution of Eq. (8) into Eq. (6) yields

$$U = \left(\frac{D_B}{\rho}\right)^{1/3}\left[k_4\left(\frac{z}{d} - \frac{1}{2}\right) + k_5\left(\ln\frac{z}{d} + 1\right)\right] + U_m \tag{9}$$

According to the difference of observed breaking wave shape, Svendsen *et al.* (1978) suggested to divide the surf zone into transition zone and inner zone. The behavior of the variation of wave height and mean water level inside the transition zone is quite different from the inner surf zone. In the transition zone, wave height decays rapidly and mean water level is relatively constant then abrupt change in slope at the transition point [Svendsen, 1984(a); and Basco and Yamashita, 1986]. Okayasu (1989) defined the transition point as the point where fully developed bore-like wave is formed. It is interesting to note that from the experimental results of Nadaoka *et al.* (1982), Okayasu *et al.* (1988) and Cox *et al.* (1994), the maximum of mean velocity occurs at the transition point. In summary, we may use four criterions to define the transition point, i.e. mean water level, wave height, mean velocity and bore formation.

The experimental results of Okayasu (1989, pp. 33 and 36–38) show that the turbulence, induced by breaking waves, in the transition zone is different from the inner zone. Since the mechanisms of turbulence induced by breaking wave (or surface roller) in these two zones are different, the different treatment is necessary. To incorporate this process, for the sake of simplicity, Eq. (9) may be written as follows.

$$U = k_6\left(\frac{D_B}{\rho}\right)^{1/3}\left[k_4\left(\frac{z}{d} - \frac{1}{2}\right) + k_5\left(\ln\frac{z}{d} + 1\right)\right] + U_m \tag{10}$$

where k_6 is the coefficient introduced herein to account for the growing of surface roller in the transition zone.

In order to investigate the validity of the model, the validation data should be compatible with the assumption on which the model itself is based. As mentioned before, the proposed model is not valid inside the bottom boundary layer. Therefore the data that used to calibrate the present model should be between the upper edge of bottom boundary layer and the wave trough. Since the experiments of Nadaoka *et al.* (1982), Hansen and Svendsen (1984) and Okayasu *et al.* (1988) were performed under the smooth bed conditions, all measured velocities below the wave trough are used in the present study. However, the experiment of Cox *et al.* (1994) was perform under the rough bed condition. Therefore only the measured velocities between the upper edge of bottom boundary layer and the wave trough were used.

The multi-regression analysis between measured U versus $(\frac{z}{d}-\frac{1}{2})$ and $(\ln\frac{z}{d}+1)$ is performed to determine the measured U_m and to justify the use of Eq. (10). Totally 76 measured undertow profiles inside the surf zone of Nadaoka *et al.* (1982), Hansen and Svendsen (1984), Okayasu *et al.* (1988) and Cox *et al.* (1994) are analyzed. The averaged regression coefficient (R^2), of 76 undertow profiles, is 0.86. This means that the Eq. (10), or Eq. (4), is fitted well with the measured undertow profiles inside the surf zone.

From the bore model (Thornton and Guza, 1983), D_B can be expressed as

$$D_B = \frac{\rho g H^3}{4Th} \tag{11}$$

where g is the acceleration of the gravity, H is the wave height, T is the wave period, and h is the mean water depth.

Substituting Eq. (11) into Eq. (10), the formula of U becomes

$$U = k_6\left(\frac{gH^3}{4Th}\right)^{1/3}\left[k_4\left(\frac{z}{d}-\frac{1}{d}\right)+k_5\left(\ln\frac{z}{d}+1\right)\right]+U_m \tag{12}$$

Equation (12) shows that the derived undertow profile consists of two parts, i.e. linear part and logarithmic part, and contains three coefficients, k_4–k_6.

In order to evaluate the accuracy of the prediction, the verification results are presented in terms of root mean square relative error (ER), which expressed as:

$$ER = 100\sqrt{\frac{\sum_{i=1}^{tn}(U_{ci}-U_{oi})^2}{\sum_{i=1}^{tn}U_{oi}^2}} \tag{13}$$

where i is the velocity number, U_{ci} is the computed velocity of number i, U_{oi} is the measured velocity of number i, tn is the total number of measured velocity.

According to Rattanapitikon and Shibayama (1993), the coefficient k_6 is taken to be 0.3 at the breaking point and to be 1 at the inner surf zone. Since the measured undertow profiles of Nadaoka *et al.* (1982) and Okayasu *et al.* (1988) show logarithmic profile at the breaking point [see Figs. 2(a), 2(d), 3(a), 3(d), 3(g) and 3(j)]. The coefficient k_4 [of the linear part of Eq. (12)] may be caused by the surface roller which is zero at the breaking point and gradually increase in transition zone until fully developed at the transition point and inner surf zone. Therefore the coefficient k_4 is taken to be 0 at the breaking point and to be 1 at the inner surf zone (including transition point). The optimal values of k_5 at the breaking point and inner surf zone are determined by trial and error. The minimum error, ER, between measured and computed undertow profile is obtained when $k_5 = -0.21$ at both the breaking point

Coefficients	Breaking point	Inner surf zone
k_4	0.00	1.00
k_5	-0.21	-0.21
k_6	0.30	1.00

and inner surf zone. The coefficients k_4–k_6 at the breaking point and inner surf zone are summarized as above.

In the transition zone, the coefficients k_4 and k_6 are assumed to increase linearly with distance from breaking point to the transition point. The coefficient k_5 is assumed to be -0.21 throughout the transition zone. The formula for undertow profile, therefore, can be written as

$$U = b_1 \left(\frac{gH^3}{4Th}\right)^{1/3} \left[b_2\left(\frac{z}{d} - \frac{1}{2}\right) - 0.21\left(\ln\frac{z}{d} + 1\right)\right] + U_m \tag{14}$$

where b_1 and b_2 are the coefficients and expressed as

$$b_1 = \begin{cases} 0.3 + 0.7\dfrac{x_b - x}{x_b - x_t} & \text{transition zone} \\ 1 & \text{inner zone} \end{cases}$$

$$b_2 = \begin{cases} \dfrac{x_b - x}{x_b - x_t} & \text{transition zone} \\ 1 & \text{inner zone} \end{cases}$$

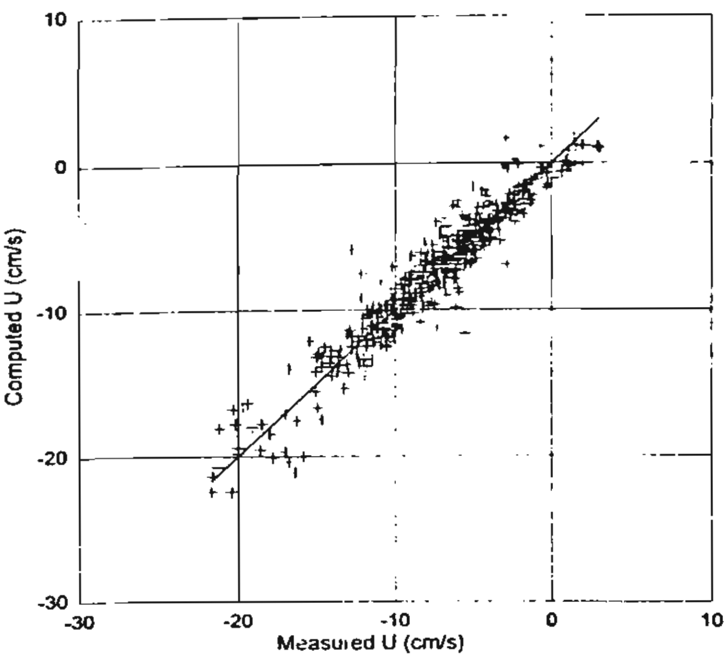

Fig. 1. Comparison between measured and computed undertow U inside the surf zone; the mean velocity U_m is given data (measured data from four sources as shown in Table 2).

where x is the position in cross-shore direction, x_b is the position at the breaking point, and x_t is the position at the transition point.

Unlike some existing models (e.g. the model of Cox and Kobayashi, 1997), calibration or adjustment of free parameters is not required for each case. All coefficients in the present model are kept to be constant for all cases of the computation. Figure 1 shows the comparison between measured U and computed U from Eq. (14) in which the measured U_m is the input data. Figures 2 and 3 show the examples of measured and computed undertow profiles in which the measured U_m is the input data. Table 2 shows the rms relative error, ER, of the present model for each case.

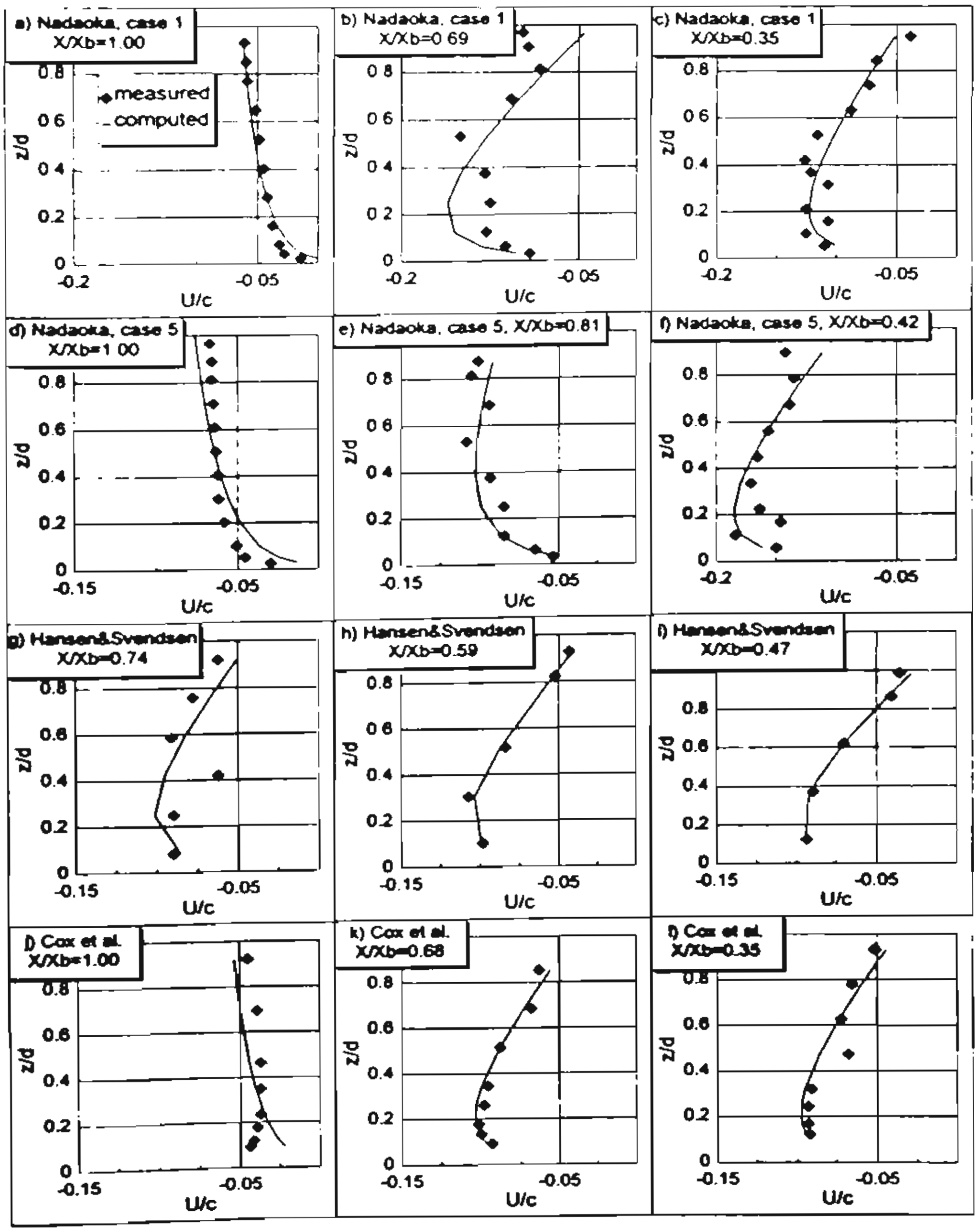

Fig. 2. Examples of measured and computed undertow profiles in which the mean velocity U_m is given data (measured data from Nadaoka *et al.*, 1982; Hansen and Svendsen, 1984; and Cox *et al.*, 1994).

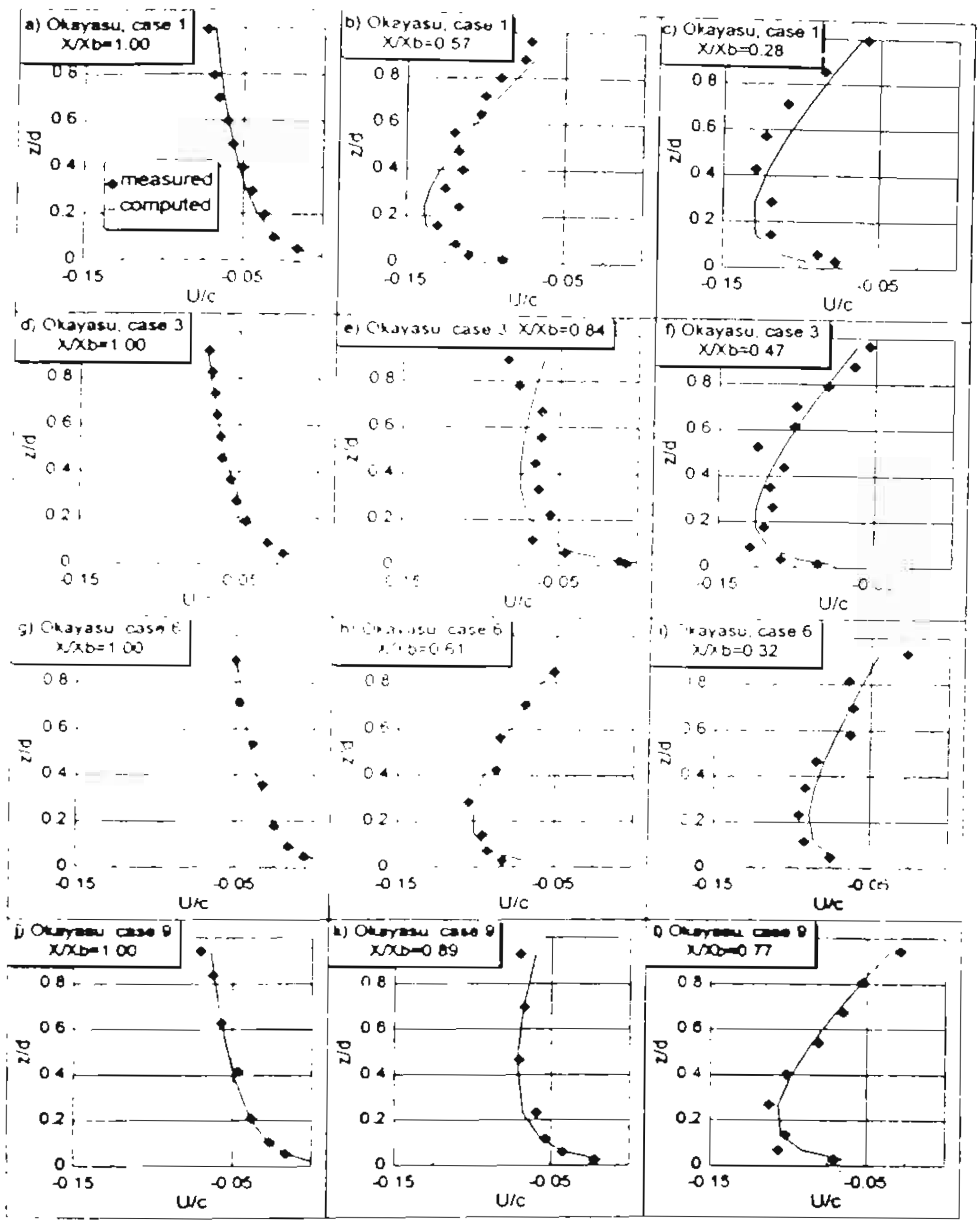

Fig. 3. Examples of measured and computed undertow profiles in which the mean velocity U_m is given data (measured data from Okayasu *et al.*, 1988).

The *rms* relative error, ER, for all 76 data sets is 15%. From Figs. 1–3 and Table 2, we can judge that the Eq. (14) is accurate enough to be used for computing the profile (or shape) of undertows in the surf zone.

4. Mean Velocity

The mean velocity, U_m, is assumed to consist of two components, one is due to the wave motion and the other one due to the surface roller [Svendsen, 1984(b)].

$$U_m = U_w + U_r \tag{15}$$

Table 2. Root mean square relative error (ER) of computed undertow from Eq. (14) in which measured u_m is the given data.

Sources	Case No.	Total No. of profiles	Total No. of data points	ER of Eq. (14)
Nadaoka *et al.* (1982)	1	6	65	19.76
	5	5	51	11.88
Hansen and Svendsen (1984)	1	4	22	13.68
Okayasu *et al.* (1988)	1	6	62	13.91
	2	6	53	16.09
	3	6	62	16.03
	4	6	54	13.99
	6	7	51	14.35
	7	6	40	16.43
	8	7	54	10.83
	9.	6	46	13.40
	10	6	43	20.20
Cox *et al.* (1994)	1	5	43	13.08
Total		76	646	15.06

where U_w is the mean velocity due to wave motion, and U_r is the mean velocity due to surface roller.

Various formulas for computing U_w and U_r have been suggested by the previous researchers. However, no direct literature has been published to describe clearly the applicability and accuracy of each formula. Therefore, the objectives of this section are to investigate the performance of each formula and to develop the appropriate one comparing with the collected experimental results. The mean velocity due to wave motion and due to surface roller are presented in Secs. 4.1 and 4.2, respectively.

4.1. *Mean velocity due to wave motion*

From the previous studies, the following explicit formulas have been suggested to compute the mean velocity due to wave motion.

(a) Svendsen [1984(b)] proposed to compute the mean velocity due to wave motion as

$$U_w = -B_0 c \left(\frac{H}{h}\right)^2 \tag{16}$$

where $B_0 = \frac{1}{T}\int_0^T (\eta/H)^2 dt$ is the wave shape parameter, which equals 1/8 for sinusoidal waves, c is the phase velocity, η is the water surface elevation measured from mean water level, and t is time.

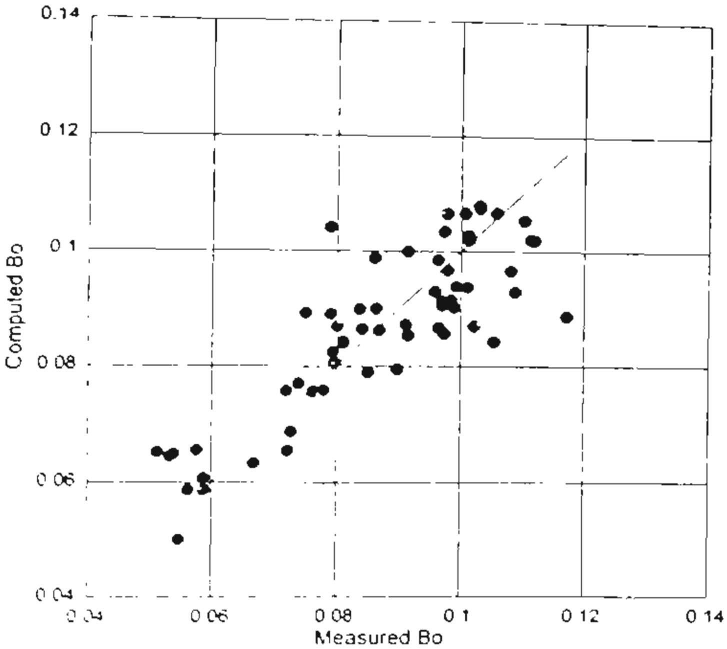

Fig. 4. Comparison between measured and computed wave shape parameter B_0 (measured data from Hansen and Svendsen, 1984, and Okayasu *et al.*, 1988).

Svendsen [1984(b)] suggested to use $B_0 = 0.08$, while Hansen and Svendsen (1987) suggested to use $B_0 = 0.09$. However, from the experimental results of Hansen and Svendsen (1984) and Okayasu *et al.* (1988), B_0 varies with a quite wide range of varieties from 0.05 to 0.11. Therefore it may not suitable to use B_0 as a constant value. Using the measured B_0 of Hansen and Svendsen (1984) and Okayasu *et al.* (1988), the following formula is fitted well with the measured B_0 in the surf zone ($R^2 = 0.81$, see Fig. 4):

$$B_0 = 0.125 + 0.6m_b - 0.089\frac{H}{h} \tag{17}$$

where m_b is the mean bottom slope.

(b) Hansen and Svendsen (1987) found that the oscillatory particle velocities are significantly smaller than predicted by linear wave theory. Therefore, equation for computing U_w of Svendsen [1984(b)] is modified to be

$$U_w = -k_7 B_0 c \left(\frac{H}{h}\right)^2 \tag{18}$$

where k_7 is the coefficient and $k_7 = 0.7$ is recommended by Hansen and Svendsen (1987).

(c) Stive and Wind (1986) proposed an empirical formula for computing the mean velocity for entire surf zone as

$$U_m = -0.1H\sqrt{\frac{g}{h}} \tag{19}$$

The coefficient 0.1 is from the best fit with the laboratory data. However, Stive and Battjes (1984) suggested using this coefficient as 0.125.

Equation (19) may be written in the form of $U_w + U_r$ as

$$U_m = -k_8 H \sqrt{\frac{g}{h}} - k_9 H \sqrt{\frac{g}{h}} \tag{20}$$

where k_8 and k_9 are the coefficients.

Therefore the mean velocity due to wave motion, U_w, of Stive and Wind (1986) can be expressed as

$$U_w = -k_8 H \sqrt{\frac{g}{h}} \tag{21}$$

(d) Sato *et al.* (1988) proposed to use Eulerian mass transport velocity as

$$U_w = \frac{1}{8}\frac{\sigma H^2 \coth(kh)}{h} \tag{22}$$

where σ is the angular frequency, and k is the wave number.

Using dispersion equation, the Eq. (22) can be rewritten as

$$U_w = -\frac{1}{8}\frac{gh^2}{ch} \tag{23}$$

As found by Hansen and Svendsen (1987) and Okayasu (1989, page 61) that linear wave theory give an overestimation of U_w, the Eq. (23) may be written as

$$U_w = -k_{10}\frac{gH^2}{ch} \tag{24}$$

where k_{10} is the coefficient and expected to be less than 1/8.

If the wave is not sinusoidal, the Eq. (24) may also be written as

$$U_w = -k_{11}\frac{B_0 gh^2}{ch} \tag{25}$$

where k_{11} is the coefficient and expected to be less than 1. It should be noted that the form of Eq. (25) will be the same as that of Eq. (18) for linear shallow water wave.

Based on the above previous studies (with some modifications) from (a) to (d), we see that there are four possible forms for computing U_w, i.e. Eqs. (18), (21), (24) and (25). The best-fit value of k_n for each equation can be determined by using regression analysis between measured U_w versus each possible formula of U_w.

At the breaking point: the effect of surface roller is very small and is negligible, gives $U_r = 0$ and $U_m = U_w$ (e.g. Basco and Yamashita, 1986; and Okayasu *et al.*, 1986). Therefore, the regression analysis between measured U_m (at the breaking point) versus each possible formula of U_w is used to determine the best-fit value

Table 3. Results of regression analysis of U_w and rms relative error (ER) of the four possible forms of U_w (using measured data at the breaking point).

Formulas	Best-fit k_n	R^2	ER (%)
Eq. (18): $U_w = -k_7 B_0 c \left(\frac{H}{h}\right)^2$	$k_7 = 0.83$	0.70	15.48
Eq. (21): $U_w = -k_8 H\sqrt{\frac{g}{h}}$	$k_8 = 0.05$	0.71	15.28
Eq. (24): $U_w = -k_{10}\frac{gH^2}{ch}$	$k_{10} = 0.05$	0.49	20.28
Eq. (25): $U_w = k_{11}\frac{B_0 gH^2}{ch}$	$k_{11} = 0.76$	0.83	11.68

of k_n in each possible formula. The results of regression analysis (the best-fit value of k_n and regression coefficient R^2) are shown in the second and third column of Table 3.

The computed results of U_w from the four possible formulas, using the best-fit value of k_n, are quantified in terms of rms relative error, ER. Using the best-fit value of k_n, the rms relative error, ER, of each possible formula (comparing with the measured data at the breaking point) is shown in the fourth column of Table 3. Through Table 3, among the four possible forms, the form of Eq. (25) appears to be the best. Therefore, the formula for computing U_w in the present study is

$$U_w = -0.76\frac{B_0 gH^2}{ch} \tag{26}$$

The form of Eq. (25) may also be derived (in the similar manner as Dean and Dalrymple, 1984, page 286) as follows:

Mass flux above the mean water level is defined as

$$M = \frac{1}{T}\int_0^T \int_h^{\eta+h} \rho u dz dt \tag{27}$$

where u is the horizontal orbital velocity above the mean water level (MWL).

Assuming u is proportional to horizontal orbital velocity at $z = h$:

$$u \propto \frac{gH}{2c}\cos(\sigma t) \tag{28}$$

or

$$u = k_{11}\frac{gH}{2c}\cos(\sigma t) \tag{29}$$

where k_{11} is the coefficient.

Substituting Eq. (29) into Eq. (27), then taking an integration:

$$M = \frac{1}{T}\int_0^T \int_h^{\eta+h} \rho k_{11} \frac{gH}{2c} \cos(\sigma t) dz dt = \frac{1}{T}\int_0^T \eta \frac{H}{2} \cos(\sigma t) \rho k_{11} \frac{g}{c} dt$$
$$= k_{11} \frac{\rho g H^2}{c} \frac{1}{T} \int_0^T \frac{\eta^2}{H^2} dt \quad (30)$$

Since $B_0 = \frac{1}{T}\int_0^T (\eta/H)^2 dt$, thus

$$M = k_{11} \frac{B_0 \rho g H^2}{c} \quad (31)$$

Since total mass transport in any section is equal to zero, net mass flux below the mean water level (MWL) balances that above MWL. This means that the mean velocity, due to mass transport, is

$$U_w = -\frac{M}{\rho h} = -k_{11} \frac{B_0 g H^2}{ch} \quad (32)$$

which is the same form as Eq. (25).

The volume flux below or above the trough level (Q_s) may be written as

$$Q_s = U_w d = k_{11} \frac{B_0 g H^2}{ch} d \quad (33)$$

It should be noted that the form of Eq. (33) is the same as that of Svendsen (1984b) for linear shallow water wave. Therefore Eq. (26) can be considered as a refinement of Svendsen (1984b)'s model.

4.2. *Mean velocity due to surface roller*

From the previous studies, the following explicit formulas have been suggested to compute the mean velocity due to surface roller.

(a) Svendsen [1984(b)] proposed to compute the mean velocity due to surface roller as

$$U_r = -\frac{A}{Th} \quad (34)$$

where A is the cross-sectional area of the roller.

Based on the experiment of Duncan (1981), Svendsen [1984(b)] proposed an empirical relation for computing cross-sectional area of surface roller as

$$A = k_{12} H^2 \quad (35)$$

where k_{12} is the coefficient and determined at 0.9 on the basis of the measurement of Dancan (1981). However, Sato *et al.* (1988) suggested using $k_{12} = 5.6$

on the basis of the best fit with the measured undertows of Okayasu *et al.* (1986) and Shimada (1982).

Substituting Eq. (35) into Eq. (34), U_r can be expressed as

$$U_r = -k_{12}\frac{H^2}{Th} \tag{36}$$

(b) Stive and Wind (1986) proposed the formula for computing U_m for the entire surf zone as shown in Eqs. (19) and (20). From Eq. (20), U_r can be expressed as follow

$$U_r = -k_9 H\sqrt{\frac{g}{h}} \tag{37}$$

(c) Okayasu *et al.* (1986) proposed to compute U_r as

$$U_r = -k_{13}\frac{cH}{d} \tag{38}$$

where k_{13} is the coefficient and determined at 0.06 on the basis of their measurements.

(d) Okayasu *et al.* (1986) and Hansen and Svendsen (1987) proposed an empirical formula for computing the cross-sectional area A as

$$A = k_{14}HL \tag{39}$$

where L is the wave length, and k_{14} is the coefficient. On the basis of the measurements the coefficient k_{14} is determined at 0.06 for Okayasu *et al.* (1986) and determined at 0.07 for Hansen and Svendsen (1987).

Substituting Eq. (39) into Eq. (34), U_r can be written as

$$U_r = -k_{14}\frac{cH}{h} \tag{40}$$

(e) Okayasu *et al.* (1988) obtained U_r by dividing the onshore mass flux by the trough level and proposed as

$$U_r = -k_{15}\frac{H^2}{dT} \tag{41}$$

where k_{15} is the coefficient and determined to be 2.3 on the basis of their measurements.

(f) Based on a hydraulic jump model of Engelund (1981), Deigaard and Fredsoe (1991) assumed the front of a broken wave is similar to that of a bore or a hydraulic jump. The cross-sectional area of the roller is approximated from the model of Engelund (1981) as

$$A = k_{16}\frac{H^3}{h} \tag{42}$$

where k_{16} is the coefficient and determined to be 1.42.

Substituting Eq. (42) into Eq. (34), U_r can be expressed as

$$U_r = -k_{16}\frac{H^3}{Th^2} \tag{43}$$

(g) It is also interesting to assume that $U_r \propto U_w$; the equation of U_r therefore can be expressed as

$$U_r = -k_{17}\frac{B_0 g H^2}{ch} \tag{44}$$

where k_{17} is the coefficient.

(h) The cross-sectional area of roller, A, may also depend on the shape of water surface. The wave shape parameter B_0 is employed as a dimensionless parameter to represent the shape of water surface. Therefore, the formulas of A in the Eqs. (35), (39) and (42) may be modified as follows

$$A = k_{18}B_0H^2 \tag{45}$$

$$A = k_{19}B_0HL \tag{46}$$

$$A = k_{20}B_0\frac{H^3}{h} \tag{47}$$

where k_{18}, k_{19}, and k_{20} are the coefficients.

Substituting Eqs. (45), (46) and (47) into Eq. (34), respectively, lead to

$$U_r = -k_{18}B_0\frac{H^2}{Th} \tag{48}$$

$$U_r = -k_{19}B_0\frac{cH}{h} \tag{49}$$

$$U_r = -k_{20}B_0\frac{H^3}{Th^2} \tag{50}$$

Based on the above previous studies (with some modifications) from (a) to (h), we will try to find out an appropriate formula for computing U_r. From Eqs. (36)–(38), (40), (41), (43), (44), (48)–(50), we see that there are ten possible forms for computing U_r.

The measured data that used in this section is the same as that in Sec. 3. The regression analysis is performed with the measured $U_m + 0.76\frac{B_0 g H^2}{ch}$ (at the breaking point and inner surf zone) versus each possible formula of U_r. The results of regression analysis (the best-fit value of k_n and regression coefficient R^2) are shown in the second and third column of Table 4. Using the best fit value of k_n, the error ER of each possible formula (comparing with the laboratory data at the breaking point and inner surf zone) is shown in the fourth column of Table 4.

Table 4. Results of regression analysis of U_r and rms relative error (ER) of the ten possible forms of U_r (using measured data at the breaking point and inner surf zone).

Formulas	Best-fit k_n	R^2	ER (%)
Eq. (36): $U_r = -k_{12}\frac{H^2}{Th}$	$k_{12} = 2.01$	0.31	33.24
Eq. (37): $U_r = -k_9 H\sqrt{\frac{g}{h}}$	$k_9 = 0.10$	0.74	20.34
Eq. (38): $U_r = -k_{13}\frac{cH}{d}$	$k_{13} = 0.08$	0.73	20.58
Eq. (40): $U_r = -k_{14}\frac{cH}{h}$	$k_{14} = 0.10$	0.74	20.35
Eq. (41): $U_r = -k_{15}\frac{H^2}{dT}$	$k_{15} = 1.56$	0.34	32.55
Eq. (43): $U_r = -k_{16}\frac{H^3}{Th^2}$	$k_{16} = 2.61$	0.10	37.89
Eq. (44): $U_r = -k_{17}\frac{B_0 g H^2}{ch}$	$k_{17} = 1.58$	0.74	20.48
Eq. (48): $U_r = -k_{18}B_0\frac{H^2}{Th}$	$k_{18} = 23.02$	0.38	31.54
Eq. (49): $U_r = -k_{19}B_0\frac{cH}{h}$	$k_{19} = 1.12$	0.75	20.06
Eq. (50): $U_r = -k_{20}B_0\frac{H^3}{Th^2}$	$k_{20} = 31.03$	0.21	35.59

Through Table 4, we see that the form of Eq. (49) has the best prediction on the mean velocity. Therefore, the formula for computing U_r in the present study is

$$U_r = -1.12B_0\frac{cH}{h} \tag{51}$$

This means that the cross-sectional area of roller, A, should be equal to $1.12B_0HL$. Up to here, we can conclude that the following formula is suitable for computing U_m.

$$U_m = \begin{cases} -0.76\dfrac{B_0 g H^2}{ch} - 1.12\dfrac{B_0 cH}{h} & \text{inner zone} \\ -0.76\dfrac{B_0 g H^2}{ch} & \text{breaking point} \end{cases} \tag{52}$$

Since there is no surface roller in the offshore zone, the value of the mean velocity caused by surface roller is zero. The formula for computing the mean velocity in the offshore zone is the same as that of at the breaking point.

Considering at the transition zone: the structure of the flow field in this zone has not yet been described in sufficient details to make it possible to identify the characteristic of the flow field. Okayasu *et al.* (1986) suggested the cross-sectional area of surface roller, A, grows linearly with distance from zero at the plunging point. Also, Basco and Yamashita (1986) suggested linear increasing of A (with distance) from zero at the breaking point for the case of spilling breaker and from zero at the plunging point for the case of plunging breaker. However, if we follow the previous researcher's assumptions, we need to define the position of the plunging point which will make the model to be more complicated. From the trial of many possible parameters, finally, we assume A increases linearly with one over square root of wave height (A is zero at the breaking point and it is fully developed at the transition point). Equation (52), therefore, can be written as

$$U_m = -0.76\frac{B_0 g H^2}{ch} - 1.12 b_3 \frac{B_0 c H}{h} \tag{53}$$

where b_3 is the coefficient and expressed as

$$b_3 = \begin{cases} 0 & \text{offshore zone} \\ \dfrac{1/\sqrt{H} - 1/\sqrt{H_b}}{1/\sqrt{H_t} - 1/\sqrt{H_b}} & \text{transition zone} \\ 1 & \text{inner zone} \end{cases}$$

where subscript b indicates the value at the breaking point, and subscript t indicates the value at the transition point.

The comparison between measured U_m and computed U_m from Eq. (53) is shown in Fig. 5. The examples of cross-shore variations of measured and computed U_m are

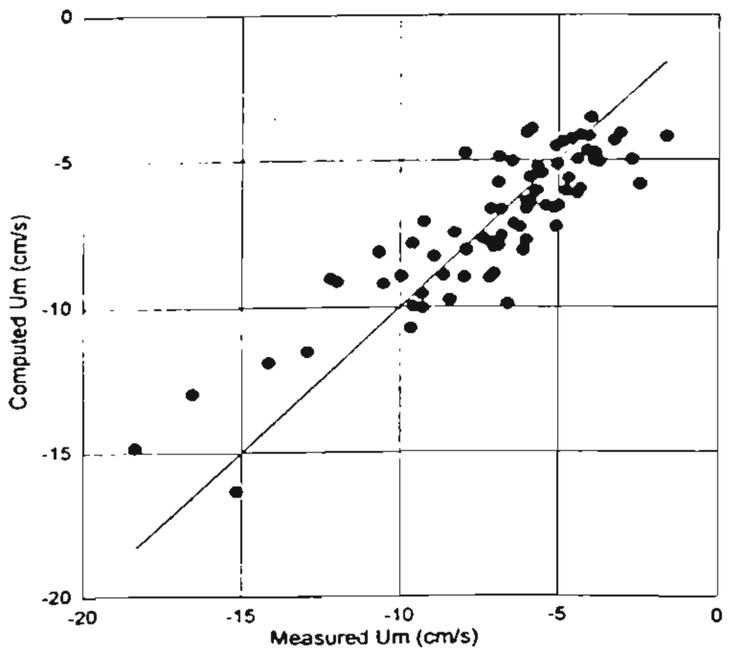

Fig. 5. Comparison between measured and computed mean velocity U_m inside the surf zone (measured data from four sources as shown in Table 2).

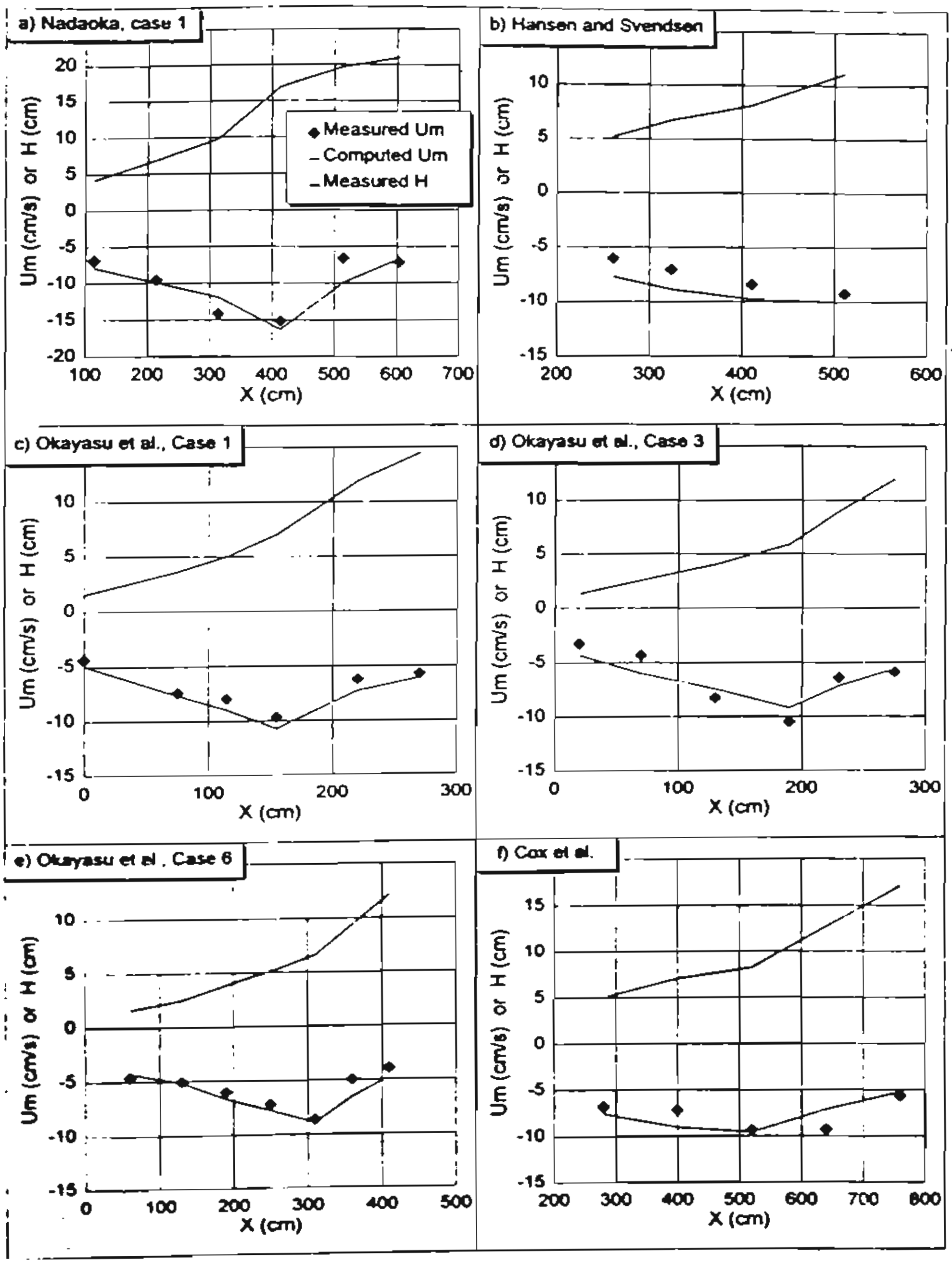

Fig. 6. Examples of cross-shore variations of measured and computed mean velocity, U_m, inside the surf zone (measured data from four sources as shown in Table 2).

shown in Fig. 6. We can see from Figs. 5 and 6 that the mean velocities are predicted well in general cases, but the variation of computed U_m is rather smoother than the measured U_m. However, for the experiment of Hansen and Svendsen (1984), the present formula gives over estimations for all points of the measurements. This may indicate the limitation of the capability of present formula. Since the experimental condition of Hansen and Svendsen (1984) is not significantly different from that of Nadaoka *et al.* (1982), Okayasu *et al.* (1988) and Cox *et al.* (1994), the limitation of present formula cannot be identified at the present. More analysis is necessary to find out the limitation.

5. Recommended Procedure for Computation of Undertow Profile

The recommended procedure for computing undertow profile, is summarized as follows:

(1) Given X, z, h, H, T, d, X_b, X_t and m_b.
(2) Compute c using linear wave theory.
(3) Compute B_0, U_m and U from Eqs. (17), (53) and (14), respectively.

Although, the present model is developed for predicting the undertow profile inside the surf zone, application of the present model to the offshore zone is possible. By assuming that the turbulence in the offshore zone (above the bottom boundary layer) is very small and is negligible, the coefficients b_1 and b_2 in Eq. (14) equal to zero. Therefore, Eq. (14) for the offshore zone becomes $U = U_m$.

6. Model Verification

In order to examine the overall performance of the model, the model has been applied to the wide range of laboratory data covering small-scale and large-scale experiments, i.e. the experiments of Nadaoka *et al.* (1982), Hansen and Svendsen (1984). Okayasu *et al.* (1988), Cox *et al.* (1994), CRIEPI (Kajima *et al.*, 1983) and SUPERTANK (Kraus and Smith, 1994). Brief summary of each experiment is given below.

The experiment of Nadaoka *et al.* (1982) was conducted to reveal the structure of velocity field inside and near the surf zone. A 16.8-m-long wooden plane beach of slope 1:20 was set in a small wave flume of 44.5 m long, 0.5 m wide and 1.0 m deep The experiments were carried out under regular wave actions for 12 cases. In most cases (except cases 1 and 5) velocities were measured at elevation 0.5 m above the bottom. Only in cases 1 and 5, the velocity profiles were measured at 7 locations (P1–P7) in cross-shore direction. The measured velocities below the trough level of cases 1 and 5 are used in this study. For case 1, the measuring locations in the offshore zone, breaking point, transition zone and inner surf zone were P7, P6, P5 and P4–P1, respectively. For case 5, the measuring locations in the offshore zone breaking point, transition zone and inner surf zone were P7–P6, P5, P4 and P3–P1, respectively. The experimental conditions are shown in Table 5.

The experiment of Hansen and Svendsen (1984) was conducted to measure velocity field inside and near the surf zone over the 1:34.3 concrete plane slope. The experiment was carried out under regular wave action in a small wave flume of 32.0 m long, 0.6 m wide and 0.6 m deep. The measured velocities below the trough level are used in this study. The velocity profiles were measured at 6 locations (L1–L6) in cross-shore direction. The first and second measuring positions (L1 and L2) were set in the offshore zone. The third measuring position (L3) was set in the transition zone. The other positions (L4–L6) were located in the inner surf zone. Only

Table 5. Root mean square relative error (ER) of the present model comparing with the small-scale experiments.

Sources	Case No.	m_b	T (s)	H_i (cm)	h_i (cm)	Total No. of profiles	Total No. of data points	ER of present model
Nadaoka *et al.* (1982)	1	1/20	1.32	21.6	70.0	7	76	27.17
	5	1/20	2.34	21.9	70.0	7	73	22.61
Hansen and Svendsen (1984)	1	1/34	2.00	12.0	36.0	4	22	22.60
Okayasu *et al.* (1988)	1	1/20	2.00	8.50	40.0	6	62	18.59
	2	1/20	2.00	5.63	40.0	6	53	28.41
	3	1/20	1.17	9.87	40.0	6	62	22.23
	4	1/20	0.91	6.69	40.0	6	54	24.73
	6	1/30	1.61	8.80	40.0	7	51	16.93
	7	1/30	1.97	6.17	40.0	6	40	21.00
	8	1/30	1.96	8.22	40.0	7	54	23.43
	9	1/30	1.12	8.26	40.0	6	46	28.18
	10	1/30	1.23	6.05	40.0	6	43	46.07
Cox *et al.* (1994)	1	1/35	2.20	13.22	28.0	6	53	22.55
Total						80	689	24.27

the velocity profiles at L3–L6 are available. The experimental condition is shown in Table 5.

The experiment of Okayasu *et al.* (1988) was constructed to measure the velocity field and to determine the Reynolds stress and eddy viscosity in the surf zone including the area close to the bottom. The experiments were carried out under regular wave actions in a small wave flume of 23.0 m long, 0.8 m wide and 1.0 m deep. Ten wave conditions were performed on 1:20 and 1:30 slopes of rubber and stainless plane beach. Only in case 5, the measuring points were taken close to the bottom and will not be used in this study. The measured velocities below the trough level of cases 1–10, except case 5, are used in this study. The velocity profiles were measured at 6 or 7 locations (L1–L7) in cross-shore direction. The first measuring position (L1) was set on the wave breaking point. The second measuring position (L2) was set in the transition zone. The other positions (L3–L7) were located in the inner surf zone. The experimental conditions are shown in Table 5.

The experiment of Cox *et al.* (1994) was conducted to measure velocity field inside and near the surf zone over a rough bottom. A single layer of sand grains with $d_{50} = 0.10$ cm was glued on the 1:35 plane beach to increase the bottom roughness. The experiment was carried out under regular wave action in a small wave flume of 33.0 m long, 0.6 m wide and 1.5 m deep. The measured velocities

Table 6. Root mean square relative error (ER) of the present model comparing with the large-scale laboratory data.

Sources	Case No	Time	D_{50} (mm)	T (s)	H_i (cm)	h_i (cm)	Total No. of profiles	Total No. of data points	ER of present study
CRIEPI (1983)	2.1	26.0 hr	0.47	6.0	180	350	13	36	38.95
	2.3	3.1 hr	0.47	3.1	66	350	10	20	25.95
	3.3	5.7 hr	0.27	12.0	81	450	5	13	35.62
		24.3 hr	0.27	12.0	81	450	6	17	32.13
		78.3 hr	0.27	12.0	81	450	5	10	18.01
	3.4	4.9 hr	0.27	3.1	154	450	5	16	29.51
		23.6 hr	0.27	3.1	154	450	4	10	42.78
		75.2 hr	0.27	3.1	154	450	4	11	46.89
	4.1	10.8 hr	0.27	3.5	31	350	5	9	53.52
		22.9 hr	0.27	3.5	31	350	5	9	50.36
	4.2	5.2 hr	0.27	4.5	97	400	7	22	37.23
		24.4 hr	0.27	4.5	97	400	8	22	47.99
		76.3 hr	0.27	4.5	97	400	7	14	64.20
	4.3	30.3 hr	0.27	3.1	151	400	25	100	48.37
		91.0 hr	0.27	3.1	151	400	23	94	50.94
	5.2	8.0 hr	0.27	3.1	74	350	16	44	51.85
		29.1 hr	0.27	3.1	74	350	20	47	45.14
		89.5 hr	0.27	3.1	74	350	21	51	47.12
	6.1	9.8 hr	0.27	5.0	166	400	5	18	25.29
		53.6 hr	0.27	5.0	166	400	16	45	31.91
	6.2	6.2 hr	0.27	7.5	112	450	19	59	36.84
SUPERTANK (1994)	STEO	s0315a	0.22	3.0	60	305	3	5	44.65
		s0316a	0.22	3.0	80	305	5	6	36.32
	STFO	s0410a	0.22	8.0	40	274	4	9	39.07
	STGO	s0415a	0.22	3.0	80	305	5	8	47.60
		s0416a	0.22	3.0	80	305	5	8	40.74
	STHO	s0508a	0.22	3.0	80	305	5	8	37.09
		s0510a	0.22	4.5	70	305	5	8	31.00
	STIO	s0513a	0.22	8.0	50	305	5	9	34.26
		s0514a	0.22	8.0	50	305	5	9	28.09
		s0515a	0.22	8.0	50	305	5	9	31.47
		s0516a	0.22	8.0	50	305	5	8	40.37
		s0607a	0.22	8.0	50	305	4	7	31.61
		s0610a	0.22	8.0	50	305	4	8	32.63
		s0612a	0.22	8.0	50	305	5	8	42.98
		s0614a	0.22	8.0	50	305	5	9	40.82
Total							299	786	39.03

between the upper edge of bottom boundary layer and the trough level are used in this study. The velocity profiles were measured at 6 locations (L1–L6) in cross-shore direction. The first measuring position (L1) was set on the wave breaking point. The second measuring position (L2) was set in the transition zone. The other positions (L3–L6) were located in the inner surf zone. The experimental condition is shown in Table 5.

The experiment of CRIEPI was performed by Kajima *et al.* (1983) at Central Research Institute of Electric Power Industry (CRIEPI). The experiments were performed under the condition of regular wave and movable bed in a large wave flume (205 m long, 3.4 m wide and 6 m deep). Coarse sand ($D_{50} = 0.47$ mm) and fine sand ($D_{50} = 0.27$ mm) were used in the experiments. The velocities were measured at various sections along the flume, covering both in offshore and surf zone. However at a few points, the vertical velocities were measured. Table 6 shows the CRIEPI experimental conditions that are used in this section.

The experiment of SUPERTANK Laboratory Data Collection Project (Kraus and Smith, 1994) was conducted to investigate cross-shore hydrodynamic and sediment transport processes, during the period of August 5 to September 13, 1992, at Oregon State University, Corvallis, Oregon, USA. A 76-m-long sandy beach was constructed in a large wave tank of 104 m long, 3.7 m wide and 4.6 m deep. The 20 major tests were performed and each major test consisted of several cases. Most of the major tests were performed under the irregular wave actions. However, five major tests were performed under regular wave actions, i.e. test No. STEO, STFO, STGO, STHO and STIO. The velocities were measured at various sections along the

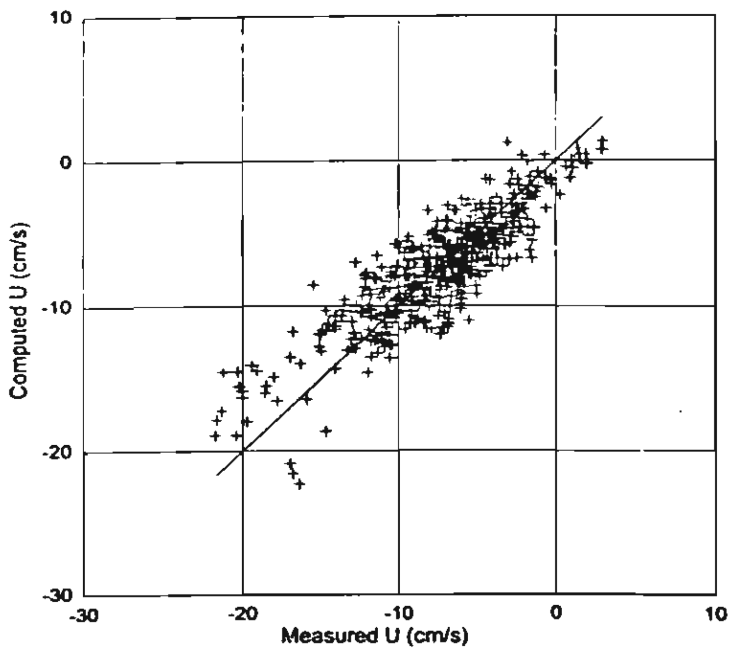

Fig. 7. Comparison between measured and computed U for all points of the measurements (measured data from four sources of small-scale experiments as shown in Table 5).

flume, covering both in offshore and surf zone. However at a few points, the vertical velocities were measured. Table 6 shows the SUPERTANK experimental conditions that are used in the verification.

6.1. *Comparison with small-scale experiments*

Four sources of the small-scale laboratory data are used to verify the present model, i.e. Nadaoka *et al.* (1982), Hansen and Svendsen (1984), Okayasu *et al.* (1988) and Cox *et al.* (1994). The undertow profiles are computed based on the procedure recommended in Sec. 5. All coefficients in the model are kept to be constant for all cases. Table 5 shows root mean square relative error (ER) of computed undertow U

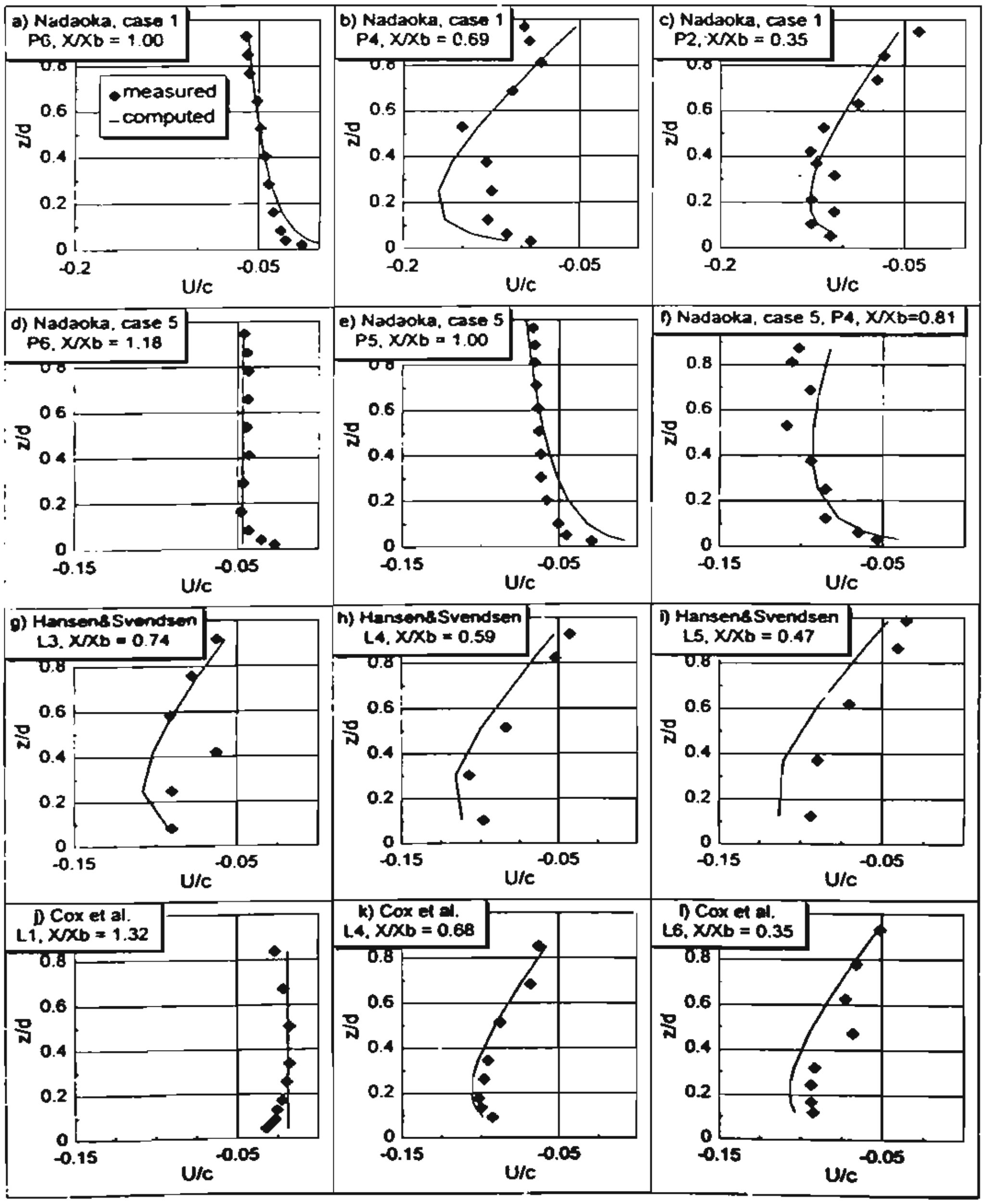

Fig. 8. Examples of measured and computed undertow profiles (measured data from Nadaoka *et al.*, 1982; Hansen and Svendsen, 1984; and Cox *et al.*, 1994).

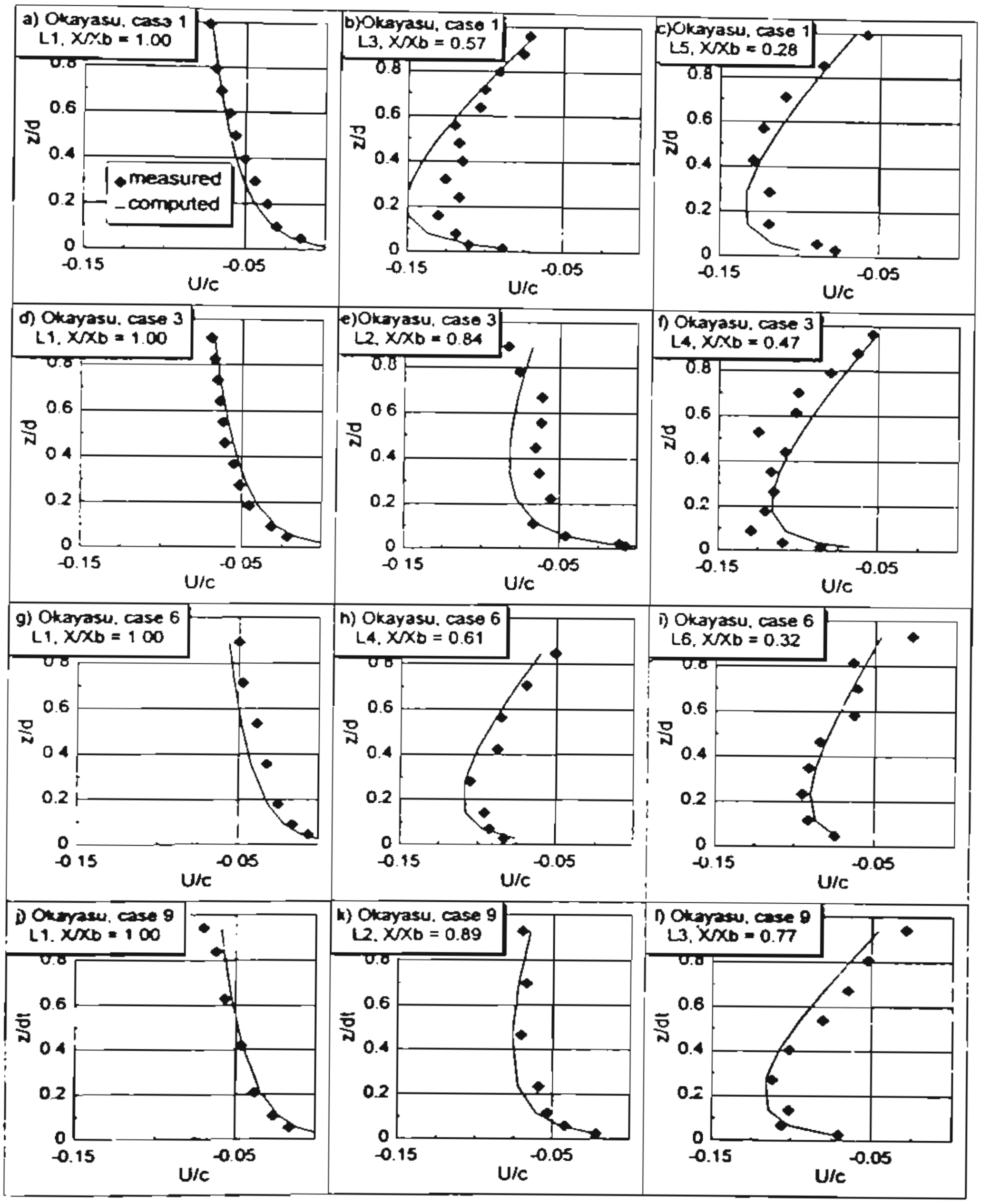

Fig. 9. Examples of measured and computed undertow profiles (measured data from Okayasu *et al.*, 1988).

for each data set. The ER of all cases is 24%. Figure 7 shows the comparison between measured and computed undertow for all points of the measurements. Examples of measured and computed undertow profiles are shown in Figs. 8–9. Through Figs. 7–9 [except 8(d) and 8(j)] and Table 5, it can be seen that the present model is quite realistic in the simulation of undertow profile in the surf zone.

The model is also applied to compute the undertow profile in the offshore zone. Figures 8(d) and 8(j) show the predicted undertow profiles in the offshore zone over the smooth bed and rough bed, respectively. The model could not predict well the velocity near and inside the bottom boundary layer. Figure 8(d) shows that the model gives under estimation of the velocity near and inside the bottom boundary layer, while Fig. 8(j) shows that the model gives over estimation. It seems to be impossible to use the simple model for predicting the velocity near and inside the bottom boundary layer in the offshore zone. However, the model gives reasonably well prediction in the region out of the bottom boundary layer. It may be accurate enough for using in the computation of suspended sediment transport above the bottom boundary layer.

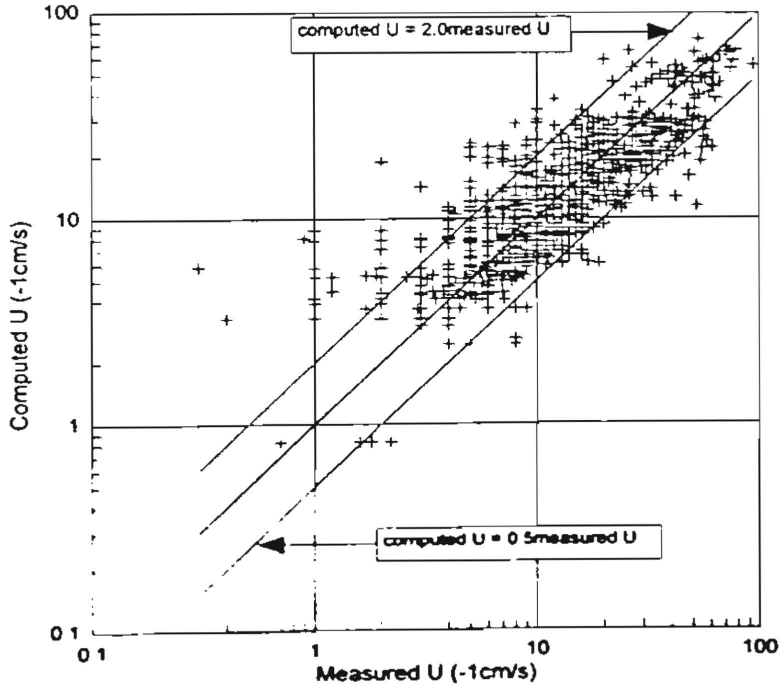

Fig. 10. Comparison between measured and computed U for all points of the measurements (measured data from two sources of large-scale experiments as shown in Table 6).

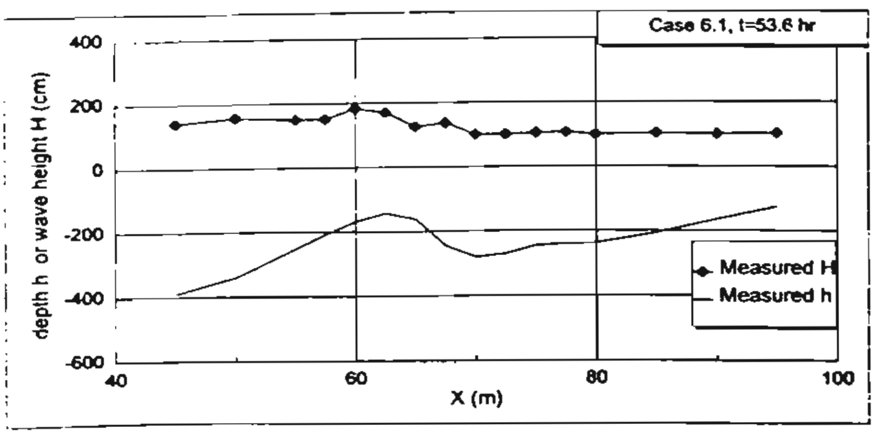

Fig. 11. Measured bottom topography and wave height variation (measured data from CRIEPI, 1983. case 6.1, time = 53.6 hr).

6.2. *Comparison with large-scale experiments*

Two sources of the large-scale laboratory data are used to verify the model, i.e. CRIEPI (Kajima *et al.*, 1983) and SUPERTANK (Kraus and Smith, 1994). The velocity profiles are computed based on the procedure recommended in Sec. 5. All coefficients in the model are kept constant for all cases in the verification. However, due to the fluctuations of measured wave heights (that is used to determine the coefficient b_3 in Eq. 53), the coefficient b_3 become negative which is impossible. To overcome this problem (only in this subsection) the coefficient b_3 is set to be equal to the coefficient b_2 in Eq. (14).

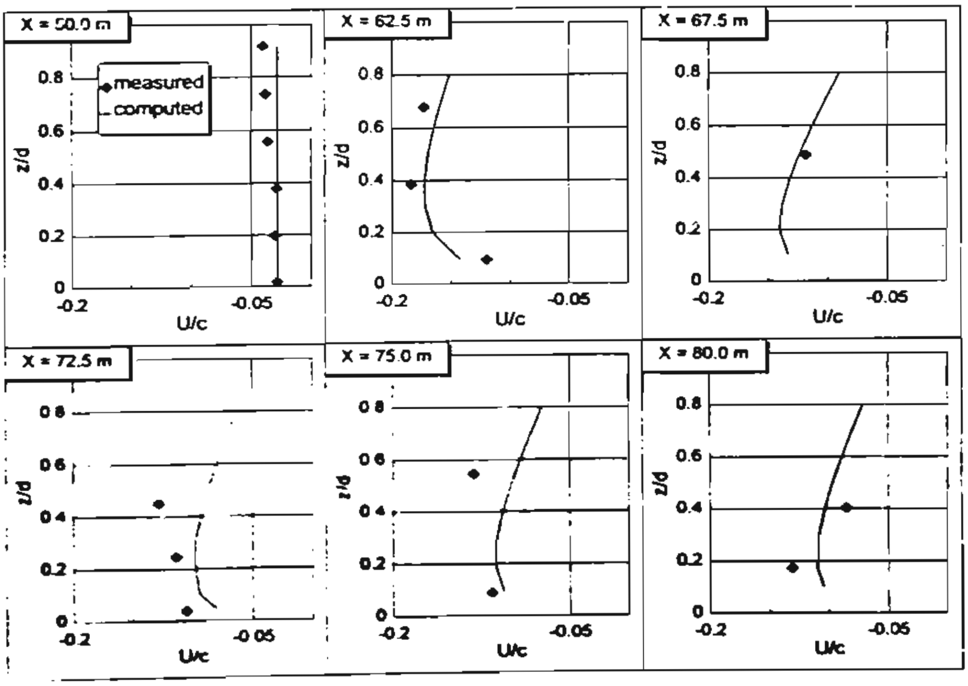

Fig. 12. Computed and measured undertow profiles (measured data from CRIEPI, 1983, case 6.1, time = 53.6 hr).

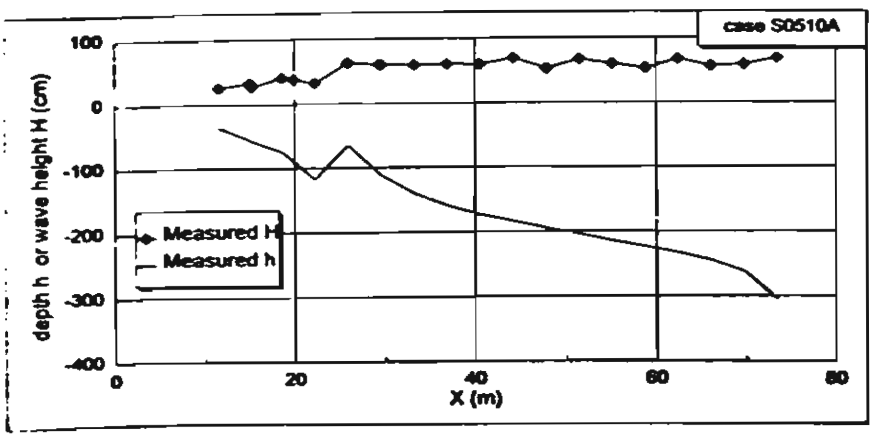

Fig. 13. Measured bottom topography and wave height variation (measured data from SUPERTANK, 1994, case s0510a).

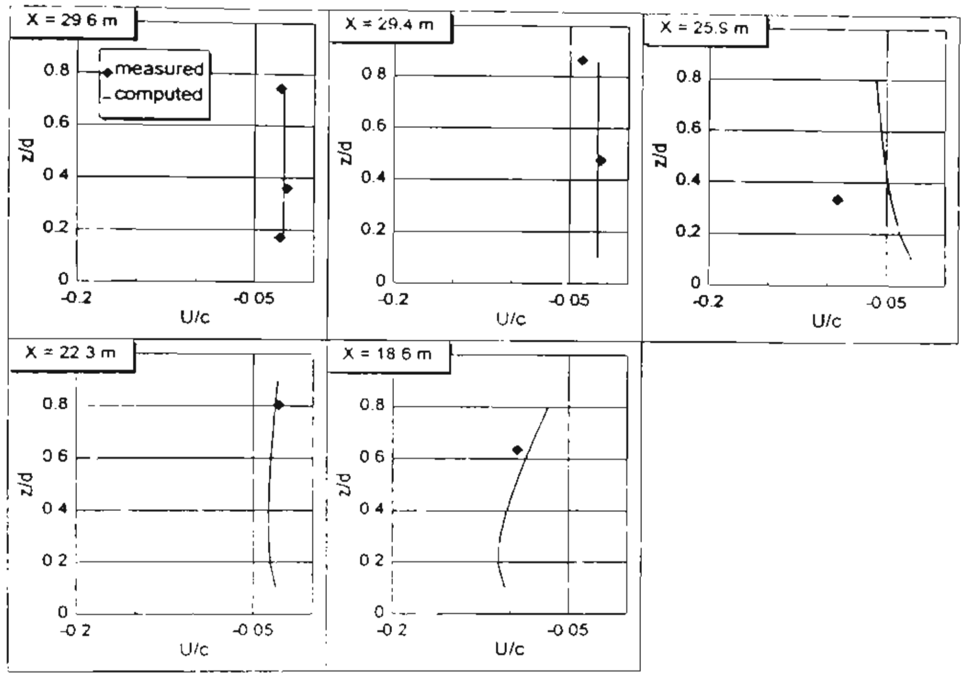

Fig. 14. Computed and measured undertow profiles (measured data from SUPERTANK, 1994, case s0510a).

The last column of Table 6 shows the *rms* relative error, ER, of the present model for each case. The *rms* relative error, ER, for all data sets is 39%. Figure 10 shows the verification results of all measuring points. It also shows about 82 percent of the predicted results are within 0.5 and 2 times the measured values Figures 12 and 14 show examples of measured and computed undertow profiles. From the general tendency of Figs. 10–14, we can judge that the present formula gives reasonably well estimations of the time-averaged velocity in the large-scale wave flume.

7. Conclusions

A simple explicit model was developed to compute undertow profile in the surf zone and then applied to the offshore zone. Published laboratory data of Nadaoka *et al.* (1982), CRIEPI (Kajima *et al.*, 1983), Hansen and Svendsen (1984), Okayasu *et al.* (1988), SUPERTANK (Kraus and Smith, 1994) and Cox *et al.* (1994) were used to calibrate and verify the model. The formula of undertow profile was derived from the eddy viscosity model. To solve the eddy viscosity model, the expression of the ratio of shear stress and eddy viscosity coefficient (τ/ν_t) should be known and one boundary condition of velocity should also be given.

The ratio of shear stress and eddy viscosity coefficient (τ/ν_t) was proposed as a function of energy dissipation rate of a broken wave. The proposed formula of τ/ν_t was used to derive the formula for determining the shape of undertow. The validity of proposed-formula (for determining the shape of undertow) was confirmed by 76 measured undertow profiles inside the surf zone and above the bottom boundary layer. The *rms* relative error, ER, of the proposed formula is 15%.

Table 7. Summary of root mean square relative error (ER) of the present model comparing with measured data of each data source.

Sources	Total No. of profiles	Total No. of data points	ER of present study
Nadaoka *et al.* (1982)	14	149	24.6
Hansen and Svendsen (1984)	4	22	22.6
Okayasu *et al.* (1988)	56	465	25.0
Cox *et al.* (1994)	6	53	22.6
CRIEPI (1983)	229	667	39.0
SUPERTANK (1994)	70	119	39.6
Total	379	1475	

The mean velocity was used as the boundary condition of the eddy viscosity model. Based on an analysis of previous formulas, the new and best formula for computing the mean velocity was proposed.

To investigate the overall performance of the model, the model was applied to the wide range of laboratory data covering small and large-scale experiments. The present model gives reasonably well estimations of the undertow profiles above the bottom boundary layers. The rms relative error, ER, of the present model for each data source is summarized in Table 7.

Acknowledgment

This research was sponsored by the Thailand Research Fund.

References

Basco, D. R. and Yamashita, T. (1986). Toward a simple model of wave breaking transition region in surf zones, *Proc. 20th Coastal Eng. Conf., ASCE*, pp. 955–970.

Cox, D. T., Kobayashi, N. and Okayasu, A. (1994). Vertical variations of fluid velocities and shear stress in surf zones, *Proc. 24th Coastal Eng. Conf., ASCE*, pp. 98–112.

Cox, D. T. and Kobayashi, N. (1997). Kinematic undertow model with logarithmic boundary layer, *J. Waterway, Port, Coastal, Ocean Eng.* **123**(6): 354–360.

Dean, R. G. and Dalrymple, R. A. (1984). Water wave mechanics for engineers and scientists, Prentice-Hall, Inc., New Jersey, USA.

Deigaard, R. and Fredsoe, J. (1991). Modelling of undertow by a one-equation turbulence model, *Coastal Eng.* **15**: 431–458.

Duncan J. H. (1981). An experimental investigation of breaking waves produced by a towed hydrofoil, *Proc. Roy. Soc. London*, Ser. **A377**: 331–348.

Engelund, F. (1981). A simple theory of weak hydraulic jumps, Institute Hydrodynamics and Hydraulic Engineering, Technical University of Denmark, Progress Report **54**: 29–32.

Hansen, J. B. and Svendsen, I. A. (1984). A theoretical and experimental study of undertow, *Proc. 19th Coastal Eng. Conf., ASCE*, pp. 2246–2262.

Hansen, J. B. and Svendsen, I. A. (1987). Surf zone breakers with current, nonlinear water waves, *IUTAM Symp.*, Tokyo/Japan, pp. 169–177.

Kajima, R., Shimizu, T., Maruyama, K. and Saito, S. (1983). On-offshore sediment transport experiment by using large scale wave flume, Collected Data No. 1–8, Central Research Institute of Electric Power Industry, Japan (in Japanese).

Kraus, N. C. and Smith, J. M. (1994). SUPERTANK laboratory data collection project, Tech. Report CERC-94-3, US Army Corps of Engineering, Waterways Experimental Station, 1–2.

Nadaoka, K., Kondoh, T. and Tanaka, N. (1982). The structure of velocity field within the surf zone revealed by means of laser-doppler anemometry, Report of the Port and Harbor Research Institute **21**(2): 50–102 (in Japanese).

Okayasu, A., Shibayama, T. and Mimura, N. (1986). Velocity field under plunging waves, *Proc. 20th Coastal Eng. Conf., ASCE*, pp. 660–674.

Okayasu, A., Shibayama, T. and Horikawa, K. (1988). Vertical variation of undertow in the surf zone, *Proc. 21st Coastal Eng. Conf., ASCE*, pp. 478–491.

Okayasu, A. (1989). Characteristics of turbulence structure and undertow in surf zone, Doctoral in Dissertation, Civil Engineering, University of Tokyo, Japan.

Rattanapitikon, W. and Shibayama, T. (1993). Vertical distribution of suspended sediment concentration in and outside surf zone, *Coastal Eng. Japan* **36**(1): 49–65.

Sato, S., Fukuhama, M. and Horikawa, K. (1988). Measurements of near-bottom velocities in random waves on a constant slope, *Coastal Eng. Japan* **31**(2): 219–229.

Shimada, M. (1982). Measurements of near-bottom velocities under irregular waves, Graduate Thesis, University of Tokyo, Japan (in Japanese).

Stive, M. J. F. and Battjes, J. A. (1984). A model for offshore sediment transport, *Proc. 19th Coastal Eng. Conf., ASCE*, pp. 1420–1436.

Stive, M. J. F. and Wind, H. G. (1986). Cross-shore mean flow in the surf zone, *Coastal Eng.* **10**: 325–340.

Svendsen, I. A., Madsen, P. A. and Hansen, J. B. (1978). Wave characteristics in the surf zone, *Proc. 16th Coastal Eng. Conf., ASCE*, pp. 520–539.

Svendsen I. A. (1984a). Wave heights and set-up in a surf zone, *Coastal Eng.* **8**: 303–329.

Svendsen I. A. (1984b). Mass flux and undertow in a surf zone, *Coastal Eng.* **8**: 347–365.

Thornton, E. B. and Guza, R. T. (1983). Transformation of wave height distribution, *J. Geophys. Res.* **88**: 5925–5983.

A.3 Verification and Modification of Breaker Height Formulas

Reprinted from:

Rattanapitikon, W. and Shibayama, T. (2000). Verification and modification of breaker height formulas, Coastal Engineering Journal (JSCE), Vol. 42, No. 4, pp. 389-406.

Coastal Engineering Journal, Vol. 42, No. 4 (2000) 389–406

VERIFICATION AND MODIFICATION OF BREAKER HEIGHT FORMULAS

WINYU RATTANAPITIKON
Sirindhorn International Institute of Technology, Thammasat University,
P.O. Box 22, Thammasat-Rangsit Post Office, Pathumthani 12121, Thailand
E-mail: winyu@siit.tu.ac.th

TOMOYA SHIBAYAMA
Department of Civil Engineering, Yokohama National University,
79-5 Tokiwadai, Hodogaya-ku, Yokohama, 240-8501, Japan
E-mail: tomo@coast.cvg.ynu.ac.jp

Received 1 May 2000
Revised 25 August 2000

This study is undertaken to find out the most reliable breaker height formulas that predict well for a wide range of hydraulic conditions. The applicability of 24 existing formulas, for computing breaking wave heights, is examined by using wide range and large amount of published laboratory data (574 cases collected from 24 sources). It is found that most formulas predict well for the breaking waves on the gentle slope ($0 < m \leq 0.07$), but the prediction is unsatisfactory for the breaking waves on the steep slope ($0.1 < m \leq 0.44$). Three formulas are selected and are modified by including the new form of bottom slope effect into the formulas. The new breaker height formulas predict well for wide range of wave and bottom slope conditions.

Keywords: Breaking wave, breaker index, incipient wave breaking.

1. Introduction

To analyze the coastal processes, breaking wave height is one of the most essentially required factors. When waves propagate from offshore to the near shore zone, wave profiles become steep. The increase in wave steepness continues until the wave breaks. In order to compute the wave height transformation in the surf zone, it is necessary to determine the initiation of breaking or wave height at the break point.

Because of the complexity of wave breaking mechanism, most predictions of the breaker heights are based on empirical or semi-empirical formulas calibrated from laboratory data. Many breaker height formulas have been suggested over the past century. Since the formulas are different, the computed results from various formulas should differ from each other and from the laboratory data. No direct approach has been made to describe clearly the accuracy of each formula over wide range of hydraulic conditions. The breaking criteria of Miche (1944), and Goda (1970) seem to be widely used. However, most of the previous formulas were developed with the limited laboratory conditions. Therefore, their validity may be limited according to the range of experimental conditions that were employed in the calibrations or verifications. There is one way to examine the validity of the empirical formulas, that

Table 1. Summary of collected laboratory data used to validate the formulas.

No.	Sources	No. of cases	Beach conditions	Bottom slopes	H_0/L_0
1	Galvin (1969)*	19	plane beach	0.05–0.20	0.001–0.051
2	Hansen and Svendsen (1979)	17	plane beach	0.03	0.002–0.069
3	Hattori and Aono (1985)	3	stepped beach	0.00	0.006–0.021
4	Horikawa and Kuo (1966)	98	plane beach	0.01–0.05	0.006–0.073
		60	stepped beach	0.00	0.007–0.100
5	Hwung *et al.* (1992)	2	plane beach	0.07	0.026–0.048
6	Iversen (1952)*	63	plane beach	0.02–0.10	0.003–0.080
7	Iwagaki *et al.* (1974)	39	plane beach	0.03–0.10	0.005–0.074
8	Maruyama *et al.* (1983)*	1	plane beach	0.03	0.091
9	Mizuguchi (1980)*	1	plane beach	0.10	0.045
10	Nadaoka *et al.* (1982)	12	plane beach	0.05	0.013–0.080
11	Nagayama (1983)	1	plane beach	0.05	0.027
		5	barred beach	0.05	0.025–0.051
		6	stepped beach	0.00–0.05	0.025–0.055
12	Okayasu *et al.* (1986)	2	plane beach	0.05	0.023–0.025
13	Okayasu *et al.* (1988)	10	plane beach	0.03–0.05	0.009–0.054
14	Ozaki *et al.* (1977)	20	plane beach	0.10	0.005–0.060
15	Saeki and Sasaki (1973)*	2	plane beach	0.02	0.005-0.039
16	Sato *et al.* (1988)	3	plane beach	0.05	0.031–0.050
17	Sato *et al.* (1989)	2	plane beach	0.03	0.019–0.036
18	Sato *et al.* (1990)	7	plane beach	0.05	0.003–0.073
19	Singamsetti and Wind (1980)*	95	plane beach	0.03–0.20	0.018–0.079
20	Smith and Kraus (1990)*	5	plane beach	0.03	0.009–0.092
		75	barred beach	0.03–0.44	0.008–0.096
21	Stive (1984)	2	plane beach	0.03	0.010–0.032
22	Ting and Kirby (1994)	2	plane beach	0.03	0.002–0.020
23	Visser (1982)*	7	plane beach	0.05–0.10	0.014-0.079
24	Walker (1974)*	15	plane beach	0.03	0.001–0.037
	Total	574		0.00–0.44	0.001–0.100

* Data from Smith and Kraus (1990).

is, to verify the computed results with the wide range of experimental conditions. The main objective of this study is to find out the most reliable breaker height formulas that predict well for a wide range of experimental conditions.

Laboratory data of broken wave height from 24 sources, including 574 cases, have been collected for examination of the formulas. The data cover wide range of wave and bottom slope conditions (deepwater wave steepness ranging between 0.001 and 0.100, and bottom slope ranging between 0 and 0.44). The data include 3 types of beach conditions, i.e. plane beach, barred beach, and stepped beach. All experiments were performed under regular wave actions and the wave propagates normally to the beach. The experiments were performed in both of small-scale and large-scale wave flumes. The experiment of Maruyama *et al.* (1983) was performed in large-scale wave flume and other experiments were performed in small-scale wave flumes. A summary of the collected laboratory data is given in Table 1.

This paper is divided into three main parts. The first part briefly reviews the existing breaker height formulas. The second part is the verification of existing formulas for identifying the best formula or the formulas that have potential to be modified. The third part describes the modification of selected potential formulas obtained from the second part.

2. Breaker Wave Height Formulas

The majority of the existing formulas present a relationship between the breaking wave height (H_b) and the variables at the breaking or deepwater conditions, i.e. water depth at breaking (h_b), wave period (T), wavelength at breaking (L_b), bottom slope (m), deepwater wavelength (L_0), and deepwater wave height (H_0). The term "breaker index" is used to describe non-dimensional breaker height. The four common indices are in the form of H_b/h_b, H_b/L_b, H_b/L_0, and H_b/H_0. Either local or deepwater conditions are used to express the breaker indices. There are four dimensionless parameters that often used to express the breaker indices, i.e. m, h_b/L_b, h_b/L_0, and H_0/L_0. Some brief reviews of selected breaker wave height formulas, that may be used in general cases, are described in the following:

(a) McCowan (1894) derived a limit of breaking wave in water of constant depth based on solitary wave theory and proposed that the breaking will occur when

$$H_b = 0.78 h_b \tag{1}$$

This formula is referred to be MC94 hereafter.

(b) Miche (1944) developed the semi-theoretical breaking criterion for periodic waves in finite water depth and proposed the limiting wave steepness as a function of h_b/L_b.

$$H_b = 0.142 L_b \tanh\left(\frac{2\pi h_b}{L_b}\right) \tag{2}$$

This formula is referred to be MI44 hereafter. Danel (1952) suggested changing the coefficient from 0.142 to be 0.12 when applying to the horizontal bottom.

(c) Le Mehaute and Koh (1967) proposed an empirical formula based on three sources of the experimental data (Suquet, 1950; Hamada, 1951; and Iversen, 1952). The experiments cover a range of $1/50 < m < 1/5$ and $0.002 < H_0/L_0 < 0.093$.

$$H_b = 0.76 H_0 \left(\frac{H_0}{L_0}\right)^{-1/4} m^{1/7} \tag{3}$$

This formula is referred to be MK67 hereafter.

(d) Galvin (1969) performed laboratory experiments with regular wave on plane beach and combined his data with the data of Iversen (1952) and McCowan (1894). The breaking criterion was developed by fitting empirical relationship between h_b/H_b and m.

$$H_b = h_b \frac{1}{1.40 - 6.85m} \qquad \text{for } m \leq 0.07 \tag{4a}$$

$$H_b = \frac{h_b}{0.92} \qquad \text{for } m > 0.07 \tag{4b}$$

This formula is referred to be GA69 hereafter.

(e) Collins and Weir (1969) derived a breaking height formula from linear wave theory and empirically included the slope effect into the formula. The experimental data from three sources (Suquet, 1950; Hamada, 1951, and Iversen, 1952) were used to fit the formula.

$$H_b = h_b(0.72 + 5.6m) \tag{5}$$

This formula is referred to be CW69 hereafter.

(f) Goda (1970) analyzed several sets of laboratory data of breaking waves on slopes obtained by several researchers (Iversen, 1952; Mitsuyasu, 1962; and Goda, 1964) and proposed a diagram presenting criterion for predicting breaking wave height. Then Goda (1974) gave an approximate expression for the diagram as

$$H_b = 0.17 L_0 \left\{1 - \exp\left[-1.5 \frac{\pi h_b}{L_0}(1 + 15m^{4/3})\right]\right\} \tag{6}$$

This formula is referred to be GO70 hereafter.

(g) Weggel (1972) proposed an empirical formula for computing breaking wave height from five sources of the laboratory data (Iversen, 1952; Reid and Bretschneider, 1953; Galvin, 1969; Jen and Lin, 1970; and Weggel and Maxwell, 1970). The experiments cover a range of $1/50 < m < 1/5$.

$$H_b = \frac{h_b g T^2 1.56/[1 + \exp(-19.5m)]}{gT^2 + h_b 43.75[1 - \exp(-19m)]} \tag{7}$$

This formula is referred to be WE72 hereafter.

(h) Komar and Gaughan (1972) used linear wave theory to derive a breaker height formula from energy flux conservation and assumed a constant H_b/h_b. After calibrating the formula to the laboratory data of Iversen (1952), Galvin (1969), and unpublished data of Komar and Simons (1968), and the field data of Munk (1949), the formula was proposed to be

$$H_b = 0.56 H_0 \left(\frac{H_0}{L_0}\right)^{-1/5} \tag{8}$$

This formula is referred to be KG72 hereafter.

(i) Sunamura and Horikawa (1974) used the same data set as Goda (1970) to plot the relationship between H_b/H_0, H_0/L_0, and m. After fitting the curve, the following formula was proposed

$$H_b = H_0 m^{0.2} \left(\frac{H_0}{L_0}\right)^{-0.25} \tag{9}$$

This formula is referred to be SH74 hereafter.

(j) Madsen (1976) combined the formulas of Galvin (1969) and Collins (1970) to be

$$H_b = 0.72 h_b (1 + 6.4m) \tag{10}$$

This formula is referred to be MA76 hereafter. Black and Rosenberg (1992) found that MA76 gives well predictions for individual breaking wave height in laboratory and field experiments.

(k) Battjes and Janssen (1978) modified Miche (1944)s formula by including the term of "$\gamma/0.88$" into the formula so that the formula can be reduced to be $H_b = \gamma h$ in shallow water condition, in which γ is an adjustable coefficient. The calibration of formula indicated that the coefficient $\gamma = 0.8$ gave the best prediction.

$$H_b = 0.14 L_b \tanh\left(\frac{0.8}{0.88}\frac{2\pi h_b}{L_b}\right) \tag{11}$$

This formula is referred to be BJ78 hereafter.

(l) Ostendorf and Madsen (1979) modified the formula of Miche (1944) by including the bottom slope into the formula. After comparison with the laboratory data, the Miche (1944)s formula was modified to be

$$H_b = 0.14 L_b \tanh\left[(0.8 + 5m)\frac{2\pi h_b}{L_b}\right] \qquad \text{for } m \le 0.1 \tag{12a}$$

$$H_b = 0.14 L_b \tanh\left[(0.8 + 5(0.1))\frac{2\pi h_b}{L_b}\right] \qquad \text{for } m > 0.1 \tag{12b}$$

This formula is referred to be OM79 hereafter.

(m) Sunamura (1980) proposed an empirical formula based on an analysis of various laboratory data (Iversen, 1952; Bowen *et al.*, 1968; Goda, 1970; and Sunamura, 1980) and obtained the following formula

$$H_b = 1.1 h_b \left(\frac{m}{\sqrt{H_0/L_0}} \right)^{1/6} \tag{13}$$

This formula is referred to be SU80 hereafter.

(n) Singamsetti and Wind (1980) conducted a laboratory experiment and proposed two empirical formulas based on their own data. The experiments cover a range of $1/40 < m < 1/5$ and $0.02 < H_0/L_0 < 0.065$.

$$H_b = 0.575 H_0 m^{0.031} \left(\frac{H_0}{L_0} \right)^{-0.254} \tag{14}$$

and

$$H_b = 0.937 h_b m^{0.155} \left(\frac{H_0}{L_0} \right)^{-0.13} \tag{15}$$

Equations (14) and (15) hereafter are referred to be SW80a and SW80b, respectively.

(o) Ogawa and Shuto (1984) obtained the following empirical formula from the same data sets as Goda (1970). The formula was suggested to be used for the range of $1/100 < m < 1/10$ and $0.003 < H_0/L_0 < 0.065$.

$$H_b = 0.68 H_0 m^{0.09} \left(\frac{H_0}{L_0} \right)^{-0.25} \tag{16}$$

This formula is referred to be OS84 hereafter.

(p) Battjes and Stive (1985) modified the formula of Battjes and Janssen (1978) by relating the coefficient γ with the deepwater wave steepness as

$$H_b = 0.14 L_b \tanh \left\{ \left[0.5 + 0.4 \tanh \left(33 \frac{H_0}{L_0} \right) \right] \frac{2\pi h_b}{0.88 L_b} \right\} \tag{17}$$

This formula is referred to be BS85 hereafter.

(q) Seyama and Kimura (1988) measured wave height deformation of individual wave of the irregular wave experiments and investigated the wave height to water depth ratio at wave breaking. The formula of Goda (1970) was modified to compute the individual wave breaking in irregular wave trains as

$$H_b = h_b \left\{ 0.16 \frac{L_0}{h_b} \left\{ 1 - \exp \left[-0.8\pi \frac{h_b}{L_0} (1 + 15 m^{4/3}) \right] \right\} - 0.96 m + 0.2 \right\} \tag{18}$$

They also found that the individual waves, derived by zero-down crossing method, tend to break before satisfying the breaking criterion for regular waves. The reduction of the wave height to water depth ratio at the breaking point was found to be about 20%. Therefore the coefficient of Eq. (18) when applying to regular wave breaking should be changed to be 1.25.

$$h_b = 1.25h_b \left\{0.16\frac{L_0}{h_b}\left\{1 - \exp\left[-0.8\pi\frac{h_b}{L_0}(1 + 15m^{4/3})\right]\right\} - 0.96m + 0.2\right\} \quad (19)$$

This formula is referred to be SK88 hereafter.

(r) Larson and Kraus (1989) developed a breaking criterion based on the large wave tank data of Kajima *et al.* (1982). The breaking height index H_b/h_b was related to the deepwater wave steepness and the local bottom slope seaward of the breaking point.

$$H_b = 1.14h_b\left(\frac{m}{\sqrt{H_0/L_0}}\right)^{0.21} \quad (20)$$

This formula is referred to be LK89 hereafter.

(s) Hansen (1990) used the laboratory data from Van Dorn (1978) and unpublished data of ISVA to plot the relationship between H_b/h_b and mL_b/h_b and proposed the following empirical formula

$$H_b = 1.05h_b\left(m\frac{L_b}{h_b}\right)^{0.2} \quad (21)$$

This formula is referred to be HA90 hereafter.

(t) Smith and Kraus (1990) proposed 2 empirical formulas based on the analysis of 11 sources of laboratory data performed on plane beach conditions. The experiments cover a range of $1/80 < m < 1/10$ and $0.001 < H_0/L_0 < 0.092$.

$$H_b = h_b\left\{\frac{1.12}{1 + \exp(-60m)} - 5.0[1 - \exp(-43m)]\frac{H_0}{L_0}\right\} \quad (22)$$

and

$$H_b = H_0(0.34 + 2.47m)\left(\frac{H_0}{L_0}\right)^{-0.30+0.88m} \quad (23)$$

Equations (22) and (23) hereafter are referred to be SK90a and SK90b, respectively.

(u) Kamphuis (1991) modified Miche (1944)s formula by introducing the exponential form of the bottom slope into the formula and applied to compute the significant wave height of the irregular wave breaking. After calibrating to his irregular breaking wave data, the formula becomes

$$H_b = 0.095\exp(4m)L_b\tanh\left(\frac{2\pi h_b}{L_b}\right) \quad (24)$$

He also found that the regular breaker height formula can be used for irregular wave to compute the significant wave height at the breaking but the coefficient has to be reduced to be around 75% of the proposed coefficient. Therefore the coefficient in Eq. (24) should be changed from 0.095 to be 0.127 when applying to the regular breaking waves as

$$H_b = 0.127 \exp(4m) L_b \tanh\left(\frac{2\pi h_b}{L_b}\right) \tag{25}$$

This formula is referred to be KA91 hereafter.

(v) Gourlay (1992) proposed an empirical formula based on seven sources of laboratory data (Bowen *et al.*, 1968; Smith, 1974; Visser, 1977; Gourlay, 1978; Van Dorn, 1978; Stive, 1984; and Hansen and Svendsen, 1979). The experiments cover a range of $1/45 < m < 1/10$ and $0.001 < H_0/L_0 < 0.066$. The data was used to plot the relationship between H_b/L_0 and H_0/L_0, the curve fitting yields

$$H_b = 0.478 H_0 \left(\frac{H_0}{L_0}\right)^{-0.28} \tag{26}$$

This formula is referred to be GL92 hereafter.

3. Formula Verifications

From Sec. 2, we see that there are 24 formulas for computing H_b, i.e. Eqs. (1)–(17), (19)–(23), and (25)–(26). All 24 formulas were developed with limited range of experimental conditions. Therefore, their validity may be limited according to the range of experimental conditions that were employed in the calibrations. However, some of them may be able to predict well for a wide range of conditions. The main objective of this section is to identify the best formula or the formulas that have the potential to be modified. The accuracy of the 24 formulas is examined against the measured breaking wave heights.

In order to evaluate the accuracy of the prediction, the verification results are presented in terms of root mean square relative error, ER, which is defined as

$$ER = 100\sqrt{\frac{\sum_{i=1}^{tn}(H_{bci} - H_{bmi})^2}{\sum_{i=1}^{tn} H_{bmi}^2}} \tag{27}$$

where i is the number of wave height, H_{bci} is the computed breaking wave height of number i, H_{bmi} is the measured breaking wave height of number i, and tn is the total number of measured breaking wave height. Smaller values of ER correspond to a better agreement.

The measured breaking wave heights from 24 sources are used to examine the validity of each formula. The experimental data cover wide range of wave and bottom conditions ($0.001 \leq H_0/L_0 \leq 0.100$, and $0 \leq m \leq 0.44$).

According to the bottom slope conditions in Eqs. (4) and (12), the group of bottom slope may be classified to be $m \leq 0.07$, $0.07 < m \leq 0.10$, and $m > 0.10$. However some formulas (e.g. MK67, SH74, and SU80) are not valid for the bottom slope $m = 0$ and the experimental data cover the range of $0 \leq m \leq 0.44$. Therefore, in this study, the bottom slope is classified into 4 groups, i.e. horizontal ($m = 0$), gentle ($0 < m \leq 0.07$), intermediate ($0.07 < m \leq 0.10$), and steep ($0.10 < m \leq 0.44$). The total number of cases of the collected data for $m = 0$, $0 < m \leq 0.07$, $0.07 < m \leq 0.10$ and $0.10 < m \leq 0.44$ are 64, 338, 102 and 70, respectively.

The computations of the breaker height formulas are carried out with 24 sources of collected data (see Table 1). All variables are computed based on the linear wave theory. The water depth (h_b) and the bottom slope (m) that used in the computation are the still water depth and the local bottom slope seaward of the breaking point. Table 2 shows the ER error of each formula for 4 groups of bottom slope and all

Table 2. The root mean square relative error (ER) of each formula for four groups of bottom slope and all cases.

Formulas		$m = 0$ (64 cases)	$0 < m \leq 0.07$ (338 cases)	$0.07 < m \leq 0.1$ (102 cases)	$0.1 < m \leq 0.44$ (70 cases)	All 574 cases
MC94	Eq. (1)	14.77	16.98	21.83	27.91	19.26
MI44	Eq. (2)	13.94	11.13	18.04	25.37	14.93
MK67	Eq. (3)	N.A.*	12.23	17.28	28.02	32.07
GA69	Eq. (4)	15.84	21.05	25.49	17.61	20.83
CW69	Eq. (5)	15.57	25.89	41.31	110.31	48.02
GO70	Eq. (6)	13.86	9.82	23.04	81.57	32.21
WE72	Eq. (7)	14.77	13.03	18.16	19.02	14.76
KG72	Eq. (8)	10.89	10.69	12.42	12.55	11.19
SH74	Eq. (9)	N.A.*	12.54	31.95	52.89	37.26
MA76	Eq. (10)	15.57	22.55	32.01	86.97	38.70
BJ78	Eq. (11)	13.31	14.34	24.24	31.41	18.78
OM79	Eq. (12)	18.86	11.13	11.68	14.44	12.45
SU80	Eq. (13)	N.A.*	14.42	14.51	20.18	31.72
SW80a	Eq. (14)	N.A.*	12.75	17.21	17.32	31.17
SW80b	Eq. (15)	N.A.*	15.73	15.53	20.66	32.23
OS84	Eq. (16)	N.A.*	10.64	18.40	24.08	31.32
BS85	Eq. (17)	20.66	18.42	28.40	29.65	21.75
SK88	Eq. (19)	14.40	13.09	13.44	35.65	17.98
LK89	Eq. (20)	N.A.*	13.39	14.43	23.54	31.73
HA90	Eq. (21)	N.A.*	14.72	20.34	29.83	33.18
SK90a	Eq. (22)	30.01	11.03	11.83	21.09	15.12
SK90b	Eq. (23)	13.90	12.61	15.61	26.78	15.71
KA91	Eq. (25)	13.84	10.11	19.14	106.41	40.64
GL92	Eq. (26)	21.23	14.54	16.43	13.18	15.23

*N.A. = Not Applicable

cases. The verification results from Table 2 can be summarized in the following points:

(a) The best formulas for predicting the breaking wave heights on the bottom slopes of $m = 0$, $0 < m \leq 0.07$, $0.07 < m \leq 0.10$, and $0.10 < m \leq 0.44$ are the formulas of KG72, GO70, OM79, and KG72, respectively. The errors ER of these formulas tend to vary with the bottom slope. Therefore they have possibility to be improved by including the new form of bottom slope effect into the formulas.
(b) The formula of KG72 gives the best prediction ($ER = 11.2\%$) over a wide range of experiments.
(c) The formula of GO70 (a commonly accepted formula) gives very well prediction for the bottom slope $m \leq 0.07$ but it may not be suitable for steep slope conditions ($m > 0.10$).
(d) Although the formula of MC94 is very simple, it seems to predict reasonably well for a wide range of experimental conditions. It can be used for rough approximation.
(e) Some formulas are not valid for the horizontal slope ($m = 0$) and give $ER = 100$ (i.e. the formulas of MK67, SH74, SU80, SW80, OS84, LK89, and HA90).
(f) Most formulas (except MC94, GA69, CW69, MA76, SW80b, and BS85) give well predictions ($ER < 15$) for the breaking height on the gentle slope ($0 < m \leq 0.07$).
(g) For the intermediate slope ($0.07 < m \leq 0.10$), the errors ER of almost all formulas are larger than those for gentle slope.
(h) For the steep slopes ($0.10 < m \leq 0.44$), the errors ER of most formulas (except GA69, WE72, KG72, OM79, SW80a, and GL92) are quite large ($ER > 20$).
(i) The formulas of CW69, GO70, SH74, MA76, and KA91 give unrealistically very large errors ($ER > 50$) for breaking wave on the steep slope ($0.10 < m \leq 0.44$). This may cause by an inappropriate bottom slope effect included in the formulas.
(j) For the non-horizontal slope ($m > 0$), the errors of most formulas (except GA69, SW80b, and GL92) tend to increase with the bottom slope.
(k) For better prediction, most formulas should have to include the new form of bottom slope effect.

4. Formula Modifications

The verification results in Table 2 show that, for bottom slope $m > 0$, the errors ER of most formula increase with the increasing of bottom slope. It is expected that the error ER of the formulas could be reduced by incorporating the new form of bottom slope effect into the formulas. Three formulas, that give the best prediction for each group of bottom slope, are selected to be modified in this study, i.e. the formulas of KG72, GO70 and OM79. To include the new form of bottom slope effect, the selected formulas will be modified as the following.

4.1. *Modification of Komar and Gaughan (1972)s formula*

The slope effect coefficient may be included in Eq. (8) by replacing the constant "0.56" to K_{KG} as

$$H_b = K_{KG} H_0 \left(\frac{H_0}{L_0}\right)^{-1/5} \tag{28}$$

where K_{KG} is the slope effect coefficient for Komar and Gaughan (1972)s formula.

From Eq. (28), the formula of K_{KG} can be written as

$$K_{KG} = \frac{H_b}{H_0}\left(\frac{H_0}{L_0}\right)^{1/5} \tag{29}$$

The measured K_{KG} of collected data (shown in Table 1) is determined by using Eq. (29). Figure 1 shows the relation between measured K_{KG} and the bottom slope (m). It can be seen from Fig. 1 that K_{KG} (y-axis) is mainly varied between 0.50 and 0.65. This narrow band of variation indicates that the effect of bottom slope (m) on the formula of KG72 is not much. Although the effect of bottom slope (m) is not much, it still has some effect. For better prediction, it is worthwhile to include the slope effect into the formula. A formula of K_{KG} is derived by using multi-regression analysis between K_{KG} and power series of m. After multi-regression analysis, the best-fit formula for K_{KG} can be expressed as

$$K_{KG} = 10.02m^3 - 7.46m^2 + 1.32m + 0.55 \tag{30}$$

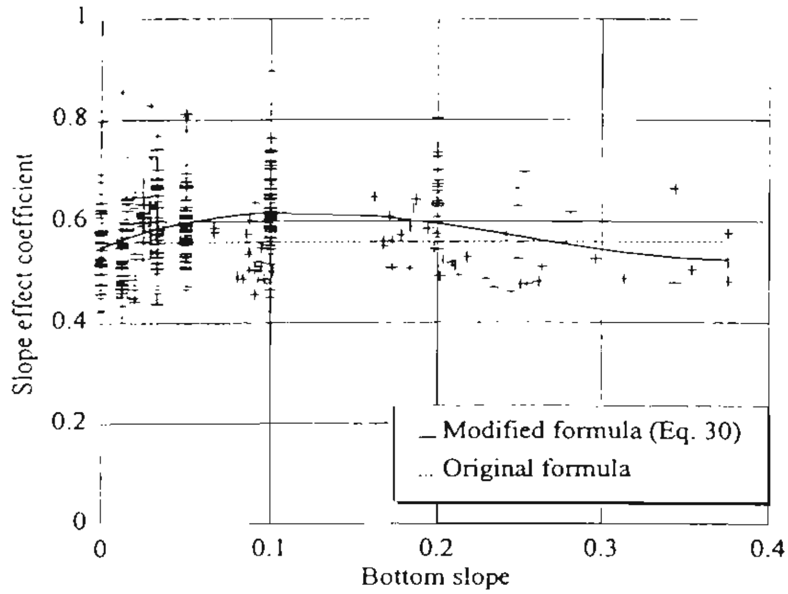

Fig. 1. Relationship between slope effect coefficient for Komar and Gaughan (1972)s formula and bottom slope (measured data from 24 sources shown in Table 1). Solid line is the computed K_{KG} from Eq. (30) and dashed line is the computed K_{KG} from the original formula [from Eq. (8), $K_{KG} = 0.56$].

Table 3. The root mean square relative error (ER) of each modified formula for four groups of bottom slope and all cases.

Formulas	$m = 0$ (64 cases)	$0 < m \leq 0.07$ (338 cases)	$0.07 < m \leq 0.1$ (102 cases)	$0.1 < m \leq 0.44$ (70 cases)	All 574 cases
MKG72 Eq. (31)	10.60	10.14	14.07	11.72	10.92
MGO70 Eq. (35)	13.01	9.92	11.89	11.99	10.73
MOM79 Eq. (39)	13.29	9.94	11.88	12.19	10.80

Substituting Eq. (30) into Eq. (28), the formula of Komar and Gaughan (1972) is modified to be

$$H_b = (10.02m^3 - 7.46m^2 + 1.32m + 0.55)H_0 \left(\frac{H_0}{L_0}\right)^{-1/5} \tag{31}$$

This formula is referred to be MKG72 hereafter. The computations of breaking wave height from Eq. (31) are carried out for 24 sources of collected data. The error ER of Eq. (31) for 4 groups of bottom slope is shown in Table 3. The error ER for all cases is 10.9%.

4.2. *Modification of Goda (1970)s formula*

The slope effect coefficient may be included in Eq. (6) by replacing the original slope effect term "$-1.5(1 + 15m^{4/3})$" as

$$H_b = 0.17L_0 \left\{1 - \exp\left[\frac{\pi h_b}{L_0}(K_{GO})\right]\right\} \tag{32}$$

where K_{GO} is the slope effect coefficient for Goda (1970)s formula.

From Eq. (32), the formula of K_{GO} can be written as

$$K_{GO} = \frac{L_0}{\pi h_b} \ln\left(1 - \frac{H_b}{0.17L_0}\right) \tag{33}$$

The measured K_{GO} of collected data (shown in Table 1) is determined by using Eq. (33). Figure 2 shows the relation between the measured K_{GO} and bottom slope (m). A formula of K_{GO} is conducted by using multi-regression analysis. After the analysis, the best-fit formula of K_{GO} can be expressed as

$$K_{GO} = 16.21m^2 - 7.07m - 1.55 \tag{34}$$

Substituting Eq. (34) into Eq. (32), the formula of Goda (1970) is modified to be

$$H_b = 0.17L_0 \left\{1 - \exp\left[\frac{\pi h_b}{L_0}(16.21m^2 - 7.07m - 1.55)\right]\right\} \tag{35}$$

This formula is referred to be MGO70 hereafter. The error ER of Eq. (35) for 4 groups of bottom slope is shown in Table 3. The error for ER all cases is 10.7%.

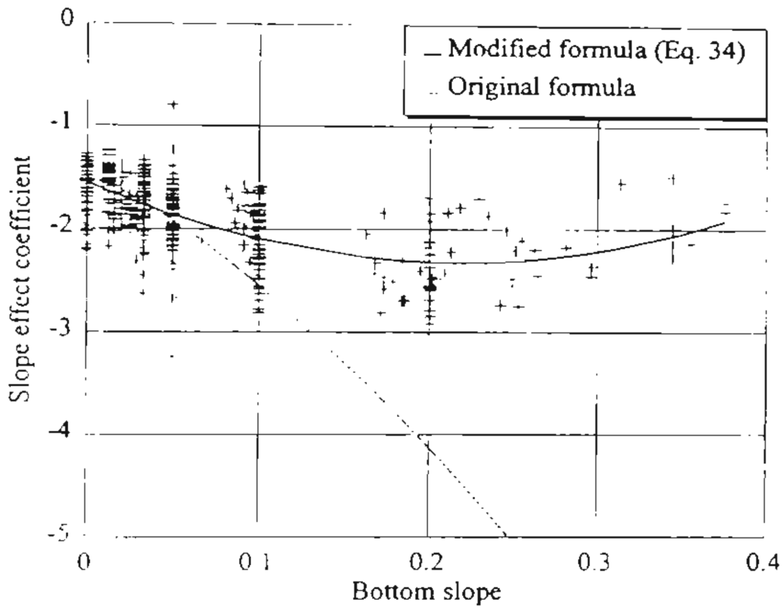

Fig. 2. Relationship between slope effect coefficient for Goda (1970)s formula and bottom slope (measured data from 24 sources shown in Table 1). Solid line is the computed K_{GO} from Eq. (34) and dashed line is the computed K_{GO} from the original formula {from Eq. (6), $K_{GO} = -1.5(1+1m^{4/3})$}.

4.3. *Modification of Ostendorf and Madsen (1979)s formula*

The slope effect coefficient may be included in Eq. (12) by replacing the original slope effect term "$(0.8 + 5m)$" as

$$H_b = 0.14L_b \tanh\left[(K_{OM})\frac{2\pi h_b}{L_b}\right] \tag{36}$$

where K_{OM} is the slope effect coefficient for Ostendorf and Madsen (1979)s formula.

From Eq. (36), the formula of K_{OM} can be written as

$$K_{OM} = \frac{L_b}{2\pi h_b}\tanh^{-1}\left(\frac{H_b}{0.14L_b}\right) \tag{37}$$

The measured K_{OM} of collected data (shown in Table 1) is determined by using Eq. (37). Figure 3 shows the relation between measured K_{OM} and the bottom slope (m). A formula of K_{OM} is conducted by using multi-regression analysis. The best-fit formula of K_{OM} can be expressed as

$$K_{OM} = -11.21m^2 + 5.01m + 0.91 \tag{38}$$

Substituting Eq. (38) into Eq. (36), the formula of Ostendorf and Madsen (1979) is modified to be

$$H_b = 0.14L_b \tanh\left[(-11.21m^2 + 5.01m + 0.91)\frac{2\pi h_b}{L_b}\right] \tag{39}$$

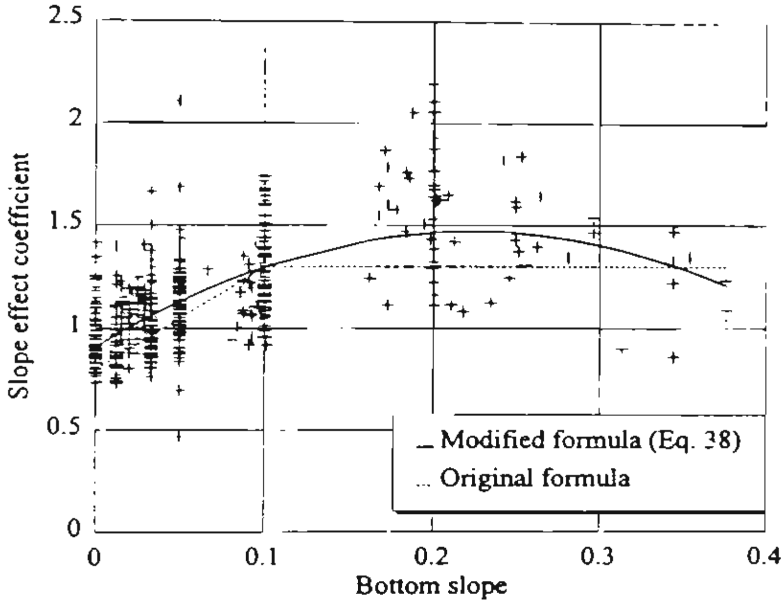

Fig. 3. Relationship between slope effect coefficient for Ostendorf and Madsen (1979)s formula and bottom slope (measured data from 24 sources shown in Table 1). Solid line is the computed K_{OM} from Eq. (38) and dashed line is the computed K_{OM} from the original formula (from Eq. (12), $K_{OM} = 0.8 + 5m$ for $m \leq 0.1$, and $K_{OM} = 1.3$ for $m > 0.1$).

This formula is referred to be MOM79 hereafter. The error ER of Eq. (39) for 4 groups of bottom slope is shown in Table 3. The error ER for all cases is 10.8%.

The results from Tables 2 and 3 can be summarized as follows:

(a) There are some ranges of m where the error increases after the modification (e.g. $0 < m \leq 0.07$ for MGO70). However, the error in most cases are decreased after the modification.
(b) The modified formulas give very well prediction for general cases and the predictions are better than the predictions of existing formulas.
(c) The MGO70 formula Eq. (35) gives the best prediction for a wide range of experiments.
(d) Although the MKG72 formula Eq. (31) is better than the original KG72 formula Eq. (8), the formula of MKG72 is long. Using the original KG72 formula is recommended for the first approximations.
(e) Since the breaking wave height (H_b) in the MKG72 formula depends on the deepwater wave height (H_0), it may have difficulty to be applied in cases where secondary breaking or refraction or diffraction effects are involved.
(f) The overall accuracies of the top four formulas in descending order are those by MGO70, MOM79, MKG72 and KG72. These formulas are recommended to be used for computing breaker wave heights in general cases.

The comparison between measured and computed breaking wave height from MGO70 formula Eq. (35) is shown in Fig. 4. One point on the upper right of the

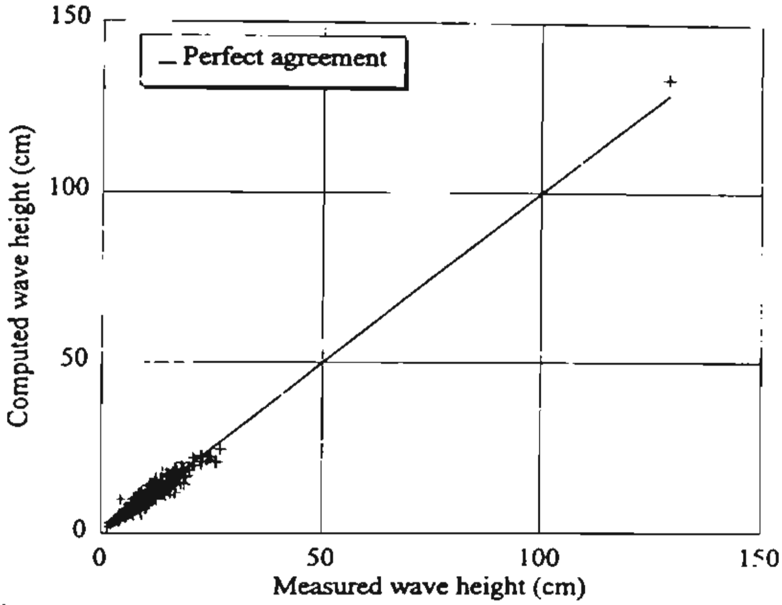

Fig. 4. Comparison between measured breaking wave height and the computed from Eq. (35) (measured data from 24 sources shown in Table 1). Solid line is the line of perfect agreement.

figure is the data from large-scale wave flume of Maruyama *et al.* (1983) and other points are the data from small-scale wave flumes. The solid line in the figure is the line of perfect agreement.

As we know, the validity of the empirical formula depends much on the range of experimental data used in formula calibration. Since the modified formulas have strong sensitivity to m and the experiments used in this study cover the range of $0 \leq m \leq 0.44$, the proposed formulas should not be used for cases of $m > 0.44$. However, based on the analysis of bottom slope of sand in the large-scale wave flume, Larson and Kraus (1989) found that the maximum slope of the sand bare ≈ 0.44. Therefore the proposed formulas can be used without care when applying to the sandy beach.

5. Conclusions

A total of 574 cases from 24 sources of published experimental results were used to verify 24 existing breaker height formulas. The experimental data cover wide range of wave and bottom conditions ($0.001 \leq H_0/L_0 \leq 0.100$, and $0 \leq m \leq 0.44$). The verification results were presented in terms of root mean square relative error (ER). It was found that the formula of Komar and Gaughan (1972) gives the best prediction, among 24 existing formulas, over a wide range of experiments. Most existing formulas predict well for the breaking waves on gentle slope ($0 < m \leq 0.07$), but predict fair for the breaking waves on the steep slope ($0.10 < m \leq 0.44$). The errors ER of most formulas vary with the bottom slopes. It was expected that incorporating the new form of bottom slope effect into the formulas could improve the accuracy of the formulas. Three formulas were selected to modify by including the new form of bottom slope effect into the formulas. The modified formulas seem to predict well for a wide range of wave and bottom slope conditions. The modified Goda (1970)s formula Eq. (35) gives the best prediction for general cases (ER = 10.7%).

Acknowledgment

This research was sponsored by the Thailand Research Fund.

References

Battjes, J. A. and Janssen, J. P. F. M. (1978). Energy loss and set-up due to breaking of random waves, *Proc. 16th Coastal Eng. Conf.*, ASCE, pp. 569–589.

Battjes, J. A. and Stive, M. J. F. (1985). Calibration and verification of a dissipation model for random breaking waves, *J. Geophy. Res.* **90**, C5, pp. 9159-9167.

Black, K. P. and Rosenberg, M. A. (1992). Semi-empirical treatment of wave transformation outside and inside the breaker line, *Coastal Eng.* **16**: 313–345.

Bowen, A. J., Inman, D. L. and Simmons, V. P. (1968). Wave set-down and set-up, *J. Geophy. Res.* **73**, 8, pp. 2569–2577.

Collins, J. I. (1970). Probabilities of breaking wave characteristics, *Proc. 12nd Coastal Eng. Conf.* ASCE, pp. 399–414.

Collins, J. I. and Weir, W. (1969). Probabilities of wave characteristics in the surf zone, Tetra Technical Report, TC-149, Pasadena, California, USA, p. 122.

Danel, P. (1952). On the limiting clapotis, Gravity waves, US Department of Commerce, National Bureau of Standards, Circular 521, pp. 35–45.

Galvin, C. J. (1969). Breaker travel and choice of design wave height, *J. Waterways Harbors Div.*, ASCE **95**, WW2, pp. 175–200.

Goda, Y. (1964). Wave forces on a vertical circular cylinder: Experiments and a proposed method of wave force computation, Report of the Port and Harbor Research Institute, Ministry of Transportation, No. 8, p. 74.

Goda, Y. (1970). A synthesis of breaker indices, *Trans. JSCE* **2**: 227–230.

Goda, Y. (1974). New wave pressure formula for composite breakwater, *Proc. 14th Coastal Eng. Conf.*, ASCE, pp. 1702–1720.

Gourlay, M. R. (1978). Wave generated currents, PhD Thesis, Department of Civil Engineering, University of Queensland.

Gourlay, M. R. (1992). Wave set-up, wave run-up and beach water table: Interaction between surf zone hydraulics and groundwater hydraulics, *Coastal Eng.* **17**: 93–144.

Hamada, T. (1951). Breakers and beach erosion, Port and Harbor Research Institute, Ministry of Transportation, Japan, p. 165.

Hansen, J. B. (1990). Periodic waves in the surf zone: Analysis of experimental data, *Coastal Eng* **14**, 1, pp. 19–41.

Hansen, J. B. and Svendsen, I. A. (1979). Regular waves in shoaling water experimental data, Series Paper No. 21, Institute of Hydrodynamics and Hydraulic Engineering, Technical University of Denmark, Denmark, p. 243.

Hattori, M. and Aono, T. (1985). Experimental study on turbulence structures under breaking waves, *Coastal Engineering Japan* **28**: 97–116.

Horikawa, K. and Kuo, C. T. (1966). A study of wave transformation inside the surf zone, *Proc. 10th Coastal Eng. Conf.*, ASCE, pp. 217–233.

Hwung, H. H., Chyan, J. M. and Chung, Y. C. (1992). Energy dissipation and air bubbles mixing inside surf zone, *Proc. 23rd Coastal Eng. Conf.*, ASCE, pp. 308-321.

Iversen, H. W. (1952). Laboratory study of breakers, Gravity Waves, Circular 52, US Bureau of Standards, pp. 9–32.

Iwagaki, Y., Sakai, T., Tsukioka, K. and Sawai, N. (1974). Relationship between vertical distribution of water particle velocity and type of breakers on beaches, *Coastal Eng. Japan*, JSCE **17**: 51–58.

Jen, Y. and Lin, P. M. (1970). Plunging wave pressures on a semi-cylindrical tube, *Proc. 12nd Coastal Eng. Conf.*, ASCE, pp. 1469–1490.

Kajima, R., Shimizu, T., Maruyama, K. and Saito, S. (1982). Experiments of beach profile change with a large wave flume, *Proc. 18th Coastal Eng. Conf.*, ASCE, pp. 1385–1404.

Kamphuis, J. W. (1991). Incipient wave breaking, *Coastal Eng.* **15**: 185–203.

Komar, P. D. and Gaughan, M. K. (1972). Airy wave theory and breaker height prediction, *Proc. 13th Coastal Eng. Conf.*, ASCE, pp. 405–418.

Larson, M. and Kraus, N. C. (1989). SBEACH: Numerical model for simulating storm-induced beach change, Report 1, Technical Report CERC-89-9, Waterways Experiment Station, US Army Crops of Engineers, p. 267.

Le Mehaute, B. and Koh, R. C. Y. (1967). On the breaking of waves arriving at an angle to the shore, *J. Hydr. Res.* **5**, 1, pp. 67–88.

Madsen, O. S. (1976). Wave climate of the continental margin: Elements of its mathematical description, eds. D. J. Stanley and D. J. P. Swift, Marine Sediment Transport in Environmental Management, Wiley, New York, pp. 65–87.

Maruyama, K., Sakakiyama, T., Kajima, R., Saito, S. and Shimizu, T. (1983). Experimental study on wave height and water particle velocity near the surf zone using a large wave flume, Civil Engineers Laboratory Report No. 382034, The Central Research Institute of Electric Power Industry, Chiba, Japan (in Japanese).

Massel, S. R. (1996). On the largest wave height in water of constant depth, *Ocean Eng.* **23**: 553–573.

McCowan, J. (1894). On the highest waves of a permanent type, Philosophical Magazine, Edinburgh **38**, Ser. 5, pp. 351–358.

Miche, R. (1944). Mouvements ondulatoires des mers en profondeur constante on decroissante, Ann. des Ponts et Chaussees, Chap. 114, pp. 131–164, 270–292, and 369–406.

Mitsuyasu, H. (1962). Experimental study on wave force against a wall, Report of the Transportation Techical Research Institute, No. 47, p. 39 (in Japanese).

Mizuguchi, M. (1980). An heuristic model of wave height distribution in surf zone, *Proc. 17th Coastal Eng. Conf.*, ASCE, pp. 278–289.

Munk, W. H. (1949). The solitary wave theory and its applications to surf problems, *Ann. New York Acad. Sci.* **51**: 376–423.

Nadaoka, K., Kondoh, T. and Tanaka. N. (1982). The structure of velocity field within the surf zone revealed by means of laser-doppler anemometry, Port and Harbor Research Institute **21**, 2, pp. 50–102 (in Japanese).

Nagayama, S. (1983). Study on the change of wave height and energy in the surf zone, Bach. Thesis, Civil Engineering, Yokohama National University, Japan, pp. 24–35.

Ogawa, Y. and Shuto, N. (1984). Run-up of periodic waves on beaches of non-uniform slope, *Proc. 19th Coastal Eng. Conf.*, ASCE, pp. 328–344.

Okayasu, A., Shibayama, T. and Mimura, N. (1986). Velocity field under plunging waves, *Proc. 20th Coastal Eng. Conf.*, ASCE, pp. 660–674.

Okayasu, A., Shibayama, T. and Horikawa, K. (1988). Verification of undertow in the surf zone, *Proc. 21st Coastal Eng. Conf.*, ASCE, pp. 478–491.

Ostendorf, D. W. and Madsen, O. S. (1979). An analysis of longshore current and associated sediment transport in the surf zone, Report No. 241, Department of Civil Engineering, MIT, p. 169.

Ozaki, A., Sasaki, M. and Usui, Y. (1977). Study on rip currents: Experimental observation of nearshore circulation on a sloping bottom, *Coastal Eng. Japan*, JSCE **20**: 147–158.

Reid, R. O. and Bretschneider, C. L. (1953). Surface waves and offshore structures, Technical Report No. 53-10, Texas A & M University.

Saeki, H. and Sasaki, M. (1973). A study of the deformation of waves after breaking, *Proc. 20th Japanese Conf. Coastal Eng.*, JSCE, pp. 559–564 (in Japanese).

Sato, S., Fukuhama, M. and Horikawa, K. (1988). Measurements of near-bottom velocities in random waves on a constant slope, *Coastal Eng. Japan*, JSCE **31**, 2, pp. 219–229.

Sato, S., Isayama, T. and Shibayama, T. (1989). Long-wave component in near bottom velocity under random waves on a gentle slope, *Coastal Eng. Japan*, JSCE **32**, 2, pp. 149–159.

Sato, S., Homma, K. and Shibayama, T. (1990). Laboratory study on sand suspension due to breaking waves, *Coastal Eng. Japan*, JSCE **33**, 2, pp. 219–231.

Seyama, A. and Kimura, A. (1988). The measured properties of irregular wave breaking and wave height change after breaking on slope, *Proc. 21st Coastal Eng. Conf.*, ASCE, pp. 419–432.

Singamsetti, S. R. and Wind, H. G. (1980). Characteristics of breaking and shoaling periodic waves normally incident on to plane beaches of constant slope, Report M1371, Delft Hydraulic Laboratory, Delft, The Netherlands, p. 142.

Smith, D. A. (1974). Radiation stress effects on wave set-up in the surf zone, MSc Thesis, Department of Civil Engineering, University of London, Imperial College.

Smith, J. M. and Kraus, N. C. (1990). Laboratory study on macro-features of wave breaking over bars and artificial reefs, Technical Report CERC-90-12, WES, US Army Corps of Engineers, p. 232.

Stive, M. J. F. (1984). Energy dissipation in wave breaking on gentle slopes, *Coastal Eng.* **8**: 99–127.

Sunamura, T. (1980). A laboratory study of offshore transport of sediment and a model for eroding beaches, *Proc. 17th Coastal Eng. Conf.*, ASCE, pp. 1051–1070.

Sunamura, T. and Horikawa, K. (1974). Two-dimensional beach transformation due to waves, *Proc. 14th Coastal Eng. Conf.*, ASCE, pp. 920–938.

Suquet, F. (1950). Experimental study on the breaking of waves, La Houille Blanche, No. 3, May to June.

Ting, C. K. and Kirby, J. T. (1994). Observation of undertow and turbulence in a laboratory surf zone, *Coastal Eng.* **24**: 51–80.

Van Dorn, W. G. (1978). Breaking invariants in shoaling waves, *J. Geophy. Res.* **83**, C6, pp. 2981–2988.

Visser, P. J. (1977). Wave set-up: Experimental investigation on normally incident waves, Report No. 77–1, Laboratory of Fluid Mechanics, Department of Civil Engineering, Delft University of Technology, Delft, The Netherlands.

Visser, P. J. (1982). The proper longshore current in a wave basin, Report No. 82-1, Laboratory of Fluid Mechanics, Department of Civil Engineering, Delft University of Technology, Delft, The Netherlands, p. 86.

Walker, J. R. (1974). Wave transformations over a sloping bottom and over a three-dimensional shoal, Miscellaneous Report No. 11, University of Hawaii, Look Lab-75-11, Honolulu, Hawaii, USA.

Weggel J. R. (1972). Maximum breaker height, *J. Waterways Harbors Coastal Eng. Div.* 98, WW4, pp. 529–548.

Weggel, J. R. and Maxwell, W. H. C. (1970). Experimental study of breaking wave pressures, *2nd Ann. Offshore Tech. Conf.*, Texas, OTC-1244.